THE ASTRONOMICAL JOURNAL, 123:3154–3198, 2002 June

VARIABLE STARS IN LEO A: RR LYRAE STARS, SHORT-PERIOD CEPHEIDS, AND IMPLICATIONS FOR STELLAR CONTENT

ANDREW E. DOLPHIN, A. SAHA, AND JENNIFER CLAVER
Kitt Peak National Observatory, National Optical Astronomy Observatory,[1] P.O. Box 26372, Tucson, AZ 85726;
dolphin@noao.edu, saha@noao.edu, jclaver@noao.edu

EVAN D. SKILLMAN
Department of Astronomy, University of Minnesota, 116 Church Street, SE, Minneapolis, MN 55455; skillman@astro.umn.edu

A. A. COLE
Department of Physics and Astronomy, 538 LGRT, University of Massachusetts, Amherst, MA 01003: cole@condor.astro.umass.edu

J. S. GALLAGHER
Department of Astronomy, University of Wisconsin, 475 North Charter Street, Madison, WI 53706; jsg@astro.wisc.edu

ELINE TOLSTOY
Kapteyn Astronomical Institute, University of Groningen, Postbus 800, NL-9700 AV Groningen, Netherlands; etolstoy@astro.rug.nl

AND

R. C. DOHM-PALMER AND MARIO MATEO
Department of Astronomy, 821 Dennison Building, University of Michigan, Ann Arbor, MI 48109-1090;
rdpalmer@astro.lsa.umich.edu, mateo@astro.lsa.umich.edu
Received 2001 November 5; accepted 2002 February 19

ABSTRACT

We present the results of a search for short-period variable stars in Leo A. We have found 92 candidate variables, including eight candidate RR Lyrae stars. From the RR Lyrae stars, we measure a distance modulus of $(m - M)_0 = 24.51 \pm 0.12$, or 0.80 ± 0.04 Mpc. This discovery of RR Lyrae stars confirms for the first time the presence of an ancient (older than $\sim$11 Gyr) population in Leo A, accounting for at least 0.1% of the galaxy's V luminosity. We have also discovered a halo of old (more than $\sim$2 Gyr) stars surrounding Leo A, with a scale length roughly 50% larger than that of the dominant young population. We also report the discovery of a large population of Cepheids in Leo A. The median absolute magnitude of our Cepheid sample is $M_V = -1.1$, fainter than 96% of SMC and 99% of LMC Cepheids. Their periods are also unusual, with three Cepheids that are deduced to be pulsating in the fundamental mode having periods of under 1 day. Upon examination, these characteristics of the Leo A Cepheid population appear to be a natural extension of the classical Cepheid period-luminosity relations to low metallicity, rather than being indicative of a large population of "anomalous" Cepheids. We demonstrate that the periods and luminosities are consistent with the expected values of low-metallicity blue helium-burning stars (BHeB's), which populate the instability strip at lower luminosities than do higher metallicity BHeB's.

Key words: Cepheids — galaxies: individual (Leo A) — Local Group

On-line material: FITS file

1. INTRODUCTION

The Local Group dwarf irregular galaxy Leo A has been a source of considerable controversy, regarding both its distance and stellar content (van den Bergh 2000). Discovered by Zwicky (1942), its first distance was determined by Demers et al. (1984) from photographic photometry. They found an unusual color-magnitude diagram (CMD), apparently containing no normal supergiants (blue or red). A large number of very blue ($B-V \sim -0.4$) stars were observed; these were interpreted as 60–120 $M_\odot$ main-sequence stars and thus evidence of very recent star formation. No red supergiants were observed. They used the three brightest blue stars to derive a distance of $(m-M)_0 = 26.8 \pm 0.4$.

A later photographic study by Sandage (1986) found significant discrepancies between the two photometry sets, strongly nonlinear (especially in B) in the sense that the photometry of Demers et al. (1984) was fainter than that of Sandage (1986) for bright stars and brighter for faint stars. Sandage (1986) thus found a "normal" CMD, with both red and blue supergiants falling in locations similar to those of other dwarf irregular galaxies. He therefore was able to use both the brightest three red star and the brightest three blue star methods to determine a distance modulus of $(m - M)_0 = 26 \pm 1$.

The photometric distance determinations were confirmed by Hoessel et al. (1994), who determined a value of $(m - M)_0 = 26.74 \pm 0.22$, based on four Cepheids. Tolstoy (1996) then used their photometric data and distance to make the first stellar population analysis of Leo A. Modeling the strong blue and red plumes in the CMD as blue and red supergiants, she concluded that Leo A has no very young stars and is apparently in a period of diminished star formation.

[1] NOAO is operated by the Association of Universities for Research in Astronomy, Inc., under cooperative agreement with the National Science Foundation. The WIYN Observatory is a joint facility of the University of Wisconsin–Madison, Indiana University, Yale University, and the National Optical Astronomy Observatory.

This picture of Leo A's distance and stellar content came into question with the *Hubble Space Telescope*–based study of Tolstoy et al. (1998). With these data, it became clear that what had been interpreted by Tolstoy (1996) as a red supergiant sequence was actually a very narrow red giant branch, and that the broadening at its base was a vertically extended red clump. The distance modulus was therefore revised to $(m - M)_0 = 24.2 \pm 0.2$, making Leo A's brightest supergiants and Cepheids 2 mag fainter than had previously been believed. The explanation for the error in the brightest supergiant distance is straightforward. For dwarf galaxies, the luminosity of the brightest star is limited by the stellar initial mass function (IMF) and small number statistics rather than by stellar astrophysics (Rozanski & Rowan-Robinson 1994). Thus, while two giant galaxies can be reasonably expected to have similar brightest supergiants, this is not true of dwarfs, in which the same supergiants could be interpreted as a small nearby system or as a large distant system with equal validity. This degeneracy was recognized by Sandage (1986) and was the reason for his 1 mag uncertainty.

However, the results of Hoessel et al. (1994) have remained a puzzle. Even with the shorter distance, there is no doubt that Leo A contains a large amount of recent star formation and therefore should contain a significant Cepheid population. As noted by Tolstoy et al. (1998), only one of the periodic variables found by Hoessel et al. (1994) falls on the Cepheid period-luminosity (P-L) relation for the shorter distance. The implication of these findings was therefore that Leo A is an unusual system—one containing a significant number of young stars and possibly an entirely young system (Tolstoy et al. 1998), but apparently without Cepheids.

By bringing the galaxy a factor of 3 closer, the blue supergiants previously assumed to be rather young were made older, thus producing the interpretation that most of Leo A's stars were formed 0.9–1.5 Gyr ago, with a much smaller number at more recent ages and perhaps none at older ages. The conclusion of Tolstoy et al. (1998) that any ancient population is very weak or perhaps nonexistent was based on the relative weakness of the red giant branch compared with that of the red clump. However, they noted that studies of Leo A main-sequence turnoff stars or RR Lyrae stars would be needed to definitively establish the existence or lack of an ancient population. With a distance of less than 1 Mpc, it is now feasible to search for RR Lyrae stars with ground-based telescopes.

The present work is a new study of variable stars in Leo A. Our observations, photometry, and variable-star search are described in §§ 2 and 3. Our variable-star results are discussed in §§ 4 and 5, while a stellar population gradient is examined in § 6. Section 7 contains the summary.

2. OBSERVATIONS AND REDUCTION

Observations of Leo A were obtained at the WIYN 3.5 m telescope on the nights of 20–22 December 2000, using the MIMO camera (described by Saha et al. (2000). Our observations are summarized in Table 1. The MIMO camera contains two 2K × 4K chips, separated by 10″. Because of its

TABLE 1
OBSERVATION LOG

Image ID	HJD (−2,451,000+)	Exposure Time (s)	Filter	Air Mass	Seeing[a]
n1080.....	899.7859	1800	*V*	1.90	0.86
n1083.....	899.8156	1800	*V*	1.54	0.77
n1084.....	899.8390	1800	*V*	1.36	0.81
n1085.....	899.8623	1800	*V*	1.23	0.68
n1086.....	899.8861	1800	*V*	1.14	0.58
n1089.....	899.9353	1800	*V*	1.03	0.66
n1095.....	900.0157	1800	*V*	1.02	0.65
n1096.....	900.0390	1800	*V*	1.05	0.81
n2081.....	900.7897	1800	*V*	1.81	1.01
n2082.....	900.8130	1800	*V*	1.54	0.88
n2083.....	900.8367	1200	*R*	1.36	0.79
n2085.....	900.8577	1200	*R*	1.24	0.72
n2086.....	900.8742	1800	*V*	1.17	0.72
n2087.....	900.8975	1800	*V*	1.10	0.71
n2088.....	900.9210	1200	*R*	1.05	0.72
n2089.....	900.9374	1200	*V*	1.02	0.79
n2098.....	901.0233	1200	*V*	1.03	0.75
n2099.....	901.0397	1500	*V*	1.06	0.75
n3060.....	901.7571	1800	*V*	2.36	0.96
n3061.....	901.7804	1800	*V*	1.90	0.76
n3063.....	901.8102	1200	*R*	1.54	0.66
n3064.....	901.8266	1200	*R*	1.41	0.58
n3065.....	901.8429	1800	*V*	1.30	0.54
n3066.....	901.8662	1800	*V*	1.19	0.51
n3068.....	901.9130	1800	*V*	1.05	0.57
n3069.....	901.9364	1200	*V*	1.02	0.61
n3074.....	902.0052	1800	*V*	1.02	0.53
n3075.....	902.0286	1800	*V*	1.05	0.55

[a] Seeing values taken from our PSF-fitting photometry.

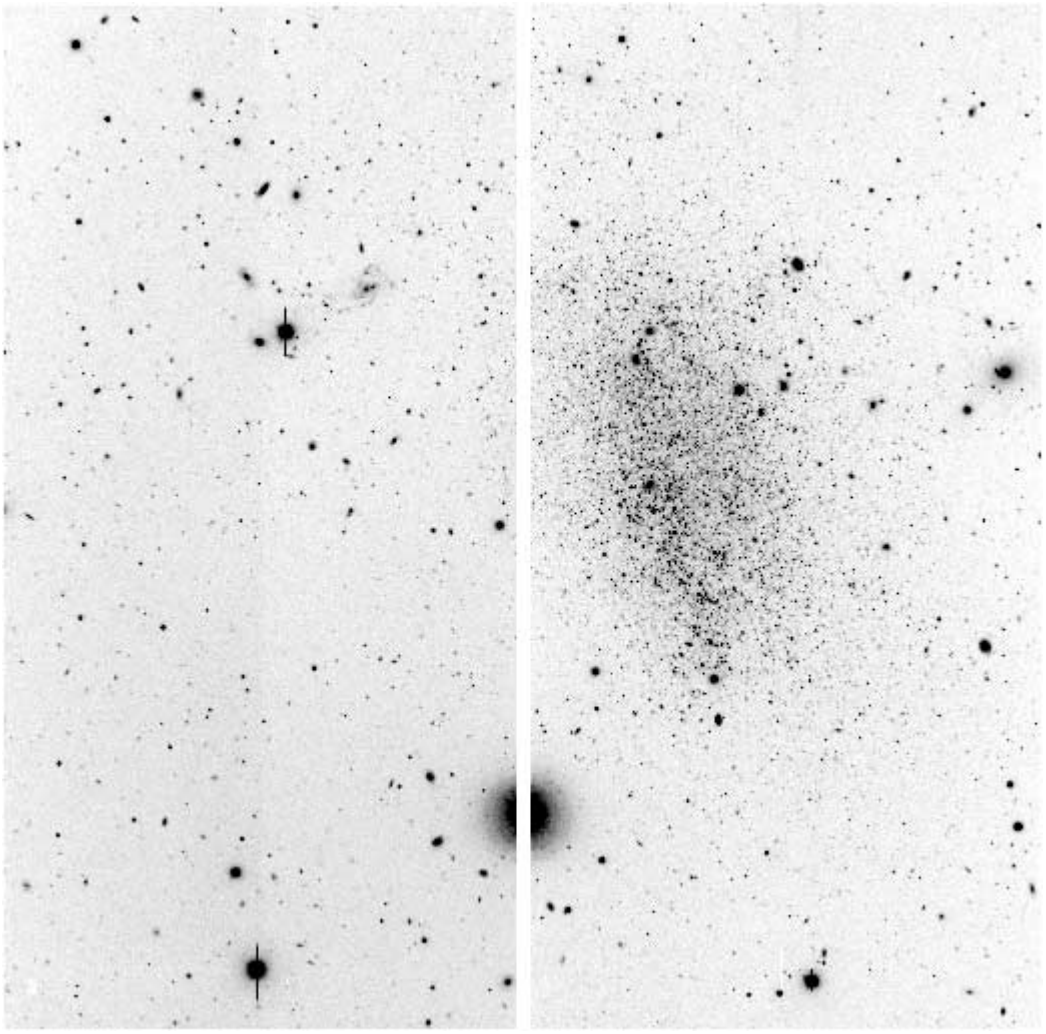

FIG. 1.—Combined *V* image of Leo A. North is to the left, and east is down. Each chip contains 2048 × 4096 pixels, with a scale of 0.″141 pixel^{-1}. The field is 9.′6 on a side.

size, shape, and orientation, Leo A fits completely on chip 2, allowing us to "hide" a bright star in the gap between the chips and obtain a halo field on chip 1. A deep *V* image is shown in Figure 1. Because of scheduling limitations, Leo A rose during the middle of the night, restricting our observing to a 6.5 hr window between its rise and morning twilight.

As indicated in Table 1, we had subarcsecond seeing for the entire run, with seeing as good as 0.″5–0.″6 (excellent image quality is typical at WIYN). This was critical for our project, both in terms of reducing blending and reducing the effective background level. As the RR Lyrae stars were near the limits of our photometry, they could not have been detected with significantly worse seeing.

To ensure a robust final result, the data were processed completely independently by two groups. A. E. D. used his own package, an adaptation of HSTPHOT (Dolphin 2000a), which includes image processing, as well as photometry programs. The reduction algorithms were similar to that implemented in IRAF, but include a more accurate overscan correction algorithm and an algorithm to mask pixels affected by cross talk between the amplifiers of MIMO. Deep frames in *V* and *R* were created by aligning all images for the filter (23 in *V* and five in *R*) to the nearest pixel and co-adding. Photometry was determined for the

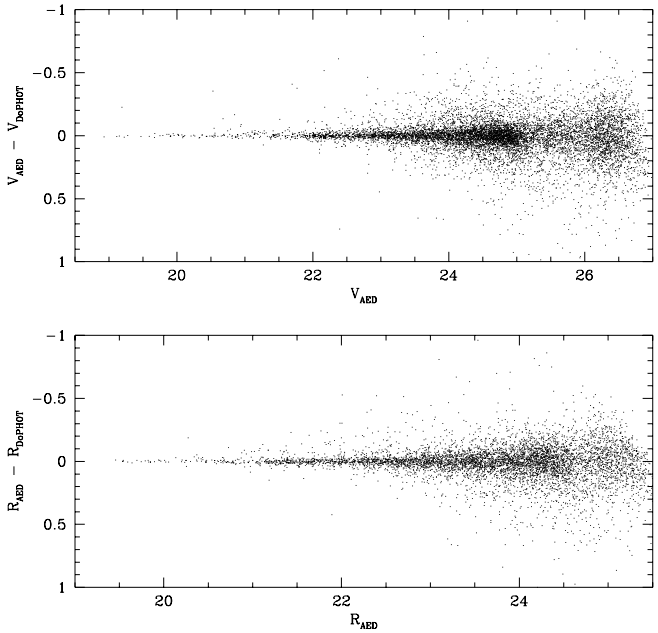

FIG. 2.—Comparison between our two sets of chip 2 deep photometry. We find no systematic differences of note.

TABLE 2

PHOTOMETRY OF VARIABLE STARS

HJD (2,450,000+)	C1-V01	C1-V02	C1-V03	C1-V04	C1-V05	C1-V06	C1-V07
				V			
899.7859.....	25.232 ± 0.241	23.412 ± 0.046	25.307 ± 0.257	24.513 ± 0.124	23.653 ± 0.057	23.864 ± 0.069	25.229 ± 0.241
899.8156.....	...	23.395 ± 0.037	25.549 ± 0.264	24.423 ± 0.094	23.659 ± 0.048	23.259 ± 0.055	25.219 ± 0.193
899.8390.....	25.761 ± 0.344	23.365 ± 0.038	...	23.969 ± 0.066	23.611 ± 0.048	23.683 ± 0.052	25.444 ± 0.252
899.8623.....	25.264 ± 0.162	23.437 ± 0.031	24.607 ± 0.089	23.705 ± 0.040	23.762 ± 0.042	23.436 ± 0.031	25.707 ± 0.243
899.8861.....	24.916 ± 0.094	23.441 ± 0.025	24.640 ± 0.073	23.548 ± 0.028	23.706 ± 0.032	23.246 ± 0.021	25.886 ± 0.227
899.9353.....	...	23.647 ± 0.032	24.563 ± 0.071	23.724 ± 0.033	23.608 ± 0.030	23.076 ± 0.019	25.633 ± 0.187
900.0157.....	...	23.895 ± 0.047	24.740 ± 0.100	23.940 ± 0.048	23.850 ± 0.045	23.164 ± 0.025	25.435 ± 0.188
900.0390.....	...	23.794 ± 0.062	25.021 ± 0.189	24.094 ± 0.081	23.839 ± 0.064	23.244 ± 0.037	...
900.7897.....	...	23.984 ± 0.075	25.170 ± 0.219	23.603 ± 0.053	23.175 ± 0.036	23.572 ± 0.052	...
900.8130.....	25.138 ± 0.177	23.993 ± 0.063	...	23.857 ± 0.056	23.137 ± 0.030	23.635 ± 0.045	25.667 ± 0.289
900.8742.....	25.466 ± 0.184	24.070 ± 0.052	25.498 ± 0.186	23.848 ± 0.043	23.260 ± 0.025	23.653 ± 0.036	25.572 ± 0.201
900.8975.....	25.459 ± 0.167	23.809 ± 0.038	25.078 ± 0.118	23.990 ± 0.045	23.374 ± 0.026	23.724 ± 0.035	25.525 ± 0.178
900.9374.....	...	23.517 ± 0.040	...	24.168 ± 0.073	23.338 ± 0.035	23.731 ± 0.048	...
901.0233.....	24.911 ± 0.132	23.368 ± 0.033	25.720 ± 0.276	24.109 ± 0.064	23.428 ± 0.035	23.816 ± 0.050	...
901.0397.....	...	23.441 ± 0.035	25.245 ± 0.176	24.081 ± 0.062	23.464 ± 0.035	23.711 ± 0.044	...
901.7571.....	...	23.959 ± 0.137	24.732 ± 0.270	...	23.913 ± 0.126	23.134 ± 0.063	...
901.7804.....	...	23.848 ± 0.105	24.806 ± 0.256	23.903 ± 0.110	23.824 ± 0.103	23.062 ± 0.052	25.086 ± 0.324
901.8429.....	25.854 ± 0.419	24.001 ± 0.077	25.046 ± 0.199	24.289 ± 0.100	23.962 ± 0.075	23.155 ± 0.036	24.622 ± 0.135
901.8662.....	25.200 ± 0.286	24.123 ± 0.107	24.876 ± 0.214	24.286 ± 0.124	24.018 ± 0.098	23.219 ± 0.048	...
901.9130.....	25.503 ± 0.259	23.864 ± 0.059	...	24.415 ± 0.097	24.023 ± 0.067	23.198 ± 0.033	25.000 ± 0.164
901.9364.....	25.784 ± 0.286	23.981 ± 0.056	25.032 ± 0.143	24.350 ± 0.077	23.954 ± 0.055	23.400 ± 0.033	25.154 ± 0.159
902.0052.....	25.176 ± 0.146	23.984 ± 0.050	25.153 ± 0.141	24.230 ± 0.061	23.691 ± 0.038	23.609 ± 0.036	25.616 ± 0.214
902.0286.....	25.359 ± 0.156	24.065 ± 0.049	25.195 ± 0.135	24.396 ± 0.065	23.640 ± 0.033	23.614 ± 0.033	25.796 ± 0.234
				R			
900.8367.....	25.180 ± 0.254	23.827 ± 0.074	...	23.767 ± 0.070	22.888 ± 0.032	23.533 ± 0.057	25.051 ± 0.225
900.8577.....	...	23.676 ± 0.063	24.865 ± 0.187	23.612 ± 0.060	22.936 ± 0.033	23.587 ± 0.059	24.967 ± 0.205
900.9210.....	25.434 ± 0.280	23.476 ± 0.047	...	23.879 ± 0.068	23.022 ± 0.031	23.615 ± 0.054	...
901.8102.....	25.077 ± 0.377	23.898 ± 0.127	24.792 ± 0.288	24.078 ± 0.150	23.407 ± 0.082	22.946 ± 0.054	...
901.8266.....	24.609 ± 0.260	23.532 ± 0.097	24.586 ± 0.255	23.745 ± 0.118	23.536 ± 0.097	22.999 ± 0.060	...

HJD (2,450,000+)	C1-V08	C1-V09	C1-V10	C2-V01	C2-V02	C2-V03	C2-V04
				V			
899.7859.....	...	23.788 ± 0.065	23.094 ± 0.034	22.892 ± 0.029	23.779 ± 0.065	23.254 ± 0.040	22.894 ± 0.029
899.8156.....	24.122 ± 0.072	23.989 ± 0.064	23.221 ± 0.032	22.728 ± 0.021	23.803 ± 0.055	23.351 ± 0.037	22.993 ± 0.027
899.8390.....	23.951 ± 0.066	24.053 ± 0.072	23.288 ± 0.036	22.687 ± 0.022	23.886 ± 0.063	23.506 ± 0.045	23.050 ± 0.030
899.8623.....	24.069 ± 0.055	24.062 ± 0.055	23.289 ± 0.028	22.606 ± 0.016	23.711 ± 0.041	23.530 ± 0.035	23.155 ± 0.025
899.8861.....	23.950 ± 0.039	23.791 ± 0.035	23.321 ± 0.023	22.619 ± 0.013	23.758 ± 0.034	23.677 ± 0.032	23.209 ± 0.021
899.9353.....	23.740 ± 0.034	23.270 ± 0.023	23.377 ± 0.025	22.593 ± 0.040	23.800 ± 0.036	23.618 ± 0.031	23.280 ± 0.023
900.0157.....	23.641 ± 0.037	23.403 ± 0.031	23.461 ± 0.032	22.855 ± 0.019	23.591 ± 0.037	23.941 ± 0.050	23.347 ± 0.030
900.0390.....	23.571 ± 0.050	23.538 ± 0.049	23.594 ± 0.052	22.941 ± 0.030	23.401 ± 0.045	23.874 ± 0.068	23.358 ± 0.043
900.7897.....	23.702 ± 0.058	23.788 ± 0.063	23.674 ± 0.057	22.657 ± 0.024	23.106 ± 0.035	23.696 ± 0.060	23.008 ± 0.032
900.8130.....	23.605 ± 0.044	23.297 ± 0.046	23.649 ± 0.047	22.707 ± 0.020	23.204 ± 0.032	23.696 ± 0.049	22.848 ± 0.024
900.8742.....	23.610 ± 0.034	23.229 ± 0.026	23.221 ± 0.024	22.849 ± 0.018	23.432 ± 0.030	23.656 ± 0.036	23.013 ± 0.021
900.8975.....	23.583 ± 0.031	23.425 ± 0.027	23.162 ± 0.022	22.923 ± 0.018	23.472 ± 0.029	23.600 ± 0.033	23.031 ± 0.020
900.9374.....	23.507 ± 0.040	23.494 ± 0.040	23.166 ± 0.030	22.948 ± 0.026	23.414 ± 0.038	23.539 ± 0.044	23.050 ± 0.028
901.0233.....	23.554 ± 0.040	23.759 ± 0.048	23.345 ± 0.033	23.162 ± 0.029	23.707 ± 0.047	...	23.318 ± 0.033
901.0397.....	23.576 ± 0.039	23.783 ± 0.048	23.350 ± 0.032	23.187 ± 0.028	23.692 ± 0.044	23.686 ± 0.044	23.324 ± 0.032
901.7571.....	23.609 ± 0.097	23.254 ± 0.070	23.743 ± 0.109	22.962 ± 0.056	...	23.606 ± 0.102	23.411 ± 0.086
901.7804.....	23.313 ± 0.065	23.398 ± 0.071	23.858 ± 0.107	22.999 ± 0.051	24.008 ± 0.127	23.986 ± 0.124	23.581 ± 0.086
901.8429.....	23.529 ± 0.050	23.506 ± 0.050	23.803 ± 0.065	23.100 ± 0.035	23.912 ± 0.073	23.971 ± 0.077	23.306 ± 0.042
901.8662.....	23.466 ± 0.060	23.580 ± 0.067	23.661 ± 0.071	23.073 ± 0.043	23.870 ± 0.087	24.023 ± 0.101	22.935 ± 0.038
901.9130.....	23.635 ± 0.048	23.668 ± 0.049	23.671 ± 0.050	23.176 ± 0.033	23.735 ± 0.053	23.938 ± 0.064	22.841 ± 0.024
901.9364.....	23.592 ± 0.040	23.801 ± 0.048	23.731 ± 0.045	23.152 ± 0.028	23.747 ± 0.046	23.893 ± 0.053	22.945 ± 0.023
902.0052.....	23.762 ± 0.041	23.935 ± 0.047	23.197 ± 0.025	23.330 ± 0.028	23.252 ± 0.026	23.792 ± 0.043	23.158 ± 0.024
902.0286.....	23.819 ± 0.039	23.849 ± 0.040	23.109 ± 0.021	23.296 ± 0.025	23.142 ± 0.022	23.543 ± 0.031	23.185 ± 0.023
				R			
900.8367.....	23.352 ± 0.048	23.051 ± 0.037	23.190 ± 0.041	22.527 ± 0.024	23.091 ± 0.040	23.457 ± 0.055	22.695 ± 0.028
900.8577.....	23.326 ± 0.046	23.145 ± 0.040	23.136 ± 0.039	22.631 ± 0.026	23.049 ± 0.037	23.485 ± 0.056	22.712 ± 0.028
900.9210.....	23.488 ± 0.048	23.265 ± 0.039	22.855 ± 0.027	22.718 ± 0.026	23.184 ± 0.039	23.207 ± 0.041	22.738 ± 0.027
901.8102.....	23.428 ± 0.083	23.386 ± 0.080	23.512 ± 0.090	22.715 ± 0.044	23.593 ± 0.098	23.573 ± 0.096	23.409 ± 0.083
901.8266.....	23.342 ± 0.082	23.340 ± 0.082	23.360 ± 0.084	22.840 ± 0.053	23.553 ± 0.101	23.570 ± 0.103	23.305 ± 0.081

TABLE 2—*Continued*

HJD (2,450,000+)	C2-V05	C2-V06	C2-V07	C2-V08	C2-V09	C2-V10	C2-V11
				V			
899.7859.....	23.816 ± 0.067	23.786 ± 0.065	23.970 ± 0.077	23.296 ± 0.042	23.691 ± 0.061	23.041 ± 0.034	22.654 ± 0.024
899.8156.....	23.715 ± 0.051	23.757 ± 0.053	24.050 ± 0.069	23.339 ± 0.036	23.646 ± 0.048	23.117 ± 0.030	22.713 ± 0.021
899.8390.....	24.165 ± 0.083	23.744 ± 0.056	23.938 ± 0.067	23.164 ± 0.033	23.756 ± 0.056	23.124 ± 0.032	22.856 ± 0.026
899.8623.....	23.804 ± 0.045	23.804 ± 0.045	24.054 ± 0.055	23.264 ± 0.027	23.589 ± 0.037	23.164 ± 0.025	22.880 ± 0.020
899.8861.....	23.800 ± 0.035	23.725 ± 0.033	23.872 ± 0.037	23.271 ± 0.022	23.668 ± 0.031	23.229 ± 0.021	22.971 ± 0.017
899.9353.....	23.870 ± 0.038	23.540 ± 0.029	23.617 ± 0.031	23.204 ± 0.022	23.622 ± 0.031	23.324 ± 0.024	23.111 ± 0.020
900.0157.....	23.858 ± 0.047	23.268 ± 0.028	23.418 ± 0.032	23.257 ± 0.027	23.703 ± 0.041	23.291 ± 0.028	23.272 ± 0.028
900.0390.....	23.818 ± 0.065	23.185 ± 0.037	23.449 ± 0.047	23.230 ± 0.039	23.683 ± 0.058	23.398 ± 0.045	23.358 ± 0.043
900.7897.....	23.644 ± 0.057	23.584 ± 0.053	23.802 ± 0.065	22.730 ± 0.025	23.502 ± 0.050	23.320 ± 0.042	22.700 ± 0.025
900.8130.....	23.916 ± 0.060	23.532 ± 0.043	23.656 ± 0.047	22.784 ± 0.022	23.478 ± 0.041	23.318 ± 0.035	22.670 ± 0.020
900.8742.....	23.750 ± 0.039	23.544 ± 0.033	23.516 ± 0.032	22.828 ± 0.018	23.542 ± 0.033	23.490 ± 0.031	22.862 ± 0.018
900.8975.....	23.723 ± 0.036	23.703 ± 0.036	23.428 ± 0.028	22.913 ± 0.018	23.580 ± 0.032	23.462 ± 0.029	22.909 ± 0.018
900.9374.....	23.975 ± 0.065	23.637 ± 0.047	23.599 ± 0.046	22.910 ± 0.025	23.663 ± 0.048	23.421 ± 0.039	22.961 ± 0.026
901.0233.....	23.754 ± 0.049	23.801 ± 0.050	23.721 ± 0.046	22.976 ± 0.024	23.606 ± 0.042	23.359 ± 0.034	23.380 ± 0.035
901.0397.....	23.834 ± 0.050	23.693 ± 0.044	23.668 ± 0.043	23.019 ± 0.024	23.699 ± 0.045	23.434 ± 0.035	23.329 ± 0.032
901.7571.....	23.130 ± 0.066	23.836 ± 0.126	23.359 ± 0.081	23.340 ± 0.081	23.154 ± 0.068	23.241 ± 0.073	23.080 ± 0.064
901.7804.....	23.231 ± 0.063	23.688 ± 0.095	23.335 ± 0.069	23.387 ± 0.072	23.211 ± 0.062	23.534 ± 0.083	22.770 ± 0.041
901.8429.....	23.484 ± 0.050	23.844 ± 0.068	23.541 ± 0.052	23.231 ± 0.039	23.390 ± 0.046	23.445 ± 0.048	22.681 ± 0.025
901.8662.....	23.472 ± 0.062	23.889 ± 0.089	23.730 ± 0.078	23.344 ± 0.054	23.378 ± 0.056	23.311 ± 0.053	22.710 ± 0.031
901.9130.....	23.501 ± 0.043	23.773 ± 0.055	23.740 ± 0.054	23.311 ± 0.037	23.337 ± 0.038	23.073 ± 0.030	22.877 ± 0.025
901.9364.....	23.566 ± 0.040	23.665 ± 0.043	23.795 ± 0.048	23.238 ± 0.030	23.447 ± 0.036	22.972 ± 0.024	22.984 ± 0.024
902.0052.....	23.699 ± 0.039	23.497 ± 0.033	23.916 ± 0.047	23.352 ± 0.029	23.470 ± 0.032	22.843 ± 0.019	23.208 ± 0.026
902.0286.....	23.769 ± 0.039	23.345 ± 0.027	23.625 ± 0.050	23.199 ± 0.024	23.491 ± 0.030	22.845 ± 0.017	23.245 ± 0.024
				R			
900.8367.....	23.110 ± 0.041	23.259 ± 0.046	23.233 ± 0.045	22.555 ± 0.025	23.125 ± 0.041	23.068 ± 0.039	22.591 ± 0.026
900.8577.....	23.293 ± 0.047	23.371 ± 0.050	23.199 ± 0.043	22.588 ± 0.025	23.177 ± 0.042	23.058 ± 0.038	22.655 ± 0.027
900.9210.....	23.285 ± 0.044	23.281 ± 0.043	23.235 ± 0.041	22.601 ± 0.024	23.164 ± 0.039	23.126 ± 0.038	22.746 ± 0.027
901.8102.....	23.121 ± 0.064	23.722 ± 0.110	23.384 ± 0.081	22.943 ± 0.054	22.936 ± 0.054	23.118 ± 0.063	22.599 ± 0.040
901.8266.....	23.066 ± 0.065	23.504 ± 0.097	23.356 ± 0.085	23.032 ± 0.063	23.020 ± 0.063	23.221 ± 0.075	22.624 ± 0.044

HJD (2,450,000+)	C2-V12	C2-V13	C2-V14	C2-V15	C2-V16	C2-V17	C2-V18
				V			
899.7859.....	24.023 ± 0.081	23.530 ± 0.052	24.052 ± 0.083	24.342 ± 0.108	23.219 ± 0.039	22.701 ± 0.025	23.198 ± 0.039
899.8156.....	23.793 ± 0.055	23.346 ± 0.037	24.071 ± 0.070	24.311 ± 0.087	23.119 ± 0.030	22.644 ± 0.020	23.203 ± 0.032
899.8390.....	23.859 ± 0.061	23.324 ± 0.038	24.160 ± 0.082	24.331 ± 0.094	23.130 ± 0.032	22.730 ± 0.026	23.304 ± 0.038
899.8623.....	24.066 ± 0.056	23.280 ± 0.028	23.950 ± 0.051	23.909 ± 0.049	23.019 ± 0.023	22.729 ± 0.017	23.401 ± 0.031
899.8861.....	24.011 ± 0.042	23.356 ± 0.024	24.016 ± 0.043	23.590 ± 0.029	22.972 ± 0.017	22.814 ± 0.015	23.424 ± 0.026
899.9353.....	23.477 ± 0.027	23.387 ± 0.025	23.661 ± 0.032	23.448 ± 0.026	22.970 ± 0.018	22.922 ± 0.017	23.499 ± 0.028
900.0157.....	23.019 ± 0.022	...	23.583 ± 0.037	23.637 ± 0.038	22.939 ± 0.021	23.010 ± 0.022	23.687 ± 0.040
900.0390.....	23.104 ± 0.034	23.720 ± 0.060	23.762 ± 0.062	23.685 ± 0.058	23.053 ± 0.033	23.011 ± 0.032	23.548 ± 0.051
900.7897.....	24.020 ± 0.080	23.819 ± 0.067	24.219 ± 0.095	24.235 ± 0.096	23.026 ± 0.033	23.577 ± 0.054	23.749 ± 0.062
900.8130.....	24.123 ± 0.073	23.757 ± 0.053	24.043 ± 0.067	23.751 ± 0.051	23.098 ± 0.029	23.659 ± 0.047	23.731 ± 0.051
900.8742.....	23.946 ± 0.047	23.748 ± 0.040	23.681 ± 0.037	23.406 ± 0.029	23.195 ± 0.024	23.656 ± 0.036	23.406 ± 0.029
900.8975.....	23.989 ± 0.046	23.768 ± 0.038	23.540 ± 0.031	23.444 ± 0.028	23.190 ± 0.023	23.610 ± 0.032	23.247 ± 0.024
900.9374.....	24.292 ± 0.085	23.616 ± 0.047	23.567 ± 0.045	23.664 ± 0.048	23.207 ± 0.032	23.653 ± 0.048	23.080 ± 0.029
901.0233.....	23.205 ± 0.029	23.704 ± 0.046	23.721 ± 0.047	23.884 ± 0.053	23.398 ± 0.035	23.778 ± 0.049	23.251 ± 0.031
901.0397.....	23.074 ± 0.026	23.659 ± 0.043	23.821 ± 0.050	23.887 ± 0.053	23.241 ± 0.030	23.698 ± 0.044	23.275 ± 0.031
901.7571.....	24.064 ± 0.157	23.100 ± 0.065	...	23.739 ± 0.115	23.245 ± 0.074	23.351 ± 0.081	23.503 ± 0.092
901.7804.....	23.864 ± 0.113	23.257 ± 0.064	23.698 ± 0.096	23.574 ± 0.086	23.292 ± 0.066	23.423 ± 0.075	23.393 ± 0.073
901.8429.....	23.876 ± 0.071	23.421 ± 0.047	23.593 ± 0.055	23.512 ± 0.051	23.440 ± 0.048	23.504 ± 0.051	23.768 ± 0.064
901.8662.....	24.045 ± 0.103	23.418 ± 0.058	23.670 ± 0.074	23.484 ± 0.062	23.436 ± 0.059	23.557 ± 0.066	23.665 ± 0.073
901.9130.....	23.873 ± 0.060	23.516 ± 0.044	23.541 ± 0.045	23.551 ± 0.045	23.413 ± 0.040	23.517 ± 0.044	23.692 ± 0.051
901.9364.....	23.871 ± 0.051	23.471 ± 0.036	23.632 ± 0.042	...	23.376 ± 0.033	23.574 ± 0.040	23.773 ± 0.047
902.0052.....	24.004 ± 0.051	23.788 ± 0.043	23.876 ± 0.046	23.835 ± 0.044	23.324 ± 0.028	23.624 ± 0.036	23.729 ± 0.040
902.0286.....	24.004 ± 0.047	23.768 ± 0.039	23.875 ± 0.042	23.874 ± 0.042	23.207 ± 0.024	23.544 ± 0.032	23.686 ± 0.036
				R			
900.8367.....	23.585 ± 0.062	23.643 ± 0.065	23.540 ± 0.059	23.432 ± 0.054	22.892 ± 0.033	23.184 ± 0.043	23.410 ± 0.053
900.8577.....	23.481 ± 0.055	23.610 ± 0.062	23.579 ± 0.061	23.265 ± 0.046	22.893 ± 0.033	23.206 ± 0.043	23.318 ± 0.048
900.9210.....	23.576 ± 0.056	23.566 ± 0.056	23.244 ± 0.042	23.279 ± 0.043	22.950 ± 0.032	23.308 ± 0.044	22.864 ± 0.030
901.8102.....	23.661 ± 0.104	23.130 ± 0.065	23.425 ± 0.084	23.337 ± 0.077	23.005 ± 0.057	23.271 ± 0.073	23.492 ± 0.089
901.8266.....	23.260 ± 0.077	23.187 ± 0.073	23.231 ± 0.076	23.262 ± 0.078	23.173 ± 0.072	23.014 ± 0.062	23.511 ± 0.097

TABLE 2—*Continued*

HJD (2,450,000+)	C2-V19	C2-V20	C2-V21	C2-V22	C2-V23	C2-V24	C2-V25
				V			
899.7859.....	23.545 ± 0.053	23.939 ± 0.077	23.489 ± 0.050	22.989 ± 0.032	23.579 ± 0.056	23.426 ± 0.048	23.150 ± 0.038
899.8156.....	23.469 ± 0.041	23.812 ± 0.056	23.513 ± 0.042	22.913 ± 0.025	23.569 ± 0.045	23.467 ± 0.041	23.031 ± 0.028
899.8390.....	23.406 ± 0.042	23.901 ± 0.065	23.541 ± 0.046	23.028 ± 0.030	23.557 ± 0.048	23.207 ± 0.035	22.863 ± 0.026
899.8623.....	23.435 ± 0.032	24.156 ± 0.061	23.630 ± 0.038	22.932 ± 0.021	23.578 ± 0.037	22.989 ± 0.022	22.445 ± 0.014
899.8861.....	23.329 ± 0.024	23.933 ± 0.040	23.649 ± 0.031	22.891 ± 0.017	23.541 ± 0.029	23.009 ± 0.018	22.247 ± 0.010
899.9353.....	23.089 ± 0.020	23.924 ± 0.040	23.681 ± 0.033	22.600 ± 0.013	23.615 ± 0.031	23.050 ± 0.019	22.148 ± 0.009
900.0157.....	22.713 ± 0.017	23.789 ± 0.045	23.587 ± 0.037	21.839 ± 0.009	23.635 ± 0.039	23.300 ± 0.029	22.263 ± 0.012
900.0390.....	22.713 ± 0.024	24.157 ± 0.089	23.689 ± 0.059	21.785 ± 0.011	23.294 ± 0.041	23.223 ± 0.038	22.420 ± 0.019
900.7897.....	22.916 ± 0.030	23.368 ± 0.044	23.229 ± 0.039	22.834 ± 0.028	23.167 ± 0.037	23.076 ± 0.034	23.458 ± 0.049
900.8130.....	22.866 ± 0.024	23.435 ± 0.040	23.223 ± 0.032	22.824 ± 0.023	23.089 ± 0.029	23.026 ± 0.027	23.245 ± 0.034
900.8742.....	22.715 ± 0.016	23.552 ± 0.033	23.061 ± 0.022	22.897 ± 0.019	23.200 ± 0.025	23.075 ± 0.022	23.317 ± 0.027
900.8975.....	22.729 ± 0.016	23.498 ± 0.030	23.092 ± 0.021	22.887 ± 0.018	23.293 ± 0.026	23.106 ± 0.021	23.215 ± 0.024
900.9374.....	22.720 ± 0.022	23.577 ± 0.045	23.123 ± 0.030	22.887 ± 0.025	23.263 ± 0.035	23.272 ± 0.034	23.159 ± 0.032
901.0233.....	22.996 ± 0.025	23.669 ± 0.045	23.345 ± 0.034	22.910 ± 0.023	23.327 ± 0.034	23.366 ± 0.034	23.261 ± 0.032
901.0397.....	22.979 ± 0.024	23.757 ± 0.047	23.401 ± 0.034	22.944 ± 0.023	23.490 ± 0.037	23.406 ± 0.034	23.320 ± 0.032
901.7571.....	22.872 ± 0.052	23.608 ± 0.102	23.802 ± 0.122	21.762 ± 0.020	23.655 ± 0.107	22.871 ± 0.052	23.149 ± 0.068
901.7804.....	22.879 ± 0.046	23.755 ± 0.102	23.881 ± 0.114	21.767 ± 0.017	...	23.047 ± 0.053	23.009 ± 0.052
901.8429.....	23.062 ± 0.034	23.895 ± 0.072	23.742 ± 0.063	21.971 ± 0.014	23.297 ± 0.042	23.288 ± 0.042	23.247 ± 0.040
901.8662.....	23.068 ± 0.043	23.891 ± 0.090	23.639 ± 0.071	22.073 ± 0.018	22.957 ± 0.039	23.208 ± 0.048	23.141 ± 0.046
901.9130.....	23.120 ± 0.031	23.918 ± 0.063	23.690 ± 0.051	22.129 ± 0.014	22.712 ± 0.022	23.290 ± 0.036	23.200 ± 0.034
901.9364.....	23.186 ± 0.029	23.767 ± 0.047	23.673 ± 0.043	22.147 ± 0.012	22.620 ± 0.018	23.279 ± 0.031	23.188 ± 0.029
902.0052.....	23.259 ± 0.027	23.688 ± 0.039	23.648 ± 0.038	22.318 ± 0.012	22.849 ± 0.019	23.437 ± 0.031	23.257 ± 0.027
902.0286.....	23.291 ± 0.026	23.638 ± 0.035	23.550 ± 0.032	22.322 ± 0.012	22.890 ± 0.018	23.412 ± 0.028	23.273 ± 0.025
				R			
900.8367.....	22.628 ± 0.027	23.289 ± 0.048	22.959 ± 0.036	22.488 ± 0.024	22.979 ± 0.037	22.702 ± 0.028	22.969 ± 0.036
900.8577.....	22.562 ± 0.025	23.212 ± 0.044	22.920 ± 0.034	22.496 ± 0.024	22.966 ± 0.035	22.761 ± 0.029	22.862 ± 0.032
900.9210.....	22.536 ± 0.023	23.463 ± 0.052	22.899 ± 0.031	22.511 ± 0.022	23.036 ± 0.035	22.889 ± 0.031	22.894 ± 0.031
901.8102.....	22.786 ± 0.047	23.644 ± 0.103	23.310 ± 0.076	21.921 ± 0.022	23.410 ± 0.084	22.876 ± 0.051	22.906 ± 0.053
901.8266.....	22.883 ± 0.055	23.766 ± 0.123	23.317 ± 0.082	21.826 ± 0.022	...	22.929 ± 0.057	22.740 ± 0.049

HJD (2,450,000+)	C2-V26	C2-V27	C2-V28	C2-V29	C2-V30	C2-V31	C2-V32
				V			
899.7859.....	23.917 ± 0.074	23.900 ± 0.073	23.274 ± 0.042	23.336 ± 0.043	23.170 ± 0.038	22.963 ± 0.032	23.397 ± 0.047
899.8156.....	23.780 ± 0.054	23.857 ± 0.057	23.184 ± 0.032	23.096 ± 0.029	23.352 ± 0.037	22.905 ± 0.025	23.283 ± 0.035
899.8390.....	23.849 ± 0.062	23.947 ± 0.067	23.238 ± 0.035	22.946 ± 0.027	23.394 ± 0.042	22.906 ± 0.027	23.238 ± 0.036
899.8623.....	23.880 ± 0.048	24.076 ± 0.057	23.348 ± 0.030	22.983 ± 0.022	23.321 ± 0.029	22.958 ± 0.021	23.213 ± 0.027
899.8861.....	23.864 ± 0.038	23.973 ± 0.041	23.374 ± 0.024	23.040 ± 0.018	23.442 ± 0.026	22.974 ± 0.017	23.031 ± 0.018
899.9353.....	23.798 ± 0.036	23.897 ± 0.039	23.345 ± 0.024	23.151 ± 0.020	23.403 ± 0.026	23.065 ± 0.019	22.899 ± 0.017
900.0157.....	23.712 ± 0.041	23.608 ± 0.037	23.388 ± 0.031	23.265 ± 0.028	23.420 ± 0.032	23.161 ± 0.026	22.772 ± 0.018
900.0390.....	...	23.426 ± 0.046	23.431 ± 0.047	23.248 ± 0.039	23.486 ± 0.049	23.279 ± 0.040	22.900 ± 0.029
900.7897.....	23.397 ± 0.046	23.667 ± 0.058	23.446 ± 0.048	23.483 ± 0.049	23.318 ± 0.043	23.326 ± 0.043	22.880 ± 0.029
900.8130.....	23.457 ± 0.040	23.928 ± 0.060	23.524 ± 0.042	23.509 ± 0.041	23.501 ± 0.042	23.362 ± 0.037	22.838 ± 0.023
900.8742.....	23.588 ± 0.034	24.115 ± 0.055	23.523 ± 0.032	23.489 ± 0.031	23.512 ± 0.032	23.230 ± 0.025	22.961 ± 0.020
900.8975.....	23.551 ± 0.031	24.081 ± 0.050	23.455 ± 0.029	23.451 ± 0.029	23.470 ± 0.029	23.008 ± 0.020	22.959 ± 0.019
900.9374.....	23.819 ± 0.057	23.918 ± 0.060	23.534 ± 0.044	23.359 ± 0.037	23.359 ± 0.037	22.529 ± 0.018	23.035 ± 0.029
901.0233.....	23.841 ± 0.053	23.874 ± 0.054	23.536 ± 0.040	23.001 ± 0.025	23.325 ± 0.034	22.471 ± 0.016	23.264 ± 0.032
901.0397.....	23.750 ± 0.047	23.951 ± 0.056	23.424 ± 0.035	22.982 ± 0.024	23.139 ± 0.028	22.509 ± 0.016	23.319 ± 0.033
901.7571.....	23.661 ± 0.108	23.447 ± 0.089	23.523 ± 0.095	23.109 ± 0.065	23.086 ± 0.064	23.400 ± 0.085	23.014 ± 0.060
901.7804.....	23.681 ± 0.095	23.500 ± 0.080	23.412 ± 0.074	23.192 ± 0.060	23.211 ± 0.062	23.585 ± 0.087	23.289 ± 0.066
901.8429.....	23.766 ± 0.064	23.690 ± 0.060	23.322 ± 0.043	23.424 ± 0.047	23.059 ± 0.034	23.459 ± 0.049	23.237 ± 0.040
901.8662.....	23.789 ± 0.082	23.724 ± 0.077	23.245 ± 0.050	23.386 ± 0.057	22.906 ± 0.037	23.441 ± 0.060	23.259 ± 0.051
901.9130.....	23.387 ± 0.039	23.789 ± 0.056	23.024 ± 0.028	23.393 ± 0.039	22.993 ± 0.028	23.407 ± 0.040	23.400 ± 0.040
901.9364.....	23.307 ± 0.032	23.851 ± 0.051	22.952 ± 0.023	23.483 ± 0.037	23.012 ± 0.025	23.376 ± 0.034	23.344 ± 0.033
902.0052.....	23.349 ± 0.029	23.895 ± 0.046	22.797 ± 0.018	23.443 ± 0.031	23.140 ± 0.024	23.387 ± 0.030	23.377 ± 0.030
902.0286.....	23.414 ± 0.028	24.106 ± 0.052	22.859 ± 0.018	23.475 ± 0.030	23.217 ± 0.024	23.452 ± 0.029	23.482 ± 0.030
				R			
900.8367.....	23.307 ± 0.049	23.572 ± 0.061	23.226 ± 0.045	23.087 ± 0.040	23.240 ± 0.046	23.398 ± 0.054	22.759 ± 0.030
900.8577.....	23.359 ± 0.050	23.675 ± 0.067	23.282 ± 0.046	23.172 ± 0.042	23.258 ± 0.046	23.217 ± 0.044	22.770 ± 0.030
900.9210.....	23.358 ± 0.047	23.622 ± 0.059	23.293 ± 0.044	23.055 ± 0.035	23.335 ± 0.046	22.610 ± 0.024	22.814 ± 0.029
901.8102.....	23.688 ± 0.107	23.341 ± 0.078	23.380 ± 0.081	23.057 ± 0.060	23.196 ± 0.069	23.177 ± 0.068	22.921 ± 0.053
901.8266.....	23.533 ± 0.100	23.400 ± 0.089	23.073 ± 0.065	23.055 ± 0.064	23.177 ± 0.072	23.181 ± 0.072	23.012 ± 0.062

TABLE 2—*Continued*

HJD (2,450,000+)	C2-V33	C2-V34	C2-V35	C2-V36	C2-V37	C2-V38	C2-V39
				V			
899.7859.....	25.114 ± 0.218	23.211 ± 0.039	23.610 ± 0.056	23.901 ± 0.073	23.480 ± 0.050	22.856 ± 0.028	22.551 ± 0.022
899.8156.....	...	23.144 ± 0.031	23.625 ± 0.047	23.823 ± 0.056	23.465 ± 0.041	22.687 ± 0.021	22.535 ± 0.018
899.8390.....	24.996 ± 0.173	23.044 ± 0.030	23.827 ± 0.061	23.765 ± 0.057	23.347 ± 0.040	22.618 ± 0.021	22.573 ± 0.020
899.8623.....	25.004 ± 0.132	23.085 ± 0.024	23.782 ± 0.044	23.832 ± 0.046	23.427 ± 0.032	22.538 ± 0.015	22.601 ± 0.016
899.8861.....	25.297 ± 0.134	23.126 ± 0.020	23.828 ± 0.036	23.872 ± 0.038	23.551 ± 0.029	22.551 ± 0.012	22.667 ± 0.013
899.9353.....	24.975 ± 0.103	23.240 ± 0.022	23.994 ± 0.043	23.934 ± 0.041	23.441 ± 0.026	22.489 ± 0.012	22.703 ± 0.014
900.0157.....	24.931 ± 0.122	23.393 ± 0.031	24.044 ± 0.056	24.151 ± 0.062	23.498 ± 0.034	22.679 ± 0.017	22.855 ± 0.019
900.0390.....	25.109 ± 0.213	23.357 ± 0.044	24.002 ± 0.077	24.239 ± 0.096	23.429 ± 0.046	22.731 ± 0.025	22.871 ± 0.028
900.7897.....	25.468 ± 0.296	23.506 ± 0.050	23.958 ± 0.076	23.621 ± 0.057	23.051 ± 0.034	22.664 ± 0.024	23.462 ± 0.048
900.8130.....	...	23.611 ± 0.046	24.108 ± 0.072	23.440 ± 0.040	23.214 ± 0.033	22.564 ± 0.018	23.436 ± 0.039
900.8742.....	25.298 ± 0.159	23.575 ± 0.034	23.839 ± 0.043	23.729 ± 0.039	23.228 ± 0.025	22.553 ± 0.014	23.395 ± 0.029
900.8975.....	...	23.528 ± 0.031	23.637 ± 0.034	23.657 ± 0.034	23.281 ± 0.025	22.556 ± 0.013	23.322 ± 0.026
900.9374.....	25.171 ± 0.187	23.438 ± 0.040	23.544 ± 0.044	23.858 ± 0.058	23.218 ± 0.033	22.528 ± 0.018	23.365 ± 0.037
901.0233.....	24.901 ± 0.136	23.682 ± 0.046	23.735 ± 0.048	24.171 ± 0.070	23.422 ± 0.036	22.788 ± 0.021	23.410 ± 0.035
901.0397.....	24.719 ± 0.111	23.638 ± 0.042	23.782 ± 0.048	24.065 ± 0.062	23.449 ± 0.036	22.841 ± 0.021	23.345 ± 0.032
901.7571.....	24.570 ± 0.248	23.601 ± 0.102	...	...	22.766 ± 0.048	22.411 ± 0.035	22.899 ± 0.054
901.7804.....	24.814 ± 0.267	23.552 ± 0.085	23.750 ± 0.101	23.867 ± 0.113	22.842 ± 0.044	22.465 ± 0.032	22.982 ± 0.050
901.8429.....	24.562 ± 0.132	23.344 ± 0.044	24.027 ± 0.081	23.632 ± 0.057	23.000 ± 0.032	22.589 ± 0.023	23.081 ± 0.035
901.8662.....	24.551 ± 0.162	23.104 ± 0.044	24.062 ± 0.105	23.618 ± 0.070	22.982 ± 0.040	22.653 ± 0.030	23.117 ± 0.045
901.9130.....	24.494 ± 0.105	23.075 ± 0.030	24.072 ± 0.073	23.750 ± 0.055	23.026 ± 0.029	22.709 ± 0.022	23.091 ± 0.030
901.9364.....	24.854 ± 0.124	23.087 ± 0.027	24.160 ± 0.068	23.836 ± 0.051	23.086 ± 0.026	22.707 ± 0.019	23.138 ± 0.027
902.0052.....	25.008 ± 0.125	23.234 ± 0.026	24.065 ± 0.054	24.011 ± 0.052	23.171 ± 0.025	22.942 ± 0.021	23.172 ± 0.040
902.0286.....	24.978 ± 0.114	23.230 ± 0.024	...	23.992 ± 0.047	23.139 ± 0.022	22.921 ± 0.019	23.232 ± 0.024
				R			
900.8367.....	24.816 ± 0.190	23.247 ± 0.046	23.705 ± 0.069	23.368 ± 0.052	22.788 ± 0.031	22.396 ± 0.022	23.091 ± 0.039
900.8577.....	...	23.191 ± 0.043	23.540 ± 0.059	23.348 ± 0.050	22.784 ± 0.030	22.405 ± 0.022	22.953 ± 0.035
900.9210.....	24.938 ± 0.195	23.284 ± 0.044	23.254 ± 0.043	23.548 ± 0.055	22.768 ± 0.028	22.443 ± 0.021	22.978 ± 0.033
901.8102.....	24.835 ± 0.305	22.985 ± 0.056	23.709 ± 0.109	23.563 ± 0.095	22.693 ± 0.043	22.434 ± 0.034	22.737 ± 0.045
901.8266.....	24.387 ± 0.217	23.104 ± 0.068	23.790 ± 0.126	23.240 ± 0.076	22.739 ± 0.049	22.412 ± 0.036	22.774 ± 0.050

HJD (2,450,000+)	C2-V40	C2-V41	C2-V42	C2-V43	C2-V44	C2-V45	C2-V46
				V			
899.7859.....	23.825 ± 0.068	23.669 ± 0.059	22.454 ± 0.020	23.108 ± 0.036	23.491 ± 0.050	23.173 ± 0.038	24.203 ± 0.098
899.8156.....	23.461 ± 0.041	23.749 ± 0.053	22.417 ± 0.016	23.024 ± 0.028	23.462 ± 0.041	23.032 ± 0.028	23.767 ± 0.054
899.8390.....	23.084 ± 0.031	23.576 ± 0.049	22.388 ± 0.017	23.057 ± 0.030	23.524 ± 0.045	22.977 ± 0.029	23.964 ± 0.068
899.8623.....	22.884 ± 0.020	23.642 ± 0.038	22.450 ± 0.014	22.857 ± 0.020	23.517 ± 0.035	23.022 ± 0.023	23.815 ± 0.046
899.8861.....	22.885 ± 0.016	23.625 ± 0.030	22.417 ± 0.011	22.718 ± 0.014	23.535 ± 0.028	23.031 ± 0.018	23.768 ± 0.035
899.9353.....	22.991 ± 0.018	23.728 ± 0.034	22.427 ± 0.011	22.599 ± 0.013	23.615 ± 0.030	23.145 ± 0.021	23.863 ± 0.039
900.0157.....	23.150 ± 0.025	23.441 ± 0.032	22.412 ± 0.014	22.597 ± 0.016	23.778 ± 0.043	23.328 ± 0.030	23.421 ± 0.032
900.0390.....	23.254 ± 0.040	23.576 ± 0.053	22.378 ± 0.018	22.651 ± 0.023	23.831 ± 0.065	23.463 ± 0.048	23.317 ± 0.042
900.7897.....	23.830 ± 0.067	23.731 ± 0.063	22.205 ± 0.016	23.185 ± 0.038	23.674 ± 0.058	23.618 ± 0.057	23.831 ± 0.067
900.8130.....	23.750 ± 0.053	23.656 ± 0.047	22.216 ± 0.014	23.206 ± 0.032	23.833 ± 0.056	23.486 ± 0.042	...
900.8742.....	23.892 ± 0.044	23.546 ± 0.033	22.222 ± 0.011	23.242 ± 0.026	23.754 ± 0.039	23.674 ± 0.037	23.855 ± 0.044
900.8975.....	23.959 ± 0.045	23.539 ± 0.031	22.254 ± 0.011	23.154 ± 0.023	23.722 ± 0.036	23.645 ± 0.034	23.788 ± 0.039
900.9374.....	23.856 ± 0.058	23.447 ± 0.040	22.213 ± 0.014	23.047 ± 0.029	23.735 ± 0.052	23.646 ± 0.048	23.764 ± 0.054
901.0233.....	22.871 ± 0.022	23.138 ± 0.028	22.350 ± 0.015	23.201 ± 0.030	23.289 ± 0.032	23.533 ± 0.040	23.832 ± 0.052
901.0397.....	22.822 ± 0.021	23.151 ± 0.028	22.340 ± 0.014	23.170 ± 0.028	23.185 ± 0.028	23.560 ± 0.040	23.741 ± 0.046
901.7571.....	24.324 ± 0.198	23.632 ± 0.105	22.424 ± 0.036	22.773 ± 0.049	23.388 ± 0.084	23.073 ± 0.064	23.960 ± 0.141
901.7804.....	23.744 ± 0.100	23.737 ± 0.099	22.367 ± 0.029	22.818 ± 0.043	23.301 ± 0.067	23.185 ± 0.061	23.726 ± 0.098
901.8429.....	23.828 ± 0.067	23.358 ± 0.044	22.369 ± 0.019	22.900 ± 0.030	23.087 ± 0.035	22.983 ± 0.032	23.269 ± 0.041
901.8662.....	23.748 ± 0.079	23.225 ± 0.049	22.334 ± 0.023	22.989 ± 0.040	23.065 ± 0.043	23.019 ± 0.041	23.253 ± 0.051
901.9130.....	23.928 ± 0.063	23.154 ± 0.032	21.858 ± 0.011	22.973 ± 0.028	23.144 ± 0.032	23.067 ± 0.030	23.369 ± 0.039
901.9364.....	23.798 ± 0.048	23.079 ± 0.026	21.765 ± 0.011	22.952 ± 0.024	23.162 ± 0.028	23.166 ± 0.028	23.541 ± 0.039
902.0052.....	23.757 ± 0.041	23.099 ± 0.023	21.714 ± 0.008	23.061 ± 0.023	23.285 ± 0.027	23.369 ± 0.029	23.558 ± 0.035
902.0286.....	23.910 ± 0.044	23.091 ± 0.021	21.728 ± 0.007	22.977 ± 0.020	23.412 ± 0.028	23.394 ± 0.028	23.608 ± 0.034
				R			
900.8367.....	23.376 ± 0.052	23.232 ± 0.045	21.881 ± 0.014	22.745 ± 0.030	23.511 ± 0.058	23.411 ± 0.054	23.396 ± 0.053
900.8577.....	23.456 ± 0.054	23.343 ± 0.050	21.904 ± 0.014	22.780 ± 0.030	23.562 ± 0.059	23.317 ± 0.049	23.620 ± 0.063
900.9210.....	23.468 ± 0.051	23.175 ± 0.040	21.827 ± 0.012	22.719 ± 0.027	23.481 ± 0.052	23.234 ± 0.042	23.332 ± 0.046
901.8102.....	23.385 ± 0.081	23.310 ± 0.076	22.075 ± 0.025	22.607 ± 0.040	22.978 ± 0.056	22.920 ± 0.053	23.277 ± 0.074
901.8266.....	23.854 ± 0.133	23.299 ± 0.080	22.086 ± 0.027	22.620 ± 0.044	22.979 ± 0.060	22.783 ± 0.051	23.109 ± 0.068

TABLE 2—*Continued*

HJD (2,450,000+)	C2-V47	C2-V48	C2-V49	C2-V50	C2-V51	C2-V52	C2-V53
				V			
899.7859.....	23.189 ± 0.038	23.750 ± 0.064	24.409 ± 0.115	23.455 ± 0.049	23.746 ± 0.063	23.859 ± 0.071	23.589 ± 0.055
899.8156.....	23.135 ± 0.030	23.789 ± 0.055	23.693 ± 0.068	23.480 ± 0.041	23.595 ± 0.046	23.806 ± 0.055	23.677 ± 0.050
899.8390.....	23.102 ± 0.032	23.819 ± 0.060	23.989 ± 0.070	23.631 ± 0.051	23.647 ± 0.051	23.863 ± 0.062	23.673 ± 0.052
899.8623.....	23.168 ± 0.025	23.792 ± 0.045	23.983 ± 0.052	23.597 ± 0.037	23.725 ± 0.041	23.866 ± 0.047	23.789 ± 0.044
899.8861.....	23.197 ± 0.021	23.777 ± 0.035	23.992 ± 0.042	23.657 ± 0.031	23.770 ± 0.034	23.900 ± 0.038	23.752 ± 0.034
899.9353.....	23.313 ± 0.024	23.739 ± 0.034	24.059 ± 0.046	23.748 ± 0.035	23.818 ± 0.036	23.808 ± 0.036	23.964 ± 0.042
900.0157.....	23.385 ± 0.031	23.498 ± 0.034	23.347 ± 0.030	23.827 ± 0.046	22.918 ± 0.020	23.795 ± 0.044	24.001 ± 0.054
900.0390.....	23.433 ± 0.046	23.516 ± 0.050	23.159 ± 0.036	23.877 ± 0.069	22.782 ± 0.026	23.848 ± 0.068	23.882 ± 0.070
900.7897.....	23.738 ± 0.062	23.637 ± 0.057	23.810 ± 0.067	23.537 ± 0.053	23.671 ± 0.057	23.780 ± 0.064	24.087 ± 0.086
900.8130.....	23.802 ± 0.054	23.624 ± 0.047	24.261 ± 0.083	23.534 ± 0.043	23.732 ± 0.050	23.771 ± 0.052	24.024 ± 0.068
900.8742.....	23.831 ± 0.042	23.783 ± 0.041	23.519 ± 0.033	23.710 ± 0.038	23.719 ± 0.038	23.700 ± 0.037	23.931 ± 0.047
900.8975.....	23.772 ± 0.038	23.615 ± 0.033	23.318 ± 0.026	23.769 ± 0.038	23.737 ± 0.036	23.603 ± 0.033	23.809 ± 0.040
900.9374.....	23.695 ± 0.049	23.779 ± 0.054	22.730 ± 0.074	23.781 ± 0.055	23.663 ± 0.048	23.297 ± 0.035	23.673 ± 0.050
901.0233.....	23.284 ± 0.032	23.442 ± 0.096	23.480 ± 0.038	...	23.686 ± 0.046	23.443 ± 0.036	23.546 ± 0.041
901.0397.....	23.154 ± 0.028	23.784 ± 0.048	23.511 ± 0.038	23.899 ± 0.054	23.579 ± 0.040	23.527 ± 0.038	23.755 ± 0.047
901.7571.....	23.723 ± 0.113	23.795 ± 0.121	23.232 ± 0.073	23.453 ± 0.090	23.296 ± 0.077	...	23.686 ± 0.110
901.7804.....	23.634 ± 0.091	23.541 ± 0.084	23.078 ± 0.055	23.460 ± 0.078	23.417 ± 0.074	23.972 ± 0.123	23.753 ± 0.102
901.8429.....	23.703 ± 0.060	23.235 ± 0.040	23.220 ± 0.040	23.838 ± 0.068	23.657 ± 0.058	23.737 ± 0.062	23.815 ± 0.067
901.8662.....	23.937 ± 0.094	23.317 ± 0.053	23.379 ± 0.057	23.785 ± 0.082	23.727 ± 0.077	23.781 ± 0.081	23.883 ± 0.089
901.9130.....	23.738 ± 0.053	23.406 ± 0.040	23.531 ± 0.045	23.883 ± 0.061	23.681 ± 0.051	23.848 ± 0.059	23.973 ± 0.066
901.9364.....	23.693 ± 0.044	...	23.487 ± 0.037	23.914 ± 0.054	23.665 ± 0.043	23.747 ± 0.046	24.075 ± 0.062
902.0052.....	23.692 ± 0.039	23.561 ± 0.035	23.748 ± 0.041	24.091 ± 0.056	23.663 ± 0.038	23.794 ± 0.042	23.729 ± 0.040
902.0286.....	23.771 ± 0.038	23.595 ± 0.033	23.807 ± 0.040	24.152 ± 0.054	23.588 ± 0.033	23.674 ± 0.035	24.000 ± 0.048
				R			
900.8367.....	23.387 ± 0.052	23.531 ± 0.060	23.827 ± 0.078	23.359 ± 0.051	23.228 ± 0.045	23.755 ± 0.073	...
900.8577.....	23.412 ± 0.052	23.587 ± 0.061	23.584 ± 0.061	23.540 ± 0.059	23.329 ± 0.048	24.051 ± 0.093	23.843 ± 0.078
900.9210.....	23.510 ± 0.053	23.658 ± 0.061	22.965 ± 0.033	23.518 ± 0.054	23.226 ± 0.041	23.243 ± 0.042	23.490 ± 0.053
901.8102.....	23.499 ± 0.090	23.160 ± 0.066	23.091 ± 0.062	23.402 ± 0.083	23.240 ± 0.071	23.549 ± 0.094	23.642 ± 0.103
901.8266.....	...	23.162 ± 0.071	22.953 ± 0.059	23.387 ± 0.087	23.262 ± 0.078	23.729 ± 0.119	...

HJD (2,450,000+)	C2-V54	C2-V55	C2-V56	C2-V57	C2-V58	C2-V59	C2-V60
				V			
899.7859.....	23.796 ± 0.066	23.048 ± 0.034	24.711 ± 0.151	23.575 ± 0.054	23.042 ± 0.033	...	22.658 ± 0.024
899.8156.....	23.875 ± 0.059	23.040 ± 0.028	25.192 ± 0.193	23.354 ± 0.037	23.173 ± 0.032	23.854 ± 0.058	22.735 ± 0.021
899.8390.....	23.782 ± 0.058	23.135 ± 0.032	25.163 ± 0.202	23.319 ± 0.038	23.085 ± 0.031	23.658 ± 0.051	22.783 ± 0.024
899.8623.....	23.598 ± 0.037	23.253 ± 0.027	25.125 ± 0.146	23.232 ± 0.027	23.137 ± 0.025	23.616 ± 0.038	22.818 ± 0.019
899.8861.....	23.499 ± 0.027	23.347 ± 0.024	25.243 ± 0.129	23.278 ± 0.022	23.080 ± 0.019	23.645 ± 0.031	22.872 ± 0.016
899.9353.....	23.310 ± 0.039	23.419 ± 0.026	25.352 ± 0.144	23.373 ± 0.025	23.125 ± 0.020	23.516 ± 0.028	23.004 ± 0.018
900.0157.....	23.441 ± 0.032	23.599 ± 0.037	25.114 ± 0.145	...	...	23.026 ± 0.023	23.103 ± 0.024
900.0390.....	23.426 ± 0.045	23.680 ± 0.058	24.872 ± 0.172	...	...	23.002 ± 0.031	23.136 ± 0.036
900.7897.....	23.640 ± 0.056	23.303 ± 0.041	24.746 ± 0.154	23.638 ± 0.056	22.528 ± 0.021	23.158 ± 0.037	23.884 ± 0.070
900.8130.....	23.703 ± 0.050	23.280 ± 0.034	...	23.726 ± 0.050	22.557 ± 0.018	23.273 ± 0.034	23.695 ± 0.049
900.8742.....	23.714 ± 0.039	23.398 ± 0.029	24.770 ± 0.097	23.505 ± 0.032	22.675 ± 0.016	23.454 ± 0.031	23.245 ± 0.026
900.8975.....	23.680 ± 0.035	23.474 ± 0.029	24.736 ± 0.090	23.311 ± 0.025	22.678 ± 0.015	23.509 ± 0.030	22.822 ± 0.017
900.9374.....	23.778 ± 0.054	23.549 ± 0.044	24.895 ± 0.146	23.218 ± 0.032	22.705 ± 0.021	23.494 ± 0.042	22.397 ± 0.017
901.0233.....	23.710 ± 0.046	23.773 ± 0.049	...	23.432 ± 0.036	22.830 ± 0.022	23.783 ± 0.049	22.396 ± 0.015
901.0397.....	23.755 ± 0.047	23.833 ± 0.050	25.345 ± 0.196	23.498 ± 0.037	22.795 ± 0.020	23.730 ± 0.046	22.501 ± 0.016
901.7571.....	23.301 ± 0.077	23.332 ± 0.079	...	23.611 ± 0.106	23.117 ± 0.066	23.791 ± 0.122	...
901.7804.....	23.494 ± 0.080	23.386 ± 0.073	24.759 ± 0.252	...	23.027 ± 0.053	23.574 ± 0.086	23.751 ± 0.101
901.8429.....	23.366 ± 0.045	23.526 ± 0.051	25.384 ± 0.277	...	...	23.546 ± 0.053	23.890 ± 0.072
901.8662.....	23.374 ± 0.056	23.721 ± 0.077	...	...	...	23.423 ± 0.059	23.824 ± 0.084
901.9130.....	23.505 ± 0.043	23.613 ± 0.048	25.391 ± 0.239	...	...	23.244 ± 0.034	23.701 ± 0.052
901.9364.....	23.451 ± 0.036	23.722 ± 0.045	25.417 ± 0.207	...	23.143 ± 0.028	23.057 ± 0.026	23.693 ± 0.044
902.0052.....	23.661 ± 0.038	23.856 ± 0.045	24.841 ± 0.108	23.296 ± 0.028	22.602 ± 0.015	23.021 ± 0.022	23.728 ± 0.040
902.0286.....	23.633 ± 0.034	23.849 ± 0.041	25.025 ± 0.118	23.256 ± 0.025	22.289 ± 0.011	23.077 ± 0.021	23.648 ± 0.035
				R			
900.8367.....	23.342 ± 0.050	23.113 ± 0.041	24.505 ± 0.143	23.472 ± 0.055	22.360 ± 0.021	23.148 ± 0.042	23.379 ± 0.052
900.8577.....	23.341 ± 0.049	23.093 ± 0.039	...	23.333 ± 0.048	22.293 ± 0.019	23.166 ± 0.042	23.227 ± 0.044
900.9210.....	23.438 ± 0.050	23.137 ± 0.038	24.420 ± 0.121	22.999 ± 0.034	22.326 ± 0.019	23.239 ± 0.042	22.375 ± 0.020
901.8102.....	23.234 ± 0.070	23.261 ± 0.073	24.717 ± 0.274	...	22.773 ± 0.047	23.506 ± 0.091	23.320 ± 0.076
901.8266.....	23.011 ± 0.062	23.186 ± 0.073	...	...	22.841 ± 0.053	23.464 ± 0.094	23.394 ± 0.088

TABLE 2—*Continued*

HJD (2,450,000+)	C2-V61	C2-V62	C2-V63	C2-V64	C2-V65	C2-V66	C2-V67
				V			
899.7859.....	23.475 ± 0.050	23.999 ± 0.080	22.761 ± 0.026	...	23.782 ± 0.065	25.165 ± 0.231	22.072 ± 0.015
899.8156.....	23.487 ± 0.042	...	22.761 ± 0.022	22.764 ± 0.022	23.708 ± 0.051	24.630 ± 0.116	22.054 ± 0.012
899.8390.....	23.306 ± 0.038	...	22.721 ± 0.023	22.825 ± 0.025	23.713 ± 0.054	24.988 ± 0.171	22.073 ± 0.013
899.8623.....	23.333 ± 0.029	...	22.747 ± 0.018	22.759 ± 0.018	23.859 ± 0.047	25.213 ± 0.160	22.088 ± 0.010
899.8861.....	23.265 ± 0.022	23.130 ± 0.020	22.707 ± 0.014	22.832 ± 0.015	23.776 ± 0.035	25.623 ± 0.181	22.091 ± 0.009
899.9353.....	23.316 ± 0.024	23.437 ± 0.026	22.795 ± 0.015	22.812 ± 0.015	23.737 ± 0.034	25.418 ± 0.153	22.172 ± 0.009
900.0157.....	23.525 ± 0.035	...	...	22.777 ± 0.018	23.535 ± 0.035	...	22.226 ± 0.012
900.0390.....	23.385 ± 0.044	...	...	22.770 ± 0.026	23.490 ± 0.048	...	22.215 ± 0.016
900.7897.....	23.678 ± 0.058	...	22.326 ± 0.018	22.191 ± 0.016	23.424 ± 0.046	24.549 ± 0.128	22.744 ± 0.025
900.8130.....	23.701 ± 0.049	...	22.289 ± 0.014	22.242 ± 0.014	23.558 ± 0.044	24.452 ± 0.097	22.684 ± 0.021
900.8742.....	23.714 ± 0.038	23.339 ± 0.027	22.365 ± 0.012	22.313 ± 0.012	23.654 ± 0.036	24.895 ± 0.110	22.757 ± 0.017
900.8975.....	23.821 ± 0.040	23.437 ± 0.028	22.388 ± 0.012	22.329 ± 0.011	23.782 ± 0.038	24.727 ± 0.089	22.805 ± 0.016
900.9374.....	23.684 ± 0.049	23.513 ± 0.042	22.397 ± 0.016	22.342 ± 0.016	23.753 ± 0.052	...	22.737 ± 0.022
901.0233.....	23.734 ± 0.047	...	...	22.402 ± 0.015	23.744 ± 0.047	...	22.760 ± 0.020
901.0397.....	23.601 ± 0.041	...	22.398 ± 0.015	22.429 ± 0.015	23.783 ± 0.048	25.738 ± 0.282	22.845 ± 0.021
901.7571.....	23.342 ± 0.080	23.201 ± 0.071	22.656 ± 0.043	22.761 ± 0.047	23.839 ± 0.128	25.062 ± 0.389	22.546 ± 0.039
901.7804.....	23.184 ± 0.061	23.198 ± 0.061	22.679 ± 0.038	22.653 ± 0.038	23.752 ± 0.101	...	22.510 ± 0.033
901.8429.....	23.305 ± 0.042	23.453 ± 0.049	...	22.797 ± 0.027	23.593 ± 0.055	...	22.340 ± 0.018
901.8662.....	23.369 ± 0.056	23.706 ± 0.076	...	22.782 ± 0.033	23.409 ± 0.058	...	22.262 ± 0.021
901.9130.....	23.456 ± 0.042	...	...	22.810 ± 0.024	23.368 ± 0.039	...	22.098 ± 0.013
901.9364.....	23.492 ± 0.037	...	...	22.828 ± 0.021	23.426 ± 0.035	24.783 ± 0.117	22.075 ± 0.011
902.0052.....	23.689 ± 0.039	23.845 ± 0.044	22.716 ± 0.017	...	23.582 ± 0.035	24.638 ± 0.090	22.117 ± 0.010
902.0286.....	23.630 ± 0.034	23.978 ± 0.046	22.710 ± 0.016	...	23.662 ± 0.035	24.840 ± 0.100	22.151 ± 0.010
				R			
900.8367.....	23.425 ± 0.054	23.222 ± 0.045	22.000 ± 0.015	21.904 ± 0.014	23.481 ± 0.056	24.493 ± 0.141	22.419 ± 0.022
900.8577.....	23.451 ± 0.054	23.193 ± 0.043	22.054 ± 0.016	21.948 ± 0.014	23.460 ± 0.054	24.288 ± 0.115	22.418 ± 0.022
900.9210.....	23.341 ± 0.047	23.190 ± 0.040	22.009 ± 0.014	21.979 ± 0.014	23.451 ± 0.050	...	22.346 ± 0.019
901.8102.....	23.222 ± 0.070	23.276 ± 0.073	22.316 ± 0.031	22.406 ± 0.034	23.524 ± 0.092	...	22.171 ± 0.027
901.8266.....	23.216 ± 0.075	23.302 ± 0.081	22.225 ± 0.031	22.386 ± 0.035	23.216 ± 0.075	...	22.144 ± 0.029

HJD (2,450,000+)	C2-V68	C2-V69	C2-V70	C2-V71	C2-V72	C2-V73	C2-V74
				V			
899.7859.....	23.428 ± 0.047	23.560 ± 0.053	23.246 ± 0.041	23.305 ± 0.042	23.188 ± 0.038	23.531 ± 0.052	23.840 ± 0.069
899.8156.....	23.363 ± 0.037	23.317 ± 0.036	23.252 ± 0.034	23.208 ± 0.032	23.310 ± 0.036	23.590 ± 0.045	23.681 ± 0.049
899.8390.....	23.530 ± 0.046	23.207 ± 0.035	23.252 ± 0.036	23.218 ± 0.034	23.289 ± 0.037	23.580 ± 0.048	23.679 ± 0.052
899.8623.....	23.444 ± 0.032	23.219 ± 0.026	23.243 ± 0.027	23.136 ± 0.025	23.442 ± 0.032	23.510 ± 0.034	23.715 ± 0.041
899.8861.....	23.529 ± 0.028	23.277 ± 0.022	23.327 ± 0.024	23.081 ± 0.019	23.513 ± 0.027	...	23.827 ± 0.036
899.9353.....	23.720 ± 0.034	23.317 ± 0.024	23.406 ± 0.026	22.925 ± 0.017	23.653 ± 0.032	23.807 ± 0.036	23.863 ± 0.038
900.0157.....	23.792 ± 0.044	23.381 ± 0.031	23.377 ± 0.031	22.721 ± 0.017	23.703 ± 0.040	23.742 ± 0.042	23.906 ± 0.049
900.0390.....	23.797 ± 0.065	23.530 ± 0.050	23.422 ± 0.046	22.635 ± 0.023	23.688 ± 0.058	23.813 ± 0.065	23.877 ± 0.069
900.7897.....	23.801 ± 0.066	23.714 ± 0.061	23.505 ± 0.051	23.183 ± 0.038	23.778 ± 0.065	23.237 ± 0.039	23.823 ± 0.066
900.8130.....	23.845 ± 0.057	23.758 ± 0.051	23.526 ± 0.043	23.079 ± 0.028	23.815 ± 0.055	23.271 ± 0.033	23.651 ± 0.047
900.8742.....	23.728 ± 0.038	23.844 ± 0.043	23.249 ± 0.026	22.926 ± 0.019	23.336 ± 0.027	23.363 ± 0.028	23.462 ± 0.031
900.8975.....	23.684 ± 0.035	23.839 ± 0.040	23.201 ± 0.023	22.778 ± 0.016	23.179 ± 0.022	23.437 ± 0.028	23.373 ± 0.027
900.9374.....	23.550 ± 0.044	23.587 ± 0.045	23.119 ± 0.031	22.778 ± 0.022	22.959 ± 0.026	23.513 ± 0.042	23.415 ± 0.039
901.0233.....	23.366 ± 0.034	23.221 ± 0.030	23.215 ± 0.030	22.732 ± 0.020	23.176 ± 0.029	23.654 ± 0.044	23.568 ± 0.041
901.0397.....	23.340 ± 0.070	23.219 ± 0.029	23.156 ± 0.028	22.705 ± 0.019	23.268 ± 0.030	23.539 ± 0.038	23.606 ± 0.041
901.7571.....	...	24.065 ± 0.157	23.418 ± 0.087	23.163 ± 0.068	23.523 ± 0.095	24.273 ± 0.188	23.553 ± 0.097
901.7804.....	23.601 ± 0.088	23.775 ± 0.104	23.452 ± 0.077	22.951 ± 0.049	23.645 ± 0.091	23.809 ± 0.106	23.589 ± 0.087
901.8429.....	23.721 ± 0.061	23.780 ± 0.065	23.723 ± 0.062	22.780 ± 0.027	23.710 ± 0.061	23.531 ± 0.052	23.690 ± 0.060
901.8662.....	23.874 ± 0.088	23.694 ± 0.076	23.562 ± 0.067	22.698 ± 0.031	23.777 ± 0.081	23.396 ± 0.057	23.721 ± 0.077
901.9130.....	23.807 ± 0.057	23.757 ± 0.054	23.565 ± 0.046	22.706 ± 0.022	23.687 ± 0.051	23.096 ± 0.030	23.838 ± 0.059
901.9364.....	23.753 ± 0.046	23.831 ± 0.050	23.634 ± 0.042	22.706 ± 0.019	23.666 ± 0.043	23.160 ± 0.028	23.763 ± 0.047
902.0052.....	23.880 ± 0.046	23.833 ± 0.044	23.687 ± 0.039	22.757 ± 0.018	23.810 ± 0.043	23.213 ± 0.026	23.929 ± 0.048
902.0286.....	23.820 ± 0.040	23.822 ± 0.040	23.636 ± 0.035	22.784 ± 0.017	23.746 ± 0.038	23.285 ± 0.025	23.857 ± 0.042
				R			
900.8367.....	23.687 ± 0.068	23.412 ± 0.053	23.134 ± 0.042	22.812 ± 0.031	23.292 ± 0.048	23.103 ± 0.040	23.328 ± 0.049
900.8577.....	23.430 ± 0.053	23.482 ± 0.056	22.978 ± 0.036	22.706 ± 0.028	23.233 ± 0.044	23.133 ± 0.041	23.217 ± 0.044
900.9210.....	23.278 ± 0.043	23.154 ± 0.042	22.854 ± 0.030	22.499 ± 0.022	22.773 ± 0.028	23.157 ± 0.039	23.084 ± 0.036
901.8102.....	23.345 ± 0.078	23.620 ± 0.100	23.345 ± 0.079	22.759 ± 0.046	23.315 ± 0.076	23.484 ± 0.088	23.396 ± 0.082
901.8266.....	23.587 ± 0.105	23.459 ± 0.093	23.219 ± 0.075	22.537 ± 0.041	23.447 ± 0.092	23.313 ± 0.082	23.477 ± 0.095

TABLE 2—*Continued*

HJD (2,450,000+)	C2-V75	C2-V76	C2-V77	C2-V78
		V		
899.7859.....	24.327 ± 0.109	23.355 ± 0.044	23.157 ± 0.038	23.729 ± 0.062
899.8156.....	24.267 ± 0.084	23.258 ± 0.034	23.330 ± 0.036	23.221 ± 0.033
899.8390.....	24.102 ± 0.077	23.117 ± 0.032	23.404 ± 0.041	22.820 ± 0.025
899.8623.....	24.186 ± 0.062	23.156 ± 0.025	23.464 ± 0.033	22.822 ± 0.019
899.8861.....	24.087 ± 0.045	23.168 ± 0.020	23.580 ± 0.029	22.874 ± 0.016
899.9353.....	23.669 ± 0.032	23.286 ± 0.023	23.889 ± 0.038	23.085 ± 0.019
900.0157.....	23.697 ± 0.041	23.447 ± 0.033	23.933 ± 0.050	...
900.0390.....	23.839 ± 0.066	23.459 ± 0.047	24.049 ± 0.081	...
900.7897.....	24.201 ± 0.094	23.896 ± 0.072	23.958 ± 0.076	23.614 ± 0.056
900.8130.....	24.162 ± 0.076	23.750 ± 0.052	23.664 ± 0.048	23.203 ± 0.032
900.8742.....	23.560 ± 0.033	23.828 ± 0.042	23.847 ± 0.043	22.815 ± 0.017
900.8975.....	23.561 ± 0.031	23.970 ± 0.045	23.837 ± 0.040	22.926 ± 0.018
900.9374.....	23.682 ± 0.049	23.874 ± 0.058	23.839 ± 0.056	23.112 ± 0.030
901.0233.....	24.016 ± 0.060	23.651 ± 0.044	24.124 ± 0.067	23.284 ± 0.032
901.0397.....	24.108 ± 0.064	23.729 ± 0.045	24.098 ± 0.064	23.342 ± 0.032
901.7571.....	...	23.347 ± 0.081	23.916 ± 0.137	23.874 ± 0.132
901.7804.....	23.731 ± 0.099	...	23.797 ± 0.105	...
901.8429.....	23.705 ± 0.060	23.204 ± 0.039	23.920 ± 0.074	...
901.8662.....	23.555 ± 0.066	23.326 ± 0.054	24.264 ± 0.125	...
901.9130.....	23.869 ± 0.060	23.355 ± 0.038	24.196 ± 0.080	...
901.9364.....	23.921 ± 0.054	23.432 ± 0.035	24.316 ± 0.077	23.067 ± 0.026
902.0052.....	24.263 ± 0.064	23.579 ± 0.035	24.205 ± 0.061	23.308 ± 0.028
902.0286.....	24.261 ± 0.060	23.727 ± 0.037	24.290 ± 0.061	23.325 ± 0.026
		R		
900.8367.....	23.695 ± 0.068	23.525 ± 0.059	23.411 ± 0.052	22.739 ± 0.029
900.8577.....	23.496 ± 0.056	23.547 ± 0.059	23.626 ± 0.064	22.624 ± 0.026
900.9210.....	23.322 ± 0.045	23.598 ± 0.058	23.817 ± 0.070	22.832 ± 0.029
901.8102.....	23.618 ± 0.100	22.951 ± 0.055	23.572 ± 0.096	23.037 ± 0.059
901.8266.....	23.328 ± 0.082	23.045 ± 0.064	23.857 ± 0.134	22.741 ± 0.049

HJD (2,450,000+)	C2-V79	C2-V80	C2-V81	C2-V82
		V		
899.7859.....	...	...	24.201 ± 0.095	23.177 ± 0.038
899.8156.....	24.756 ± 0.130	25.698 ± 0.309	24.389 ± 0.094	23.179 ± 0.031
899.8390.....	...	...	24.232 ± 0.087	23.316 ± 0.038
899.8623.....	24.819 ± 0.110	...	24.071 ± 0.056	23.323 ± 0.029
899.8861.....	24.828 ± 0.088	25.445 ± 0.153	23.746 ± 0.033	23.350 ± 0.024
899.9353.....	25.022 ± 0.107	25.690 ± 0.195	23.482 ± 0.027	23.489 ± 0.027
900.0157.....	25.014 ± 0.133	25.033 ± 0.133	23.707 ± 0.040	23.557 ± 0.035
900.0390.....	...	24.947 ± 0.181	23.789 ± 0.064	...
900.7897.....	25.195 ± 0.234	...	23.506 ± 0.051	23.476 ± 0.048
900.8130.....	24.886 ± 0.144	25.321 ± 0.214	23.537 ± 0.042	23.523 ± 0.042
900.8742.....	25.167 ± 0.140	25.638 ± 0.214	23.688 ± 0.037	23.493 ± 0.031
900.8975.....	25.002 ± 0.113	25.906 ± 0.258	23.864 ± 0.041	23.509 ± 0.030
900.9374.....	25.435 ± 0.240	...	23.843 ± 0.056	23.616 ± 0.046
901.0233.....	...	25.637 ± 0.260	24.208 ± 0.072	23.549 ± 0.040
901.0397.....	25.444 ± 0.214	25.243 ± 0.178	24.178 ± 0.068	23.506 ± 0.037
901.7571.....	...	...	23.629 ± 0.105	23.798 ± 0.121
901.7804.....	25.491 ± 0.495	...	23.900 ± 0.115	23.795 ± 0.105
901.8429.....	...	25.306 ± 0.258	23.851 ± 0.069	23.463 ± 0.049
901.8662.....	...	...	24.064 ± 0.104	23.708 ± 0.075
901.9130.....	25.495 ± 0.262	25.385 ± 0.237	24.022 ± 0.069	23.528 ± 0.044
901.9364.....	25.409 ± 0.205	25.104 ± 0.155	24.082 ± 0.062	23.557 ± 0.039
902.0052.....	25.069 ± 0.133	25.815 ± 0.261	24.250 ± 0.063	23.109 ± 0.023
902.0286.....	25.189 ± 0.137	...	24.186 ± 0.056	23.046 ± 0.020
		R		
900.8367.....	24.337 ± 0.121	24.818 ± 0.191	23.348 ± 0.051	23.091 ± 0.040
900.8577.....	24.213 ± 0.109	25.498 ± 0.348	23.411 ± 0.052	23.267 ± 0.046
900.9210.....	24.452 ± 0.124	25.120 ± 0.228	23.521 ± 0.053	23.259 ± 0.042
901.8102.....	24.578 ± 0.240	...	23.516 ± 0.091	23.188 ± 0.068
901.8266.....	23.930 ± 0.143	24.801 ± 0.317	23.338 ± 0.083	23.217 ± 0.075

deep frames, with the resulting star list used as a template (after determining appropriate coordinate transformations) for each of the individual epochs. By restricting the star positions, we obtain more accurate photometry in the individual epochs, as each star has only one free parameter (brightness), instead of three (X, Y, and brightness).

J. C. and A. S. made a parallel reduction using IRAF and photometry using DoPHOT (Schechter, Mateo, & Saha 1993). In this reduction, the images were adjusted prior to IRAF reduction, correcting for overscan and cross talk using an IDL routine written by A. S. The normal IRAF procedure was then used to reduce the data. The DoPHOT photometry consisted of two passes, similar in concept to that made by A. E.D. In the first pass, each individual epoch image was photometered, along with the deep frames. Coordinate transformations were made between the deep and individual star lists, and photometry was rerun on the individual frames. A comparison between our two sets of chip 2 deep photometry is shown in Figure 2; there are no obvious inconsistencies between the two reductions.

Because only one of the three nights was photometric, we could not make independent photometric solutions for each night. Instead, we observed two standard fields—SA 92 (Landolt 1992) and NGC 2419 (Stetson 2000)—and used Leo A observations at similar air mass (n2086 and n2083; see Table 1) to define secondary standards in our Leo A field. Unfortunately, we did not observe SA 92 in R, and the Stetson (2000) R standards in NGC 2419 cover only the region north of NGC 2419 (corresponding to chip 1 on our images). Thus we were forced to use the chip 1 R transformation for chip 2 also, under the assumption that the color term of the R-band transformation is the same in the two chips. Data for other WIYN and MIMO studies have shown this to be nearly true; we increase our R error bars by 0.02 mag to account for this source of uncertainty. The resulting photometric calibration is accurate to ± 0.02 mag in V and ± 0.04 mag in R.

Using our secondary standards within the Leo A images, we calibrated both photometry sets by forcing the mean difference between the calibrated and point-spread function-fitted magnitudes of all secondary standards to be zero. This resulted in a large photometric database consisting of the deep positions and magnitudes of all stars, as well as the magnitudes determined for each epoch.

3. VARIABLE-STAR IDENTIFICATION

Variable stars were identified according to the procedure described by Dolphin et al. (2001b), except that only the V observations were used for locating variables. Because of smaller error bars in the photometry, we adopted A. E. D.'s point-spread function–fitting photometry as our primary measurement (Table 2). We believe that the smaller errors in A. E. D.'s photometry resulted because his point-spread function (PSF) formulation (an analytical function plus a residual image) permitted a more accurate modeling of the oddly shaped PSFs (due to tracking errors) found in our data than does the DoPHOT PSF formulation (analytical function only). The measured magnitudes were nearly identical in the two reductions as noted above; however, the smaller (and more accurate) error bars were necessary to accurately identify variable stars.

For a star to be classified as a variable star, it had to meet a strict set of criteria. The first criterion was that the PSF-fitting photometry had to detect and classify it as a well-fitted star in the deep V frame. We define "well fitted" to mean that the χ^2 of the fit had to be 4.0 or less, the sharpness had to be between -0.25 and 0.25 (a sharpness of zero is a perfect star), and the signal-to-noise ratio had to be 5.0 or more. Additionally, the star had to be well photometered in at least 12 of the 23 V epochs and at least one R epoch, and contamination from bright neighbors had to contribute no more than 20% of the star's light within a PSF-sized aperture.

Stars that met these criteria had to pass additional variability tests. First, to eliminate nonvariable stars, we required that the reduced χ^2 of the V observations be 2.0 or greater and the standard deviation of the V measurements be at least 0.14 mag. The first criterion eliminates stars that appear variable because their measurements have large uncertainties; the second eliminates stars for which small systematic errors in the measurements could cause false detections. Additionally, in case a star was spuriously flagged because of one or two bad points, we eliminated one-third of the points contributing the most to χ^2 and required that this "robust" χ^2 value be 0.5 or more.

Our final automatic variability test for periodicity and was made using the Lafler-Kinman Θ statistic (Lafler & Kinman 1965) as implemented by Saha & Hoessel (1990). For a variety of trial periods, the value $\Theta(p)$ was calculated using

$$\Theta(p) = \frac{\sum_{i=1}^{N}(V_i - V_{i+1})^2}{\sum_{i=1}^{N}(V_i - \overline{V})^2} , \qquad (1)$$

where N is the number of epochs at which the star was observed, V_i is the V magnitude at epoch i, and $\overline{V}$ is the mean V magnitude. For uncorrelated data, Θ will be ≈ 2, since the typical difference between any two data points would be $\sqrt{2}$ times the standard deviation (the denominator). However, if the data are periodic and the correct trial period is used, V_i and V_{i+1} will be correlated, thus reducing Θ. We required $\Theta \leq 1.0$. Finally, we visually examined the image and light curves of each star, eliminating any candidate variables that either appeared nonstellar or nonperiodic.

We found three additional variable stars from the DoPHOT photometry that were not recovered in our initial variable-star search. (C2-V09 had $\sigma V = 0.13$, C2-V30 had $\chi^2 = 4.4$ in the photometry, C2-V57 had $\sigma V = 0.12$.) After visual inspection, these three stars were added to our list of variables. In all, we found 92 variable stars, of which 82 have very good light curves.

Our list of variable stars is presented in Table 3, finding charts in Figure 3, and light curves in Figure 4. The values given in Table 3 are the variable-star ID, chip and position (the FITS file from which the positions are taken is available in the electronic edition of the Journal), period-averaged V and R magnitudes (Dolphin et al. 2001b), period, and light-curve quality on a scale of 0, the worst, to 4, the best (Dolphin et al. 2001b). We note that our relatively short observing window created a large number of stars with possibly aliased periods; these are indicated in Table 3 and Figure 4 by the same star ID being shown with multiple periods.

Only one of our variable stars (our C2-V25 corresponds to their V10) is in common with the list of Hoessel et al.

TABLE 3

VARIABLE STARS

ID[a]	Chip	X	Y	V	R	P (days)	Q[b]	Class[c]
C1-V01	1	691.71	844.00	25.38 ± 0.11	25.21 ± 0.23	0.11 ± 0.01	2	RR
C1-V02	1	1443.33	2494.99	23.75 ± 0.06	23.66 ± 0.10	0.59 ± 0.02	3	C-FO
C1-V03	1	1561.26	2010.57	25.03 ± 0.09	24.78 ± 0.06	0.61 ± 0.02	3	RRab
C1-V04	1	1663.61	2872.98	24.02 ± 0.07	23.76 ± 0.03	0.44 ± 0.01	2	C
C1-V04	1	1663.61	2872.98	24.18 ± 0.11	23.76 ± 0.03	0.86 ± 0.04	2	C
C1-V05	1	1712.41	3989.46	23.56 ± 0.09	23.17 ± 0.12	1.58 ± 0.21	4	C-FM?
C1-V06	1	1735.66	1215.41	23.44 ± 0.08	23.27 ± 0.15	0.61 ± 0.02	4	C-FO
C1-V07	1	1761.25	2635.05	25.23 ± 0.13	25.01 ± 0.03	0.43 ± 0.01	3	RRc
C1-V08	1	1778.02	2486.54	23.75 ± 0.08	23.36 ± 0.02	0.83 ± 0.04	3	C-FM
C1-V09	1	1836.01	956.66	23.64 ± 0.06	23.19 ± 0.08	0.45 ± 0.01	4	C-FO/SO
C1-V10	1	1923.00	1934.91	23.48 ± 0.06	23.16 ± 0.16	0.56 ± 0.01	2	C
C1-V10	1	1923.00	1934.91	23.56 ± 0.06	23.15 ± 0.20	1.13 ± 0.02	3	C
C2-V01	2	61.12	3722.22	22.97 ± 0.08	22.67 ± 0.09	0.85 ± 0.05	4	C-FO
C2-V02	2	142.80	1760.57	23.52 ± 0.06	23.30 ± 0.11	0.65 ± 0.02	4	C-FO
C2-V03	2	157.58	2897.08	23.67 ± 0.06	23.43 ± 0.08	0.60 ± 0.02	2	C
C2-V03	2	157.58	2897.08	23.72 ± 0.06	23.40 ± 0.11	1.17 ± 0.06	2	C
C2-V04	2	180.87	2063.72	23.14 ± 0.05	22.94 ± 0.17	0.35 ± 0.01	2	C
C2-V04	2	180.87	2063.72	23.23 ± 0.06	22.97 ± 0.19	0.53 ± 0.02	2	C
C2-V05	2	230.94	2618.02	23.61 ± 0.09	23.19 ± 0.05	0.54 ± 0.02	3	C-FO
C2-V06	2	237.06	2014.71	23.60 ± 0.04	23.40 ± 0.08	0.68 ± 0.01	3	C-FO
C2-V07	2	249.07	2033.99	23.68 ± 0.06	23.28 ± 0.03	0.43 ± 0.02	3	C
C2-V07	2	249.07	2033.99	23.75 ± 0.07	23.29 ± 0.04	0.87 ± 0.02	3	C
C2-V08	2	277.29	2951.84	23.08 ± 0.12	22.76 ± 0.14	1.70 ± 9.99[d]	4	C
C2-V09	2	287.17	2532.65	23.47 ± 0.10	23.06 ± 0.07	1.22 ± 0.18	4	C-FO
C2-V10	2	297.66	1729.13	23.18 ± 0.07	23.13 ± 0.04	0.79 ± 0.04	4	C-FO
C2-V11	2	317.32	2079.96	23.04 ± 0.08	22.67 ± 0.05	0.51 ± 0.01	4	C-SO
C2-V12	2	322.49	3299.65	23.62 ± 0.14	23.57 ± 0.05	0.53 ± 0.03	2	C
C2-V12	2	322.49	3299.65	23.55 ± 0.23	23.59 ± 0.04	1.06 ± 0.04	2	C
C2-V13	2	342.66	2481.67	23.58 ± 0.04	23.38 ± 0.11	0.64 ± 0.01	3	C-FO
C2-V14	2	364.83	3020.08	23.79 ± 0.05	23.36 ± 0.08	0.32 ± 0.01	3	C
C2-V14	2	364.83	3020.08	23.82 ± 0.06	23.38 ± 0.09	0.47 ± 0.02	3	C
C2-V14	2	364.83	3020.08	23.89 ± 0.06	23.38 ± 0.10	0.94 ± 0.03	3	C
C2-V15	2	392.70	1445.98	23.82 ± 0.10	23.34 ± 0.05	0.47 ± 0.01	3	C-FO
C2-V16	2	444.82	1062.55	23.18 ± 0.04	23.00 ± 0.07	0.75 ± 0.02	4	C-FO
C2-V17	2	452.70	1432.99	23.27 ± 0.09	23.22 ± 0.05	1.47 ± 0.13	4	C-FM
C2-V18	2	475.87	3022.91	23.45 ± 0.06	23.25 ± 0.14	0.61 ± 0.02	4	C-FO
C2-V19	2	495.83	2489.02	23.13 ± 0.10	22.72 ± 0.08	0.82 ± 0.04	3	C-FO
C2-V20	2	498.92	2900.82	23.69 ± 0.05	23.50 ± 0.10	0.65 ± 0.03	3	C-FO
C2-V21	2	501.97	2756.53	23.42 ± 0.06	23.08 ± 0.09	0.64 ± 0.02	3	C
C2-V21	2	501.97	2756.53	23.54 ± 0.08	23.08 ± 0.11	1.33 ± 0.13	3	C
C2-V22	2	533.98	2050.36	22.53 ± 0.15	22.16 ± 0.16	1.67 ± 0.13	4	C-FM
C2-V23	2	543.16	2838.83	23.26 ± 0.09	23.18 ± 0.13	1.52 ± 0.20	3	C-FM
C2-V24	2	557.82	3022.99	23.27 ± 0.08	22.80 ± 0.06	0.47 ± 0.02	3	C-FO/SO
C2-V25	2	564.82	2569.75	22.91 ± 0.14	22.88 ± 0.03	1.39 ± 0.15	3	C-FM
C2-V26	2	569.46	2480.98	23.63 ± 0.05	23.45 ± 0.07	0.61 ± 0.02	3	C-FO
C2-V27	2	576.01	2941.31	23.74 ± 0.07	23.50 ± 0.07	0.55 ± 0.02	4	C-FO
C2-V28	2	580.26	1573.64	23.22 ± 0.08	23.18 ± 0.05	0.80 ± 0.04	3	C-FO
C2-V29	2	588.69	1556.76	23.28 ± 0.04	23.07 ± 0.01	0.59 ± 0.02	3	C-FO
C2-V30	2	597.29	1850.02	23.25 ± 0.05	23.23 ± 0.03	0.75 ± 0.06	3	C-FO
C2-V31	2	597.32	2021.21	23.10 ± 0.11	22.99 ± 0.17	1.46 ± 0.20	4	C-FM
C2-V32	2	610.25	1971.24	23.15 ± 0.08	22.87 ± 0.07	0.78 ± 0.04	4	C-FO
C2-V33	2	619.20	3024.54	24.96 ± 0.08	24.68 ± 0.12	0.72 ± 0.04	2	RR
C2-V34	2	623.99	2424.54	23.39 ± 0.04	23.16 ± 0.05	0.68 ± 0.01	3	C-FO
C2-V35	2	625.81	1618.98	23.85 ± 0.05	23.59 ± 0.10	0.39 ± 0.01	4	C-FO/SO
C2-V36	2	635.97	2072.98	23.92 ± 0.07	23.50 ± 0.04	0.52 ± 0.02	2	C
C2-V36	2	635.97	2072.98	23.87 ± 0.05	23.49 ± 0.05	0.34 ± 0.01	2	C
C2-V37	2	646.88	2654.01	23.16 ± 0.10	22.74 ± 0.02	1.28 ± 0.12	4	C-FM
C2-V38	2	654.39	2694.43	22.71 ± 0.07	22.42 ± 0.02	0.47 ± 0.02	4	C-SO
C2-V39	2	666.37	2974.68	23.05 ± 0.11	22.88 ± 0.07	1.69 ± 0.05	4	C-FM
C2-V40	2	702.00	1343.75	23.55 ± 0.21	23.45 ± 0.05	1.17 ± 0.02	3	C-FM
C2-V41	2	706.34	1509.98	23.38 ± 0.11	23.26 ± 0.04	0.87 ± 0.05	3	C-FM/FO
C2-V42	2	709.10	2136.04	22.17 ± 0.10	21.96 ± 0.06	1.73 ± 0.23	4	C-FO
C2-V43	2	728.98	2209.79	22.99 ± 0.05	22.67 ± 0.03	1.61 ± 0.05	4	C-FM
C2-V44	2	743.34	3186.82	23.45 ± 0.06	23.24 ± 0.14	0.75 ± 0.03	4	C-FO

TABLE 3—*Continued*

ID[a]	Chip	X	Y	V	R	P (days)	Q[b]	Class[c]
C2-V45	2	758.02	1581.99	23.35 ± 0.06	23.08 ± 0.13	0.66 ± 0.02	3	C-FO
C2-V46	2	768.59	1827.79	23.67 ± 0.06	23.30 ± 0.05	0.60 ± 0.02	3	C-FO
C2-V47	2	773.21	1373.99	23.54 ± 0.06	23.49 ± 0.02	1.25 ± 0.03	4	C-FM
C2-V48	2	801.67	1693.65	23.61 ± 0.05	23.39 ± 0.12	0.59 ± 0.03	3	C-FO
C2-V49	2	807.70	2488.27	23.72 ± 0.16	23.29 ± 0.28	0.86 ± 0.02	3	C-FM
C2-V50	2	818.83	2468.22	23.74 ± 0.10	23.47 ± 0.04	0.49 ± 0.01	4	C-FO
C2-V51	2	824.51	1270.23	23.41 ± 0.13	23.24 ± 0.01	0.54 ± 0.03	3	C-FO
C2-V52	2	850.27	2903.02	23.70 ± 0.05	23.62 ± 0.10	0.70 ± 0.06	2	C
C2-V53	2	879.84	2184.60	23.83 ± 0.04	23.67 ± 0.08	0.39 ± 0.01	2	C
C2-V53	2	879.84	2184.60	23.81 ± 0.04	23.65 ± 0.07	0.63 ± 0.03	2	C
C2-V54	2	886.59	2699.69	23.58 ± 0.04	23.26 ± 0.08	0.61 ± 0.01	4	C-FO
C2-V55	2	896.01	2998.07	23.45 ± 0.09	23.13 ± 0.02	0.46 ± 0.02	3	C
C2-V55	2	896.01	2998.07	23.41 ± 0.19	23.13 ± 0.03	0.94 ± 0.03	3	C
C2-V56	2	911.13	683.76	24.98 ± 0.09	24.56 ± 0.07	0.40 ± 0.02	2	RR
C2-V56	2	911.13	683.76	25.00 ± 0.07	24.57 ± 0.08	0.66 ± 0.04	2	RR
C2-V57	2	921.60	3592.23	23.47 ± 0.05	23.21 ± 0.15	0.36 ± 0.01	3	C
C2-V57	2	921.60	3592.23	23.51 ± 0.04	23.21 ± 0.16	0.54 ± 0.01	3	C
C2-V58	2	940.38	1718.02	22.84 ± 0.12	22.53 ± 0.12	1.46 ± 0.17	3	C-FM
C2-V59	2	964.71	2747.65	23.40 ± 0.06	23.31 ± 0.07	0.64 ± 0.02	4	C-FO
C2-V60	2	987.72	2004.47	23.16 ± 0.15	22.89 ± 0.26	1.32 ± 0.11	4	C-FM
C2-V61	2	995.38	2382.95	23.54 ± 0.04	23.31 ± 0.04	0.64 ± 0.01	4	C-FO
C2-V62	2	1030.01	1635.68	23.62 ± 0.12	23.21 ± 0.01	0.47 ± 0.01	3	C-FO
C2-V63	2	1031.99	1510.28	22.54 ± 0.13	22.12 ± 0.07	2.29 ± 9.99[d]	3	C
C2-V64	2	1047.48	1842.02	22.52 ± 0.20	22.14 ± 0.15	2.01 ± 9.99[d]	3	C
C2-V65	2	1057.63	3135.79	23.64 ± 0.04	23.42 ± 0.05	0.61 ± 0.01	3	C-FO
C2-V66	2	1062.41	2604.56	24.94 ± 0.14	24.39 ± 0.07	0.36 ± 0.02	2	RR
C2-V66	2	1062.41	2604.56	25.02 ± 0.16	24.39 ± 0.07	0.54 ± 0.03	2	RR
C2-V67	2	1107.01	1657.93	22.50 ± 0.10	22.27 ± 0.06	2.13 ± 0.06	4	C-FM
C2-V68	2	1135.14	1589.98	23.64 ± 0.04	23.46 ± 0.08	0.63 ± 0.01	3	C-FO
C2-V69	2	1146.02	2148.28	23.65 ± 0.12	23.37 ± 0.14	1.15 ± 0.04	3	C-FM
C2-V70	2	1147.09	1590.18	23.39 ± 0.05	23.10 ± 0.12	1.47 ± 0.26	4	C-FM
C2-V71	2	1152.43	1307.52	22.96 ± 0.13	22.64 ± 0.11	0.93 ± 0.02	4	C-FO
C2-V72	2	1177.03	2359.03	23.45 ± 0.07	23.15 ± 0.14	0.61 ± 0.02	4	C-FO
C2-V73	2	1210.49	769.61	23.47 ± 0.07	23.25 ± 0.08	0.60 ± 0.01	3	C
C2-V73	2	1210.49	769.61	23.66 ± 0.14	23.28 ± 0.09	1.23 ± 0.05	3	C
C2-V74	2	1236.99	1834.70	23.66 ± 0.04	23.31 ± 0.07	0.67 ± 0.04	4	C-FO
C2-V75	2	1294.01	1756.03	23.98 ± 0.08	23.50 ± 0.12	0.46 ± 0.01	3	C-FO
C2-V76	2	1327.86	1894.33	23.55 ± 0.07	23.27 ± 0.14	0.65 ± 0.02	4	C-FO
C2-V77	2	1352.80	384.51	23.70 ± 0.23	23.61 ± 0.14	0.90 ± 0.06	4	C-FM
C2-V78	2	1516.13	1461.38	23.31 ± 0.15	22.88 ± 0.08	0.50 ± 0.02	4	C-FO/SO
C2-V79	2	1521.82	2097.56	25.06 ± 0.10	24.16 ± 0.15	0.84 ± 0.07	3	RRab
C2-V80	2	1600.98	1996.23	25.38 ± 0.10	24.99 ± 0.11	0.35 ± 0.02	2	RR
C2-V81	2	1608.14	2434.63	23.89 ± 0.07	23.37 ± 0.03	0.44 ± 0.01	3	C
C2-V81	2	1608.14	2434.63	24.01 ± 0.07	23.36 ± 0.02	0.86 ± 0.03	3	C
C2-V82	2	1909.10	1158.70	23.42 ± 0.07	23.16 ± 0.05	0.45 ± 0.02	3	C-FO/SO

[a] Stars listed multiple times have periods with multiple potential aliases.

[b] Variable-star quality is based on the cleanness of the light curves, uniqueness of the period, and coherence between V and R light curves, where 4 is highest quality and 0 is lowest quality.

[c] RR Lyrae stars classified into subclasses (RRab, RRc, and RRd) when possible. Cepheid classifications: (FM) fundamental mode, (FO) first overtone, (SO) second overtone, made only for objects with unambiguous periods and quality ratings of 3 or 4.

[d] Upper limits of the periods of stars C2-V08, C2-V63, and C2-V64 are unconstrained.

(1994), albeit with a period of 1.4 days instead of 13 days. Three of their other variables (V7, V9, and V13) are also clearly variable in our data. However, none of the three passed our PSF-fitted cut of $\chi^2 \leq 4.0$ (all were more extended than a typical star and thus are likely blends), so these three were excluded from our list. Of their other objects, their V3 appears to be a galaxy in our images and V8 is also clearly elongated, thus being rejected as nonstellar objects by our photometry. We see no sign of variability for the majority of their variables (V1, V2, V4, V5, V6, V11, V12, and V14); this is undoubtedly because of the sampling difference: they had a baseline of a decade but only one pair of observations separated by less than 1 day, while we had a baseline of only 2.25 days but frequent observations during that period. We note that the periods they determined for V2 (1.76 days), V11 (2.01 days), and V12 (0.51 days) are inconsistent with our data; we should have seen such variability during our 2.25 day baseline. These period inconsistencies can be attributed to their poor sampling of timescales of a few days. These concerns were raised in a

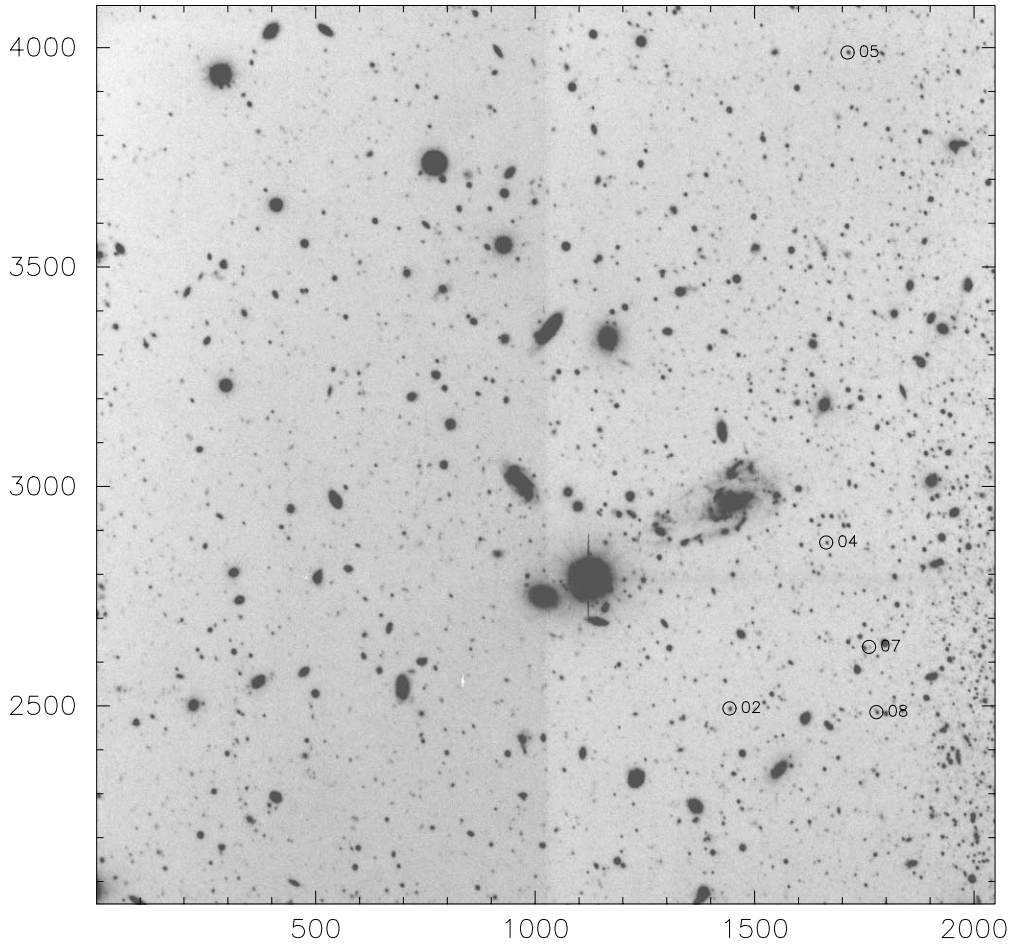

FIG. 3*a*

FIG. 3.—Variable-star finding chart for (*a*) the top half of chip 1, (*b*) the bottom half of chip 1, (*c*) the top half of chip 2, and (*d*) the bottom half of chip 2

later paper by the same authors (Saha et al. 1996), who noted the possibility that some of their Leo A Cepheids were long-period red variables.

A color-magnitude diagram showing our variable stars is given in Figure 5, with the variable stars marked as circles (size represents the light-curve quality). We emphasize that colors and magnitudes were not used to determine our sample; the restriction of variable stars into two populations on the CMD is therefore real and not a selection effect. We interpret the brighter population (*open circles*) as classical Cepheids and the fainter population (*solid circles*) as RR Lyrae stars.

4. RR LYRAE STARS

Our primary goal in this project was a search for RR Lyrae stars. Eight candidates were found. An expanded CMD detailing this region is shown in Figure 6. Two of these (C1-V03 and C1-V07) have extremely clean light curves without period aliasing, were well photometered and isolated from any source of potential contamination, and have colors that place them in the instability strip. We therefore claim that these are bona fide RR Lyrae stars. C1-V03 has a period and light-curve shape (rapid rise, slow descent) that make it appear to be an RRab. C1-V07 has a shorter period and longer ascent time, making it appear to be an RRc.

A third (C2-V79) is another good candidate. Its red color appears to be the result of a bad point in *R*, as well as of phase coverage; eliminating the point moves the star bluer by 0.3 mag and accounting for the fact that it was observed in *R* only near maximum moves it bluer by an additional 0.2 mag. We cannot make a type classification from its light curve, as it was not observed while ascending. However, its long period would make it an RRab. Finally, C2-V66 also appears to be a very likely RR Lyrae; its having two possible periods lowered it to a quality rating of 2 and makes a classification impossible. As with C2-V79, it was observed only in *R* near maximum and is thus bluer than its listed color.

We are less certain of the nature of the other four candidates. C1-V01 has a period that seems too short to be an RR Lyrae (though it could be an RRd). C2-V33 does not have the light-curve shape one would expect to see at that period, perhaps indicating that it is an anomalous Cepheid rather than an RR Lyrae. C2-V56 fits an RRc template light curve reasonably well at the period of 0.40 days, but a few points fall well off that template. (Its red color is caused by poor phase coverage; it is likely 0.15–0.2 mag bluer than our measured color of $V-R = 0.42$.) Finally, C2-V80 is our faintest candidate and thus has large error bars that prohibit a definitive classification.

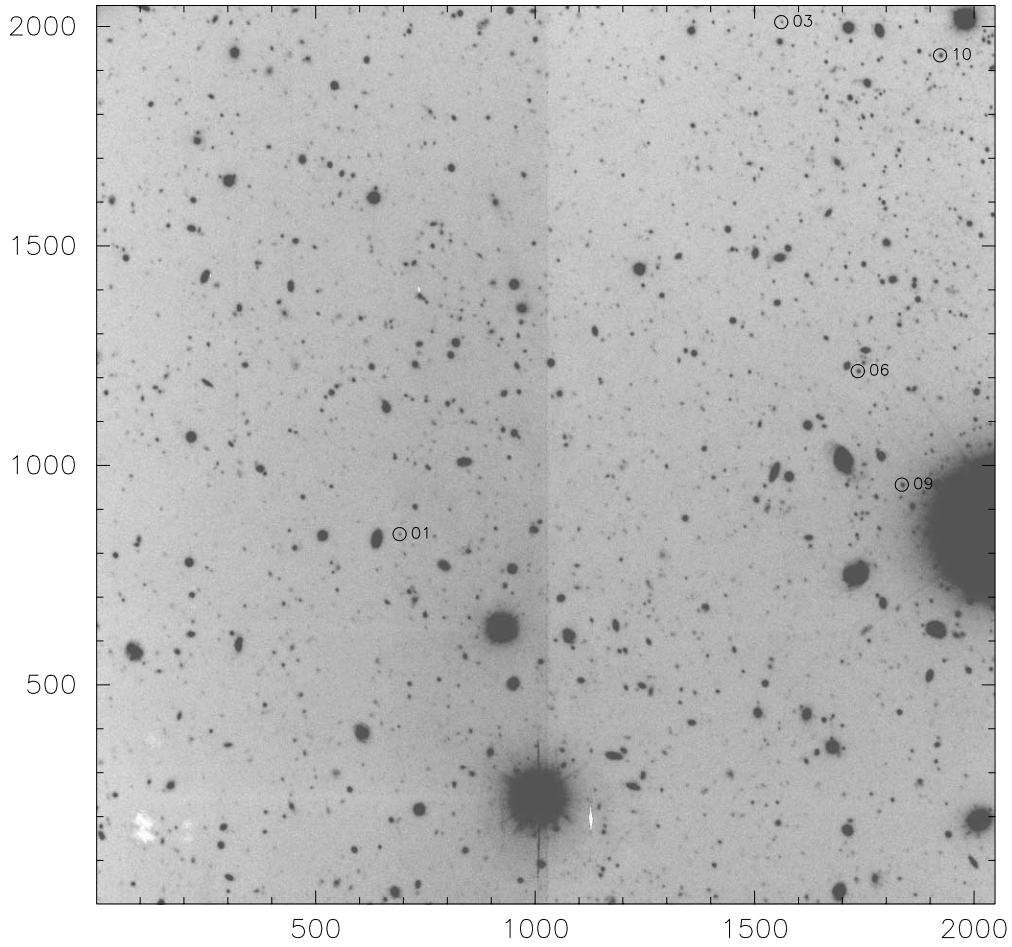

FIG. 3*b*

By weighting by the light-curve qualities of all eight candidate RR Lyrae stars, we measure a mean magnitude of $\langle V \rangle = 25.11 \pm 0.06$, where the quoted uncertainty is the uncertainty in the mean. Using only the four best RR Lyrae stars, we find $\langle V \rangle = 25.08 \pm 0.05$. Finally, the two bona fide RR Lyrae stars produce a mean magnitude of $\langle V \rangle = 25.10 \pm 0.09$. We adopt the final value, which is the most conservative of the values. The DoPHOT magnitudes are not significantly different from these values. Given that our completeness reached well beyond the RR Lyrae stars ($V \sim 25$) in the halo of Leo A (where all eight candidates are located), we find it unlikely that our calculated mean magnitude is biased.

To determine the distance, we adopt the RR Lyrae absolute magnitude calibration of Carretta et al. (2000):

$$M_V = (0.18 \pm 0.09)([\mathrm{Fe/H}] + 1.5) + (0.57 \pm 0.07) \; . \qquad (2)$$

We choose this calibration largely because its zero point is nearly identical to what we measured in IC 1613 ($M_V = 0.61 \pm 0.08$ at $[\mathrm{M/H}] = -1.3 \pm 0.2$); see Dolphin et al. (2001b) for a more detailed discussion of the various RR Lyrae zero-point values. As is demonstrated below, the slope of the relation is irrelevant to this discussion.

Since no spectroscopy exists for stars in Leo A, the metallicity of Leo A RR Lyrae stars is very uncertain. We can attempt to estimate this value with two methods. First, we can fit the WFPC2 data of Tolstoy et al. (1998) to the theoretical isochrones of Girardi et al. (2000), assuming an age of 10–15 Gyr. We find that the red giant branch (RGB) color can be fitted with a metallicity of $[\mathrm{M/H}] = -1.8 \pm 0.3$. The advantage of this determination is that it is based on old stars; the disadvantage is that metallicities measured by broadband photometry are less accurate than those determined spectroscopically.

An additional constraint is given by the present-day metallicity, as measured by H II region spectra ($[\mathrm{O/H}] = -1.5 \pm 0.2$; van Zee, Skillman, & Haynes 1999). Adopting an [O/Fe] ratio, we can use this as an upper limit to the metallicity of the RR Lyrae stars in Leo A. While older stars in our galaxy (halo and globular cluster stars) at the metallicity of Leo A show α-element enhancements of $\sim$0.4 dex and those in the Draco, Ursa Minor, and Sextans dSph galaxies show enhancements of $\sim$0.3 dex (Shetrone, Côté, & Sargent 2001), these enhancements are not seen in the young populations of other metal-poor dwarf irregular galaxies, such as the SMC (Venn 1999) and NGC 6822 (Venn et al. 2001). Thus we adopt an α-element enhancement of $[\mathrm{O/Fe}] = 0.2 \pm 0.2$ dex, which results in a present-day metallicity of $[\mathrm{M/H}] = -1.7 \pm 0.3$.

We believe the spectroscopic determination is more accurate (given uncertainties in the isochrones) and thus adopt the value of $[\mathrm{Fe/H}] = -1.7 \pm 0.3$, which results in an RR Lyrae absolute magnitude of $M_V = 0.53 \pm 0.08$. Adopting

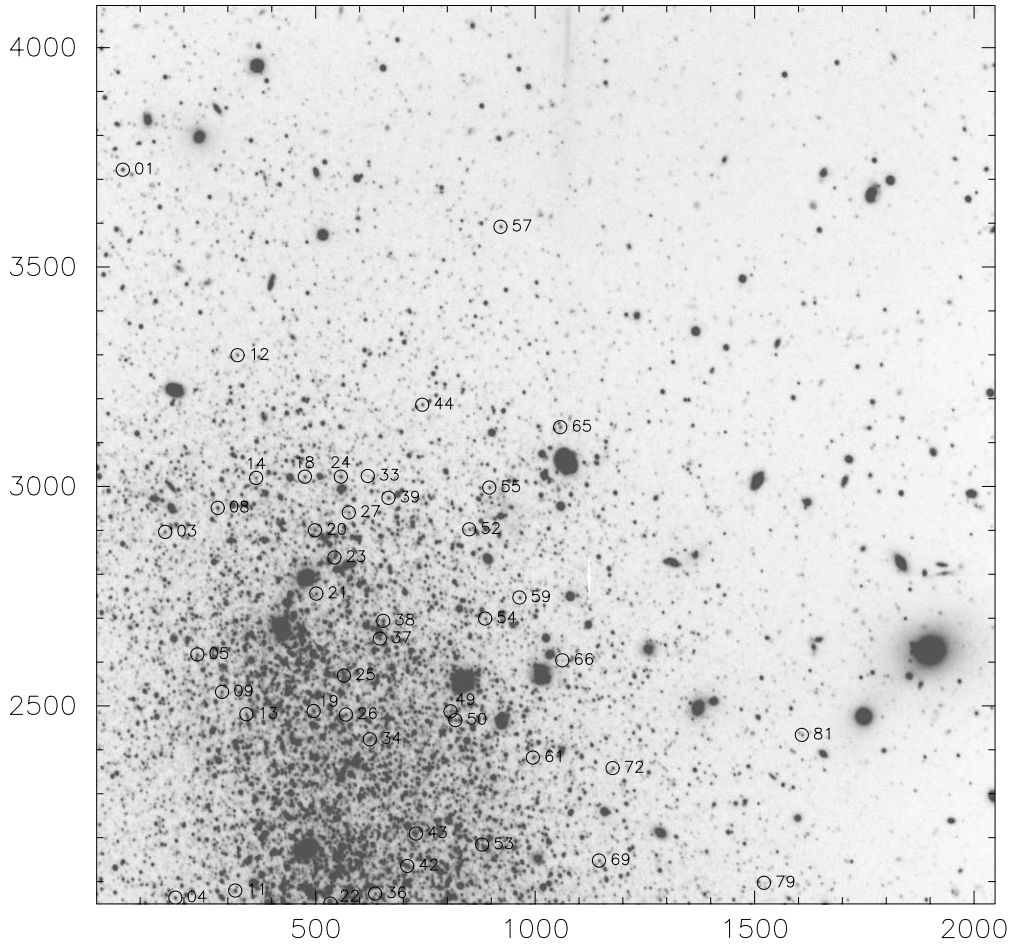

FIG. 3*c*

an extinction of $A_V = 0.06$ (Schlegel, Finkbeiner, & Davis 1998), we measure a true distance modulus of $(m - M)_0 = 24.51 \pm 0.12$, corresponding to a distance of 0.80 ± 0.04 Mpc. Because the metallicity is very close to [Fe/H] $= -1.5$, the assumed slope in the RR Lyrae absolute magnitude calibration has little effect on the distance. Adopting a steeper slope of 0.30 mag dex^{-1} (Sandage 1993), for example, would only increase the distance modulus by 0.02 mag; adding this difference in quadrature to our 0.12 mag uncertainty does not increase the uncertainty.

Our preferred distance is a factor of 3 smaller than that of $(m - M)_0 = 26.74$ measured by Hoessel et al. (1994), but consistent with that of $(m - M)_0 = 24.5 \pm 0.2$ determined from the RGB tip by Tolstoy et al. (1998). [They were unsure whether or not a population older than 1.5 Gyr existed in Leo A, leading them to base their final distance of $(m - M)_0 = 24.2 \pm 0.2$ largely on the blue loop and red clump positions rather than on that of the RGB tip, which is not a standard candle at ages younger than $\sim$2 Gyr.] We also note that their "young RC" distance of $(m - M)_0 = 24.2 \pm 0.2$ is based on an assumed red clump absolute magnitude of $M_I \simeq -0.4$; the semiempirical (and thus less model dependent) technique described by Dolphin et al. (2001b) produces a more accurate absolute magnitude of $M_I = -0.67 \pm 0.1$ for the metallicity and age assumed by Tolstoy et al. (1998), thus increasing their red clump distance by $\sim$0.3 mag and making it consistent with the other distances. This 15% change in the Leo A distance could significantly alter the star formation history they determined; that problem should thus be revisited in light of our revised distance.

We note the possibility that the stars we are detecting are anomalous Cepheids rather than RR Lyrae stars. We believe this not to be the case for several reasons. As anomalous Cepheids tend to be $\sim$0.5 mag brighter than RR Lyrae stars, this would push the Leo A distance to $(m - M)_0 = 25.0$ and would be inconsistent with the RGB tip and red clump distances quoted above. Additionally, we do see short-period variables, discussed in the following section, which are about half a magnitude brighter than the RR Lyrae stars.

With the discovery of RR Lyrae stars in Leo A, we have definitively located a population of "ancient" (more than $\sim$11 Gyr; Walker 1989) stars in Leo A, a galaxy previously considered a candidate for a delayed onset of star formation (Tolstoy et al. 1998). A quantitative estimate of the extent of this population is extremely difficult to determine because of the completeness of our RR Lyrae survey, which is zero inside the region where young stars are present. Scaling from the relatively uncrowded chip 1, we estimate a total of $\sim$50 RR Lyrae stars in the entire galaxy, with a 1 σ lower limit of $\sim$10. Adopting the well-populated horizontal branch of M5 (Reid 1996) and its 65 known RR Lyrae stars (Kaluzny et al. 2000) as typical of an ancient population, we

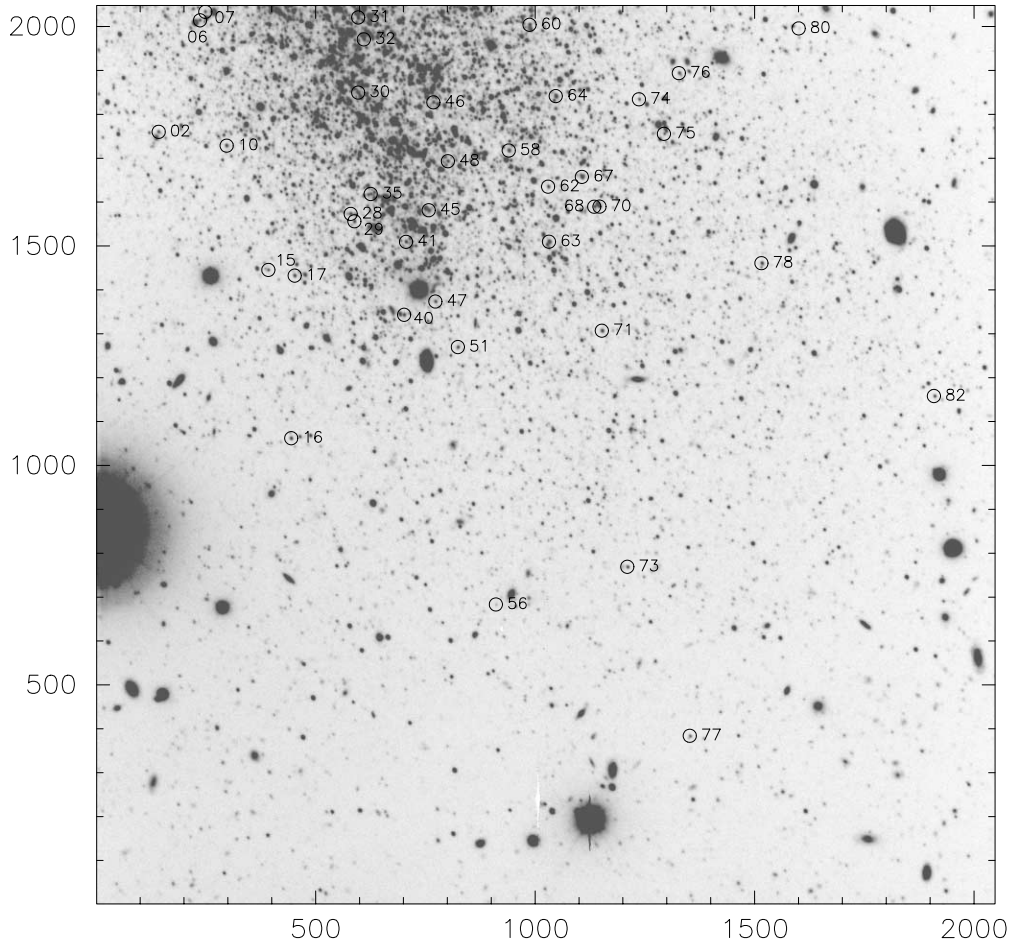

FIG. 3*d*

estimate that such an M5-like population would account for 0.1%–1% of the V luminosity of Leo A. Instead, by using a globular cluster with proportionally fewer RR Lyrae stars (such as M13), the ancient population could be larger by an order of magnitude or more; we thus quote only a value of 0.1% as the lower limit of the contribution. Because of the large uncertainties in this calculation, an accurate quantification of the ancient population would require photometry reaching the ancient main-sequence turnoffs ($M_V \sim +4$).

5. SHORT-PERIOD CEPHEIDS

Although the primary goal of our project was the detection of RR Lyrae stars in Leo A, our 2 day baseline made us sensitive to any variable star with a period of 2 days or less. It was perhaps surprising, given the lack of previously known Cepheids in Leo A, that 91% of our detected variable stars (84 out of 92) are brighter than $V = 24.5$, fall in or near the instability strip, and therefore are apparently Cepheids. Figure 7 shows our CMD, expanded around the area of the instability strip; small dots represent all stars, while the circles represent our variables. The sizes of the circles indicate the light-curve quality. Note that the majority of objects lie near the intersection of the blue loop with the instability strip. Variables with ambiguous periods, as well as those with quality ratings of 2 or lower (Dolphin et al. 2001b), are omitted, leaving 66 Cepheids with accurately measured periods and excellent light curves. We plot the P-L diagram of these variables in Figure 8.

Because of the change in the P-L relation slope at a period of 2 days (Bauer et al. 1999), we had to calculate P-L relations for short-period Cepheids such as those seen in Leo A instead of using the published relations of Madore & Freedman (1991) or Udalski et al. (1999b). To do this, we selected objects with periods of 2 days or less from the OGLE SMC Cepheid database (Udalski et al. 1999a) and fitted the following relations for fundamental mode and first-overtone pulsators:

$$M_V(\mathrm{FM}) = -3.14 \log (P) - 1.04 , \quad (3)$$

$$M_V(\mathrm{FO}) = -3.39 \log (P) - 1.73 . \quad (4)$$

Using the distance modulus of $(m-M)_0 = 24.51 \pm 0.12$ determined from the RR Lyrae stars, we plot the P-L relations as lines on Figure 8.

Since we have insufficient phase coverage to attempt Fourier decomposition, we must classify Cepheids simply on their positions in the P-L diagram. From Figure 8, we classify 19 of our 66 Cepheids as fundamental mode, 38 as first overtone, and two as second overtone. The remaining seven Cepheids fall between the relations and thus cannot be definitively classified.

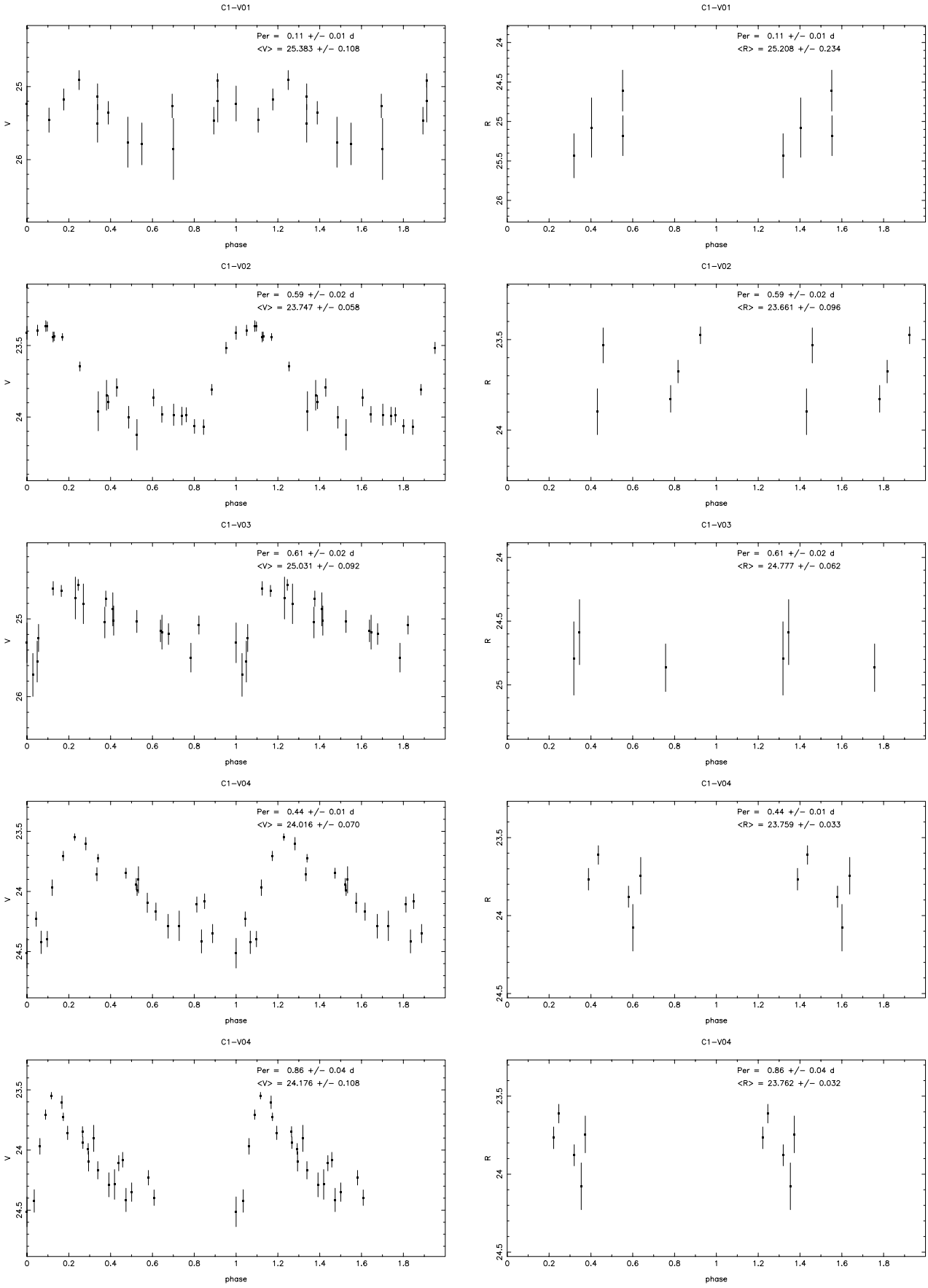

FIG. 4.—Light curves of Leo A variable stars

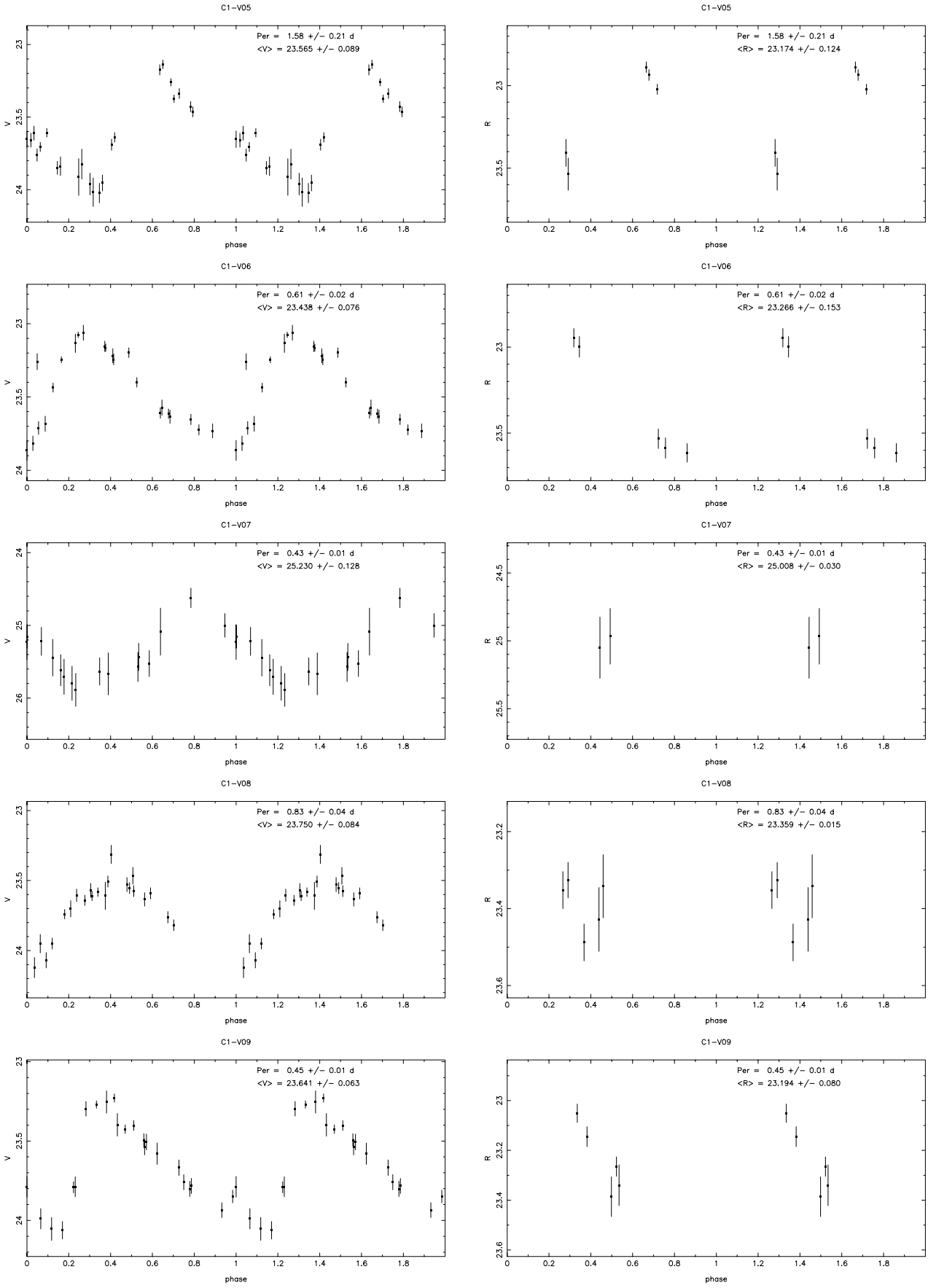

FIG. 4.—*Continued*

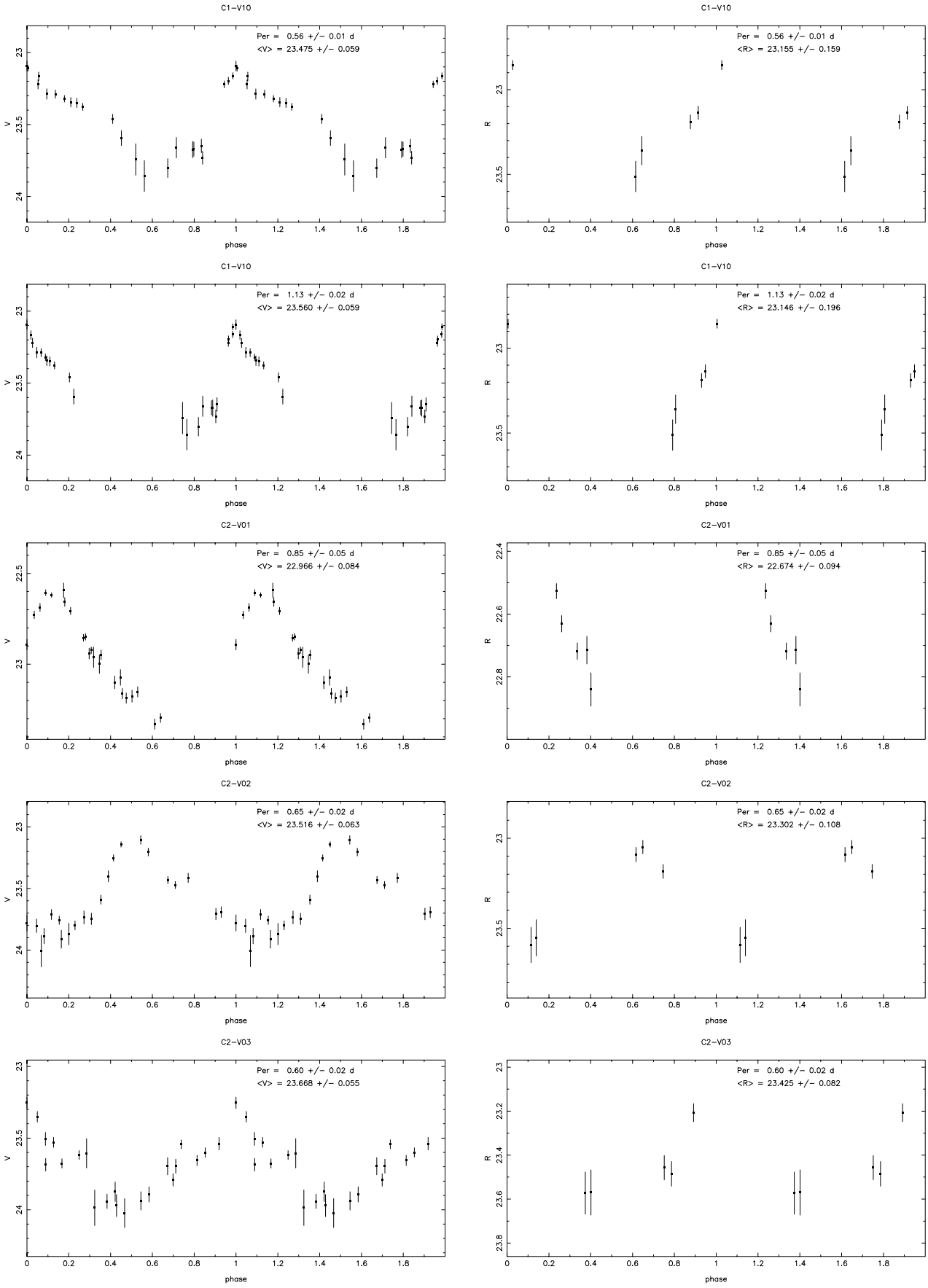

FIG. 4.—*Continued*

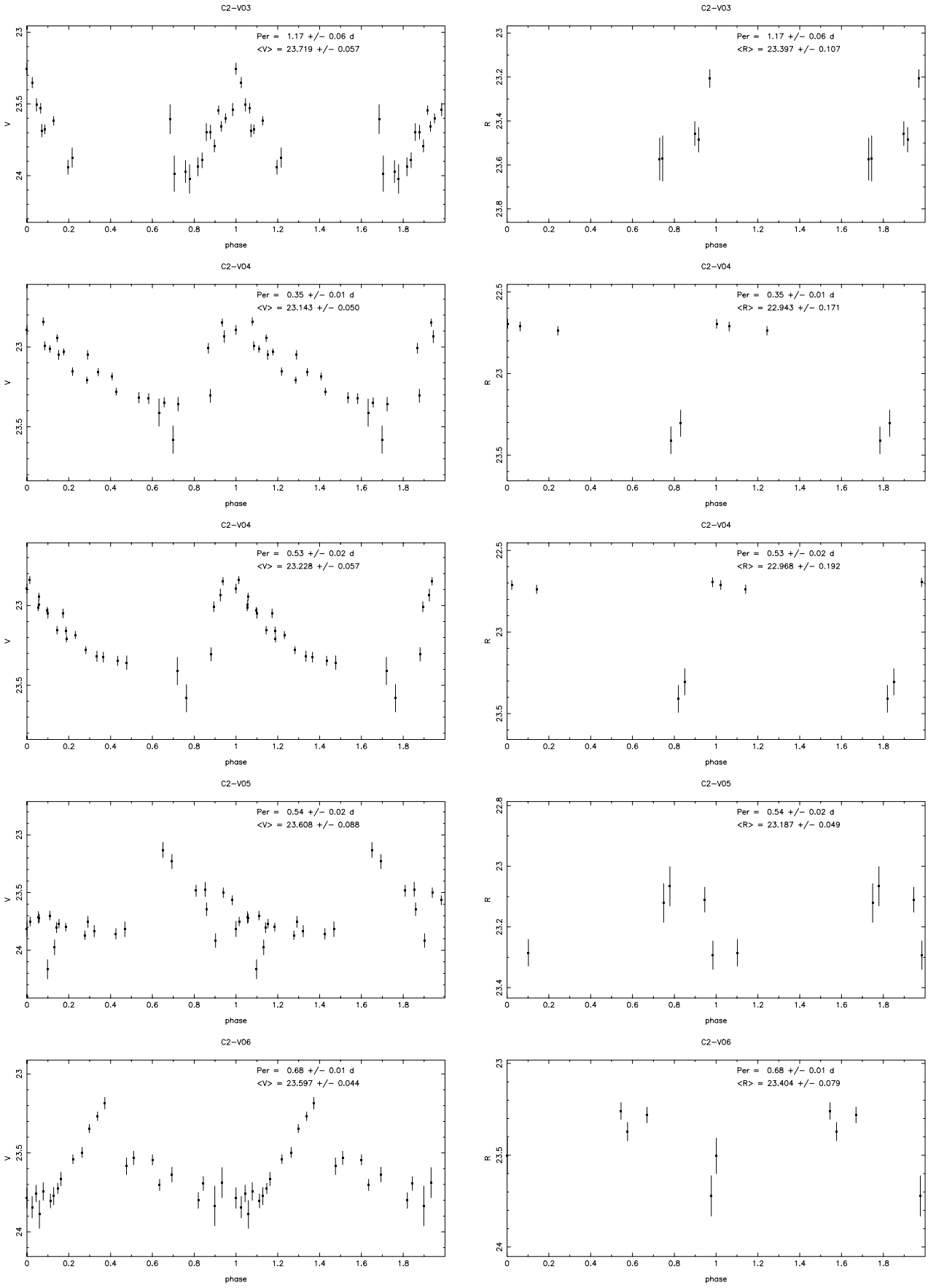

FIG. 4.—*Continued*

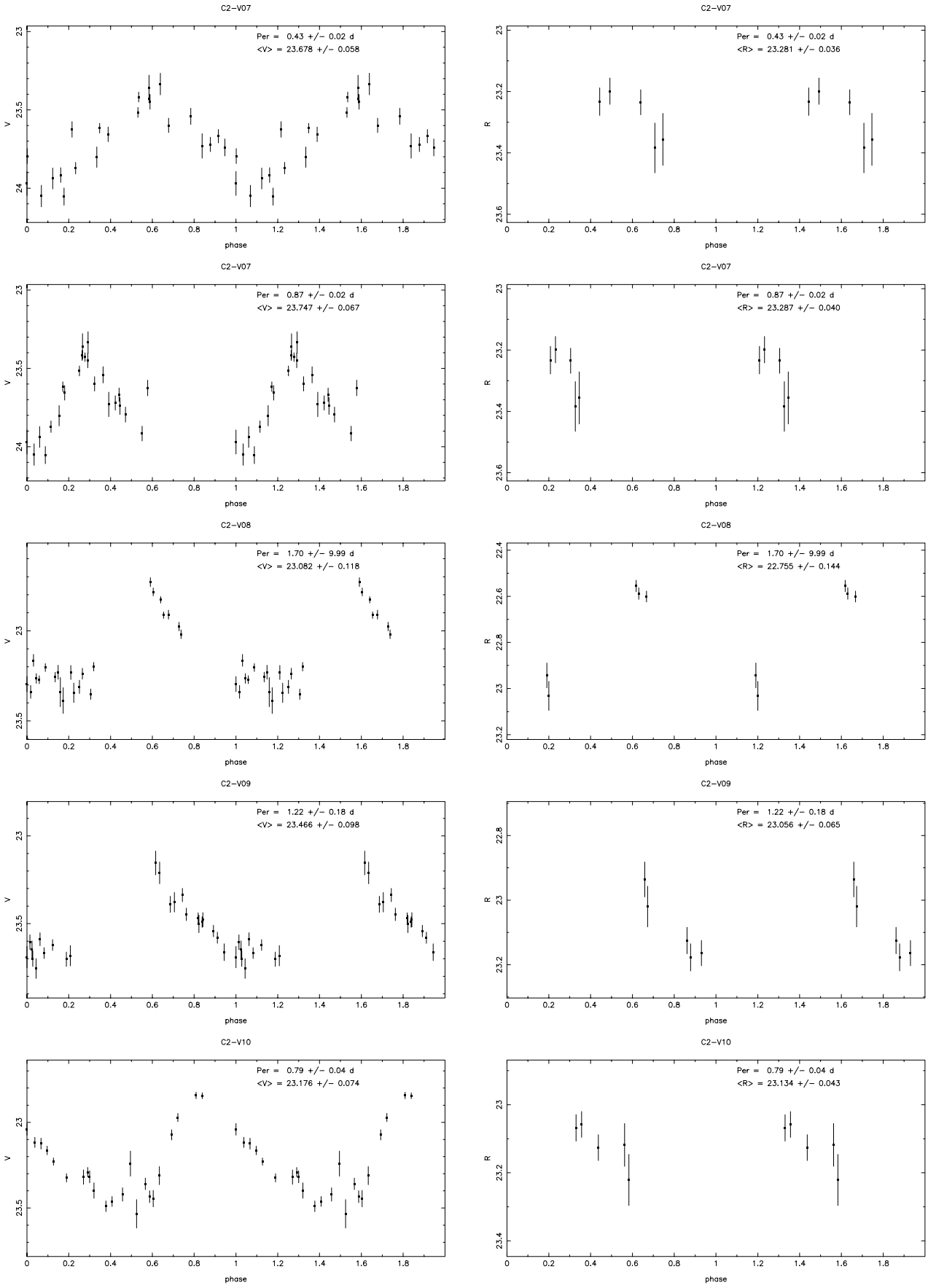

FIG. 4.—*Continued*

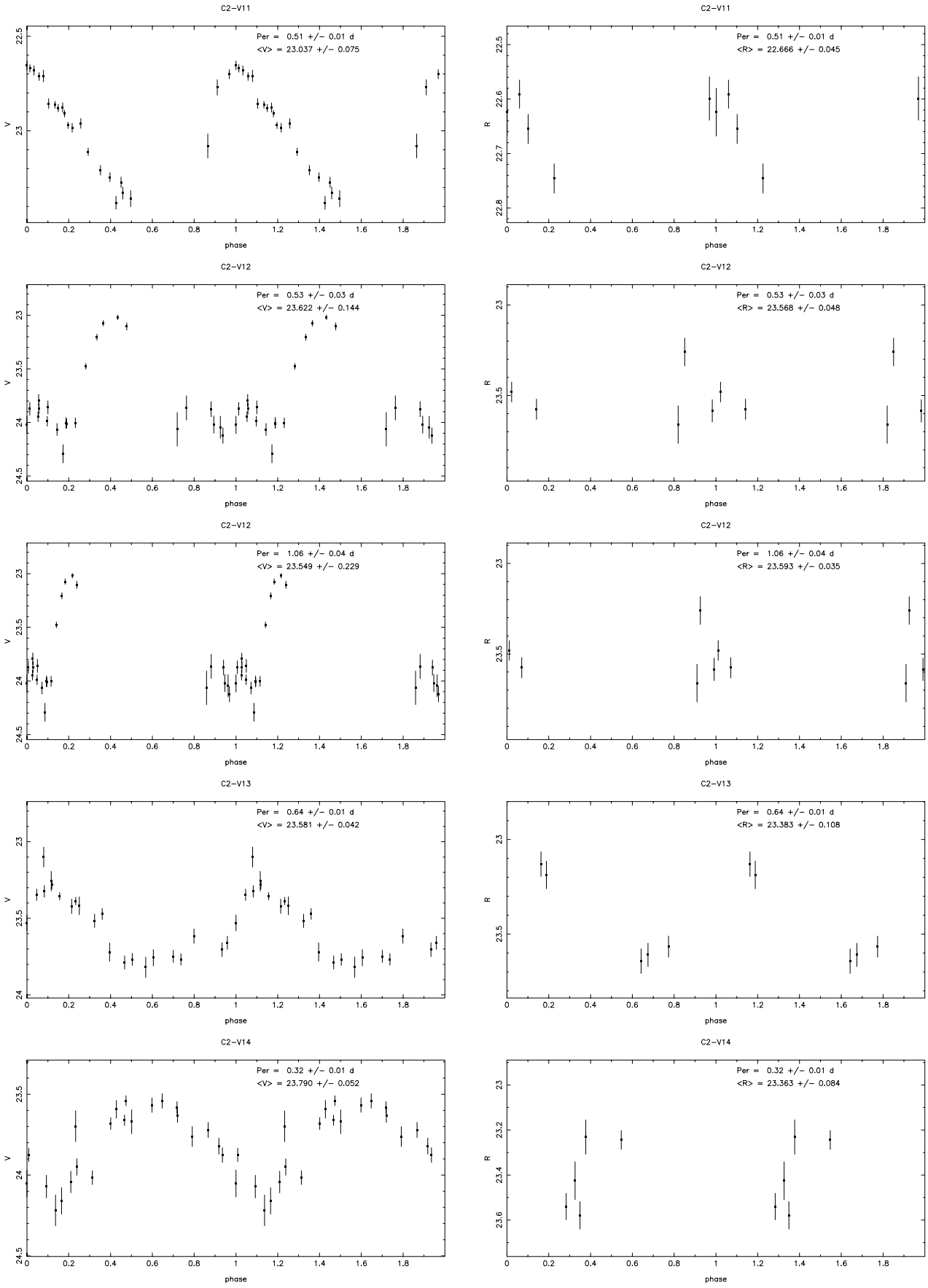

FIG. 4.—*Continued*

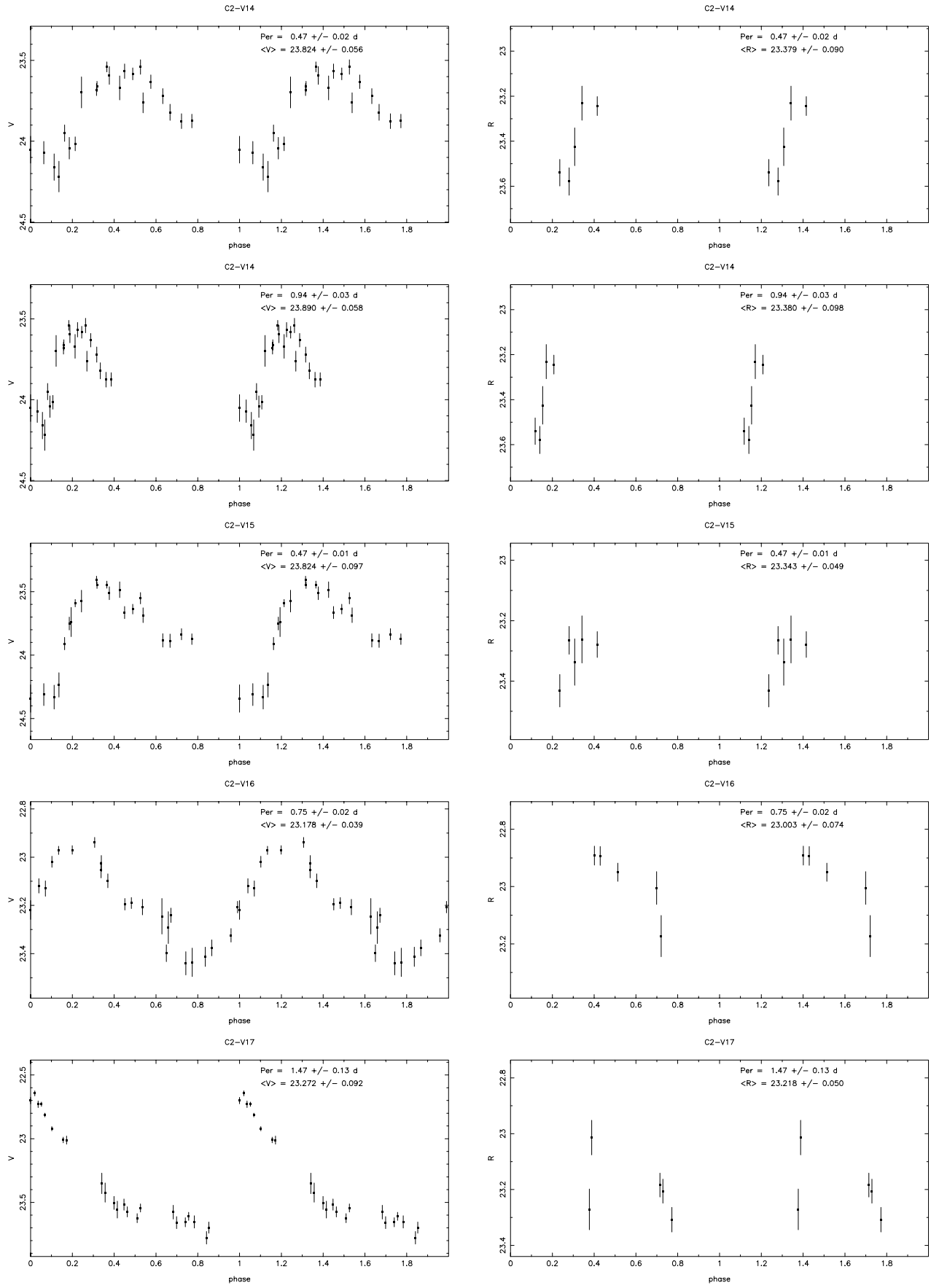

FIG. 4.—*Continued*

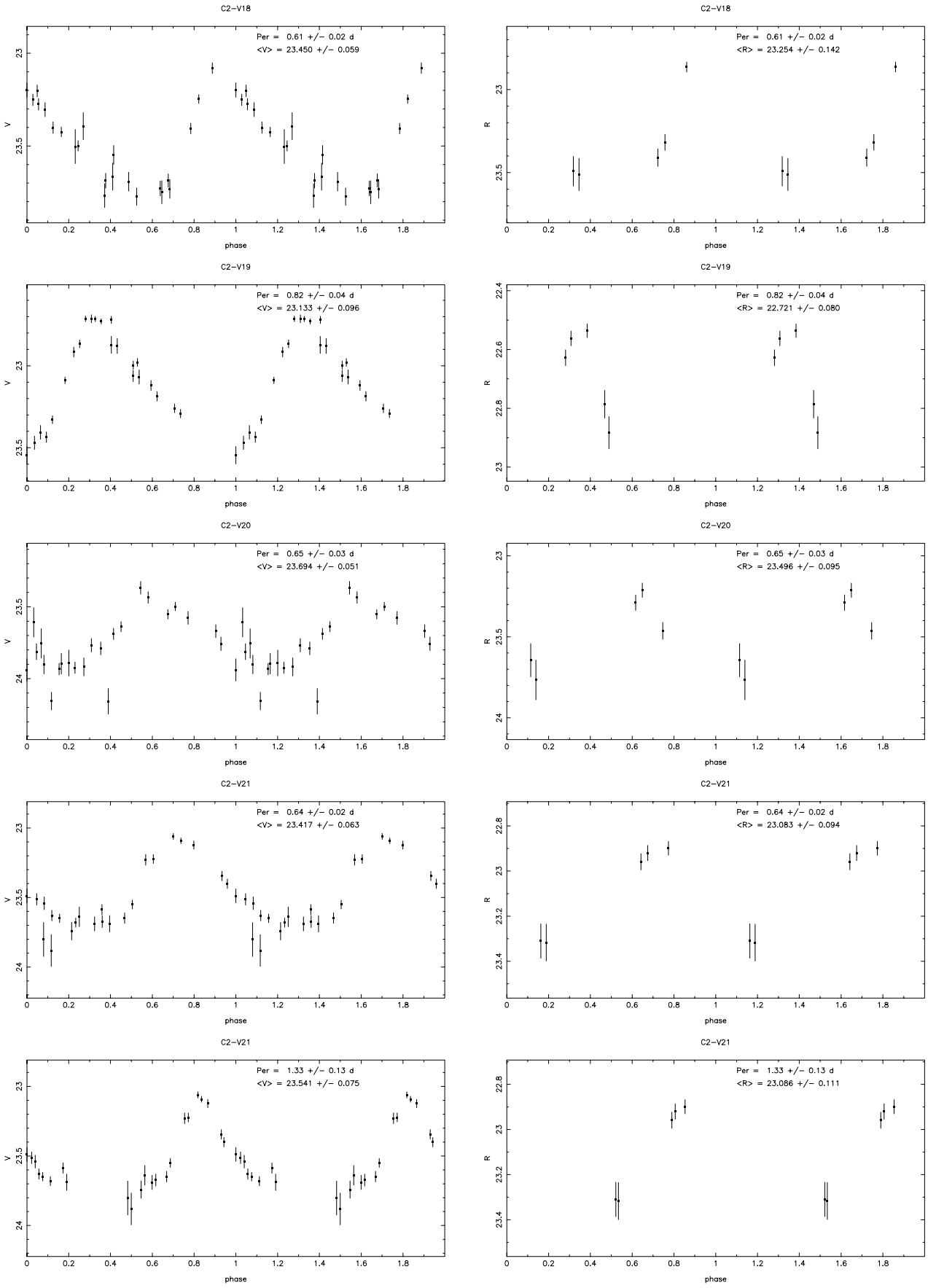

FIG. 4.—*Continued*

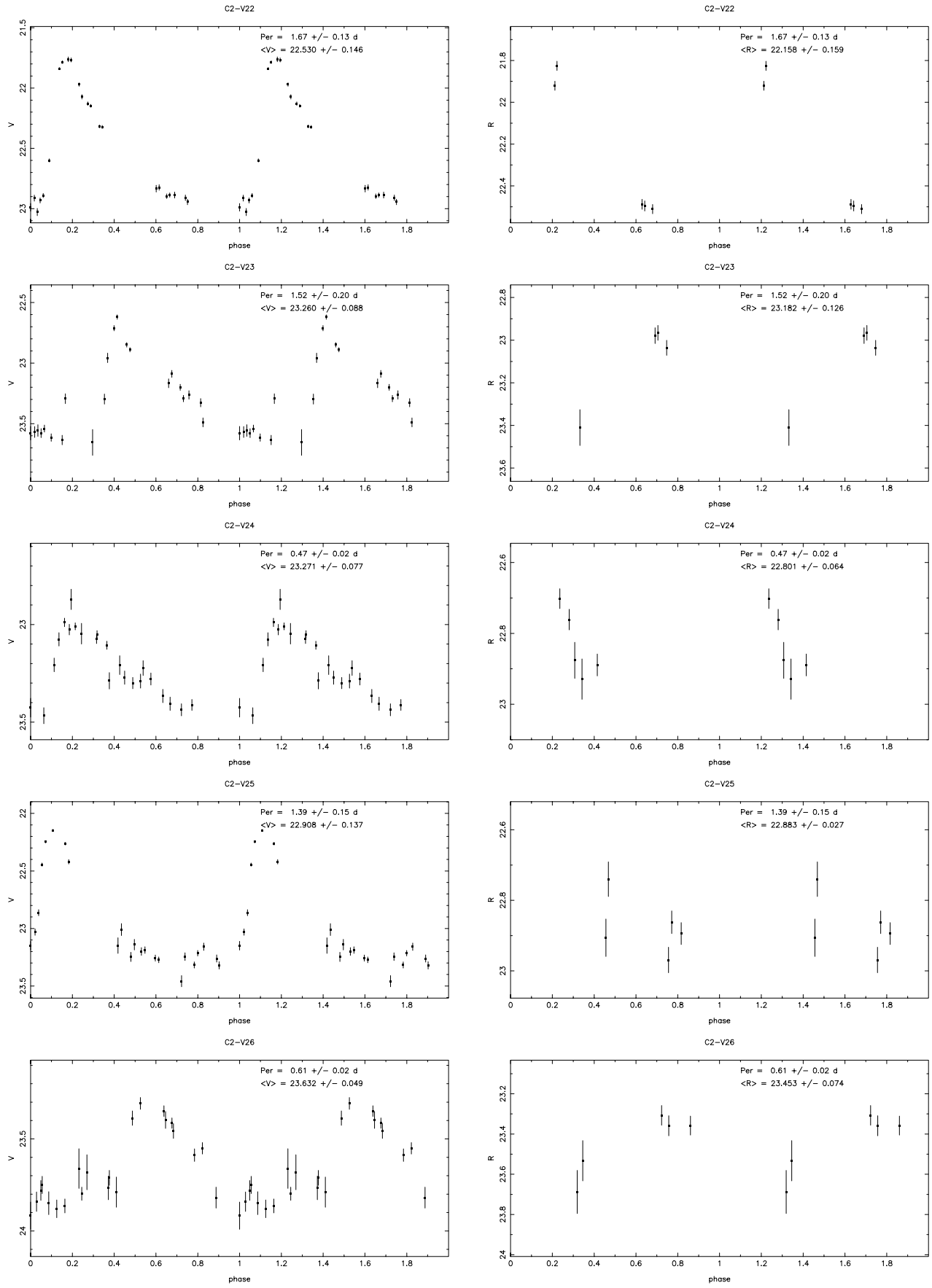

FIG. 4.—*Continued*

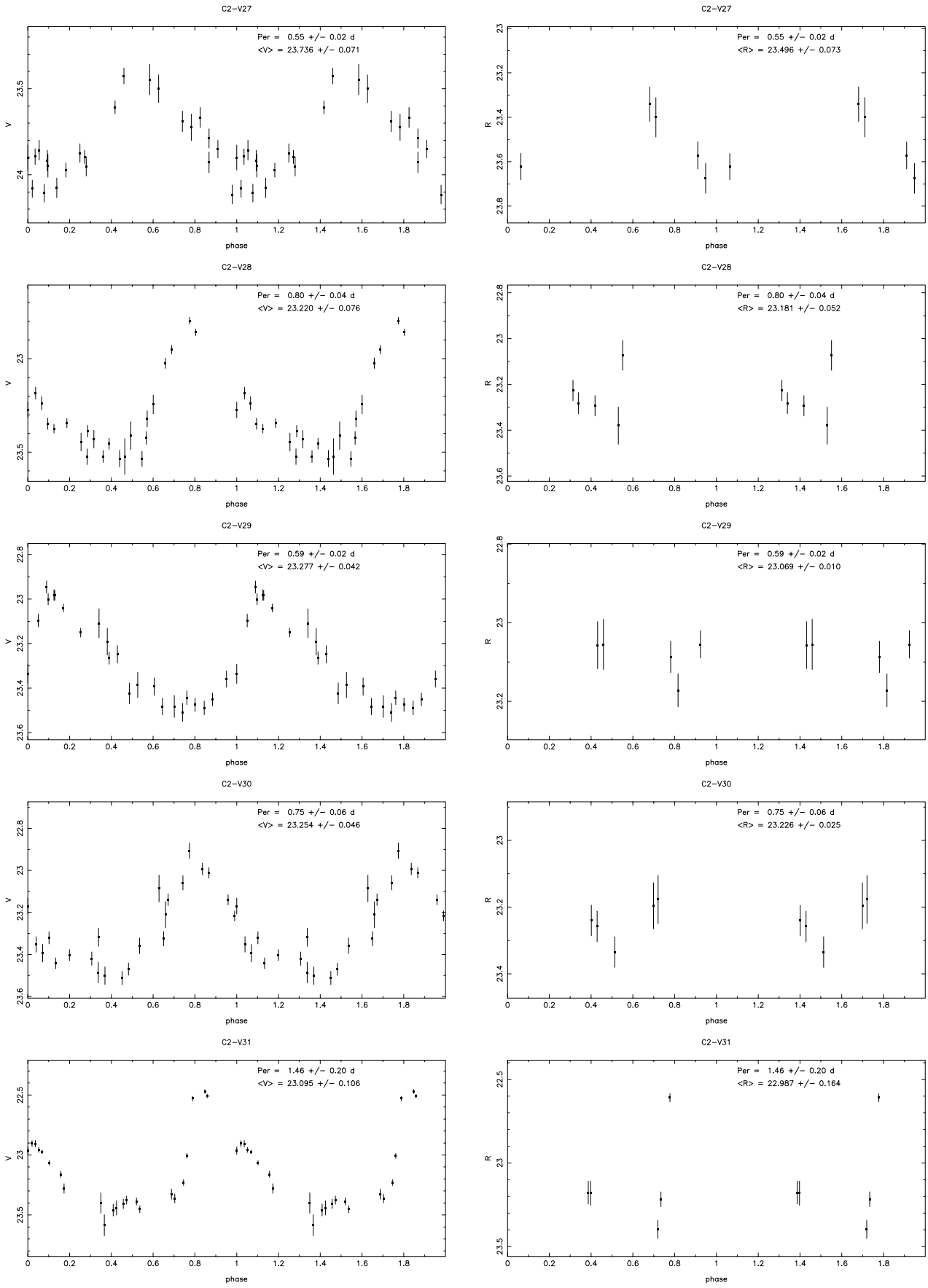

FIG. 4.—*Continued*

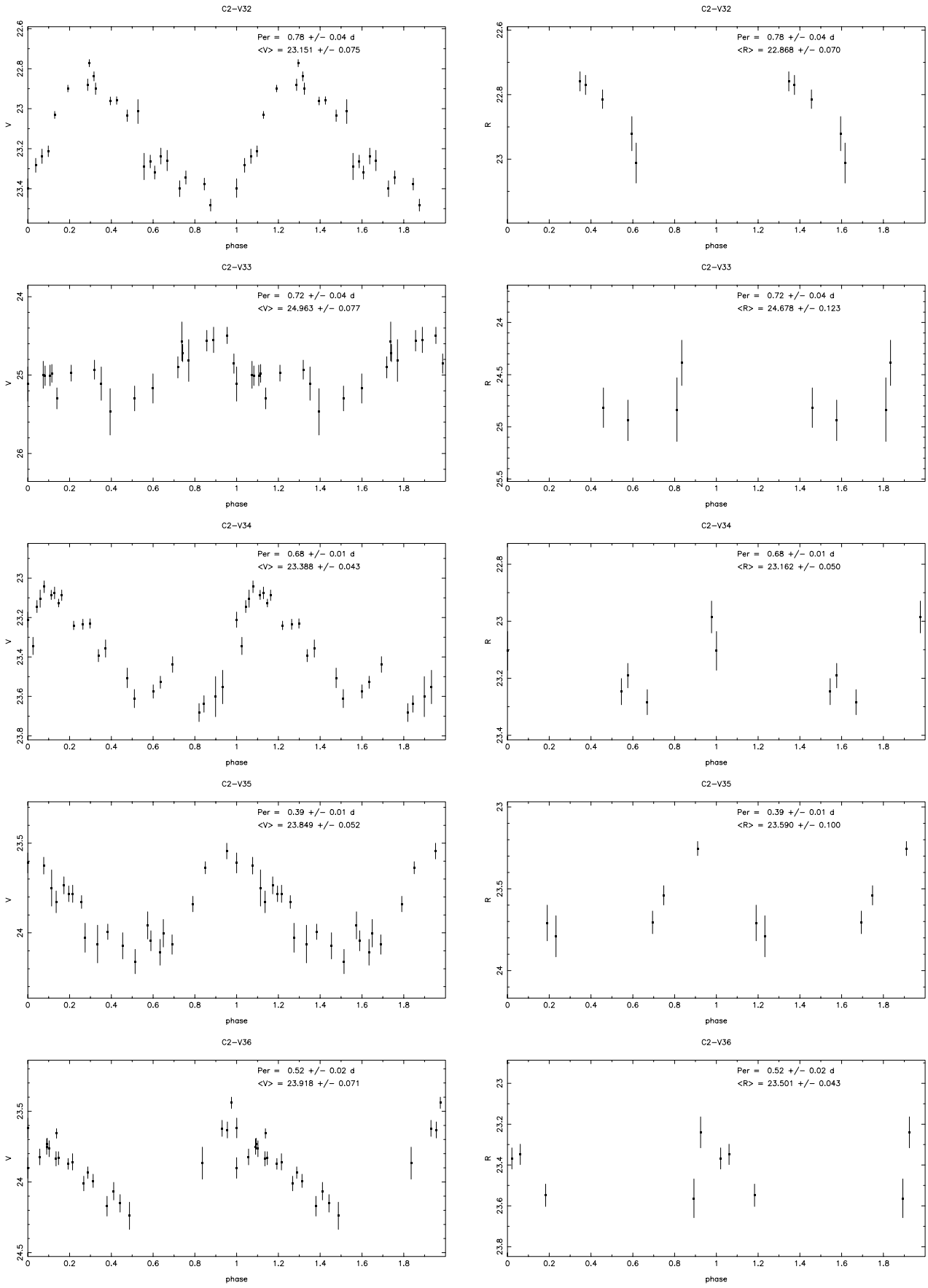

FIG. 4.—*Continued*

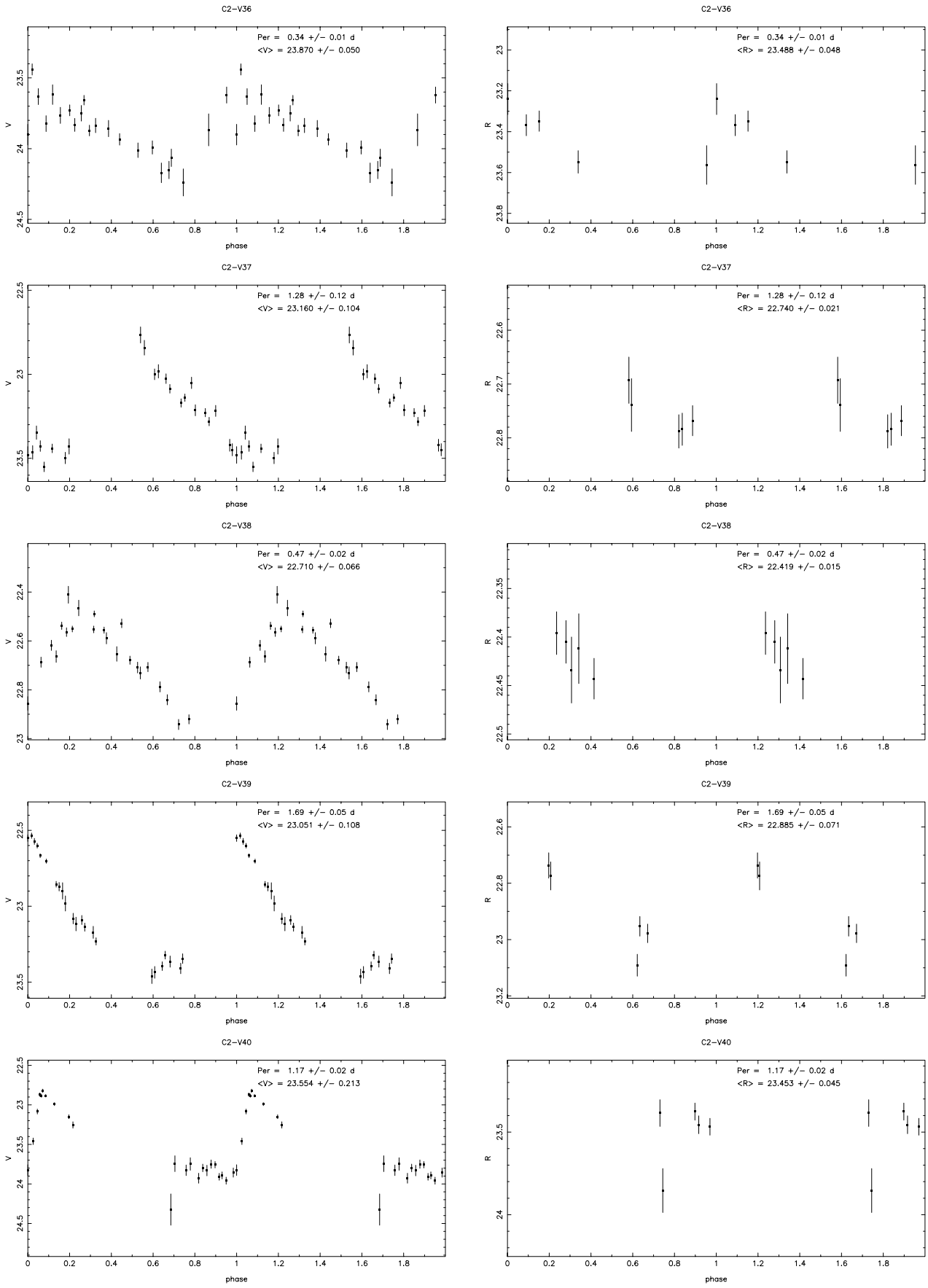

FIG. 4.—*Continued*

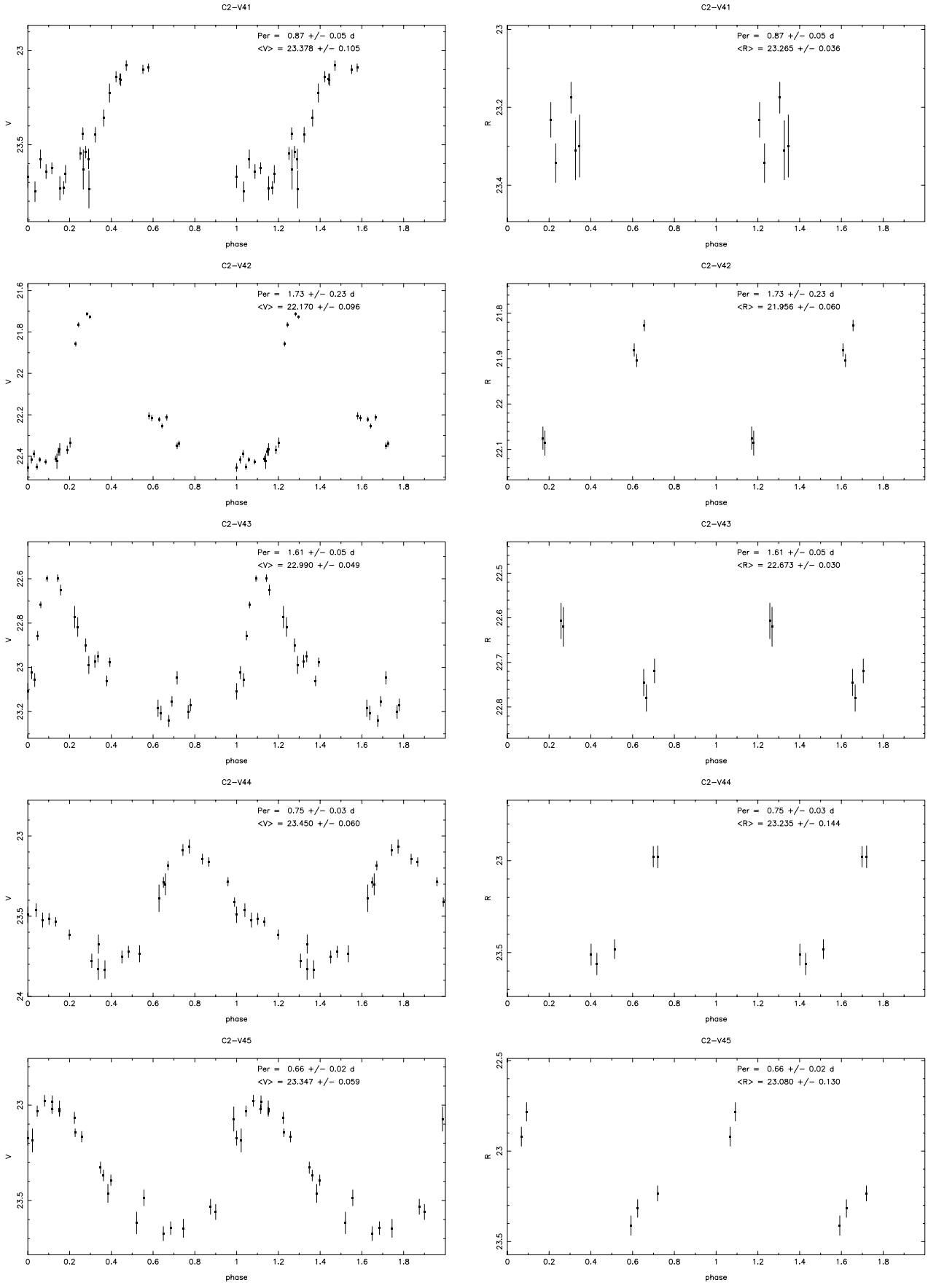

FIG. 4.—*Continued*

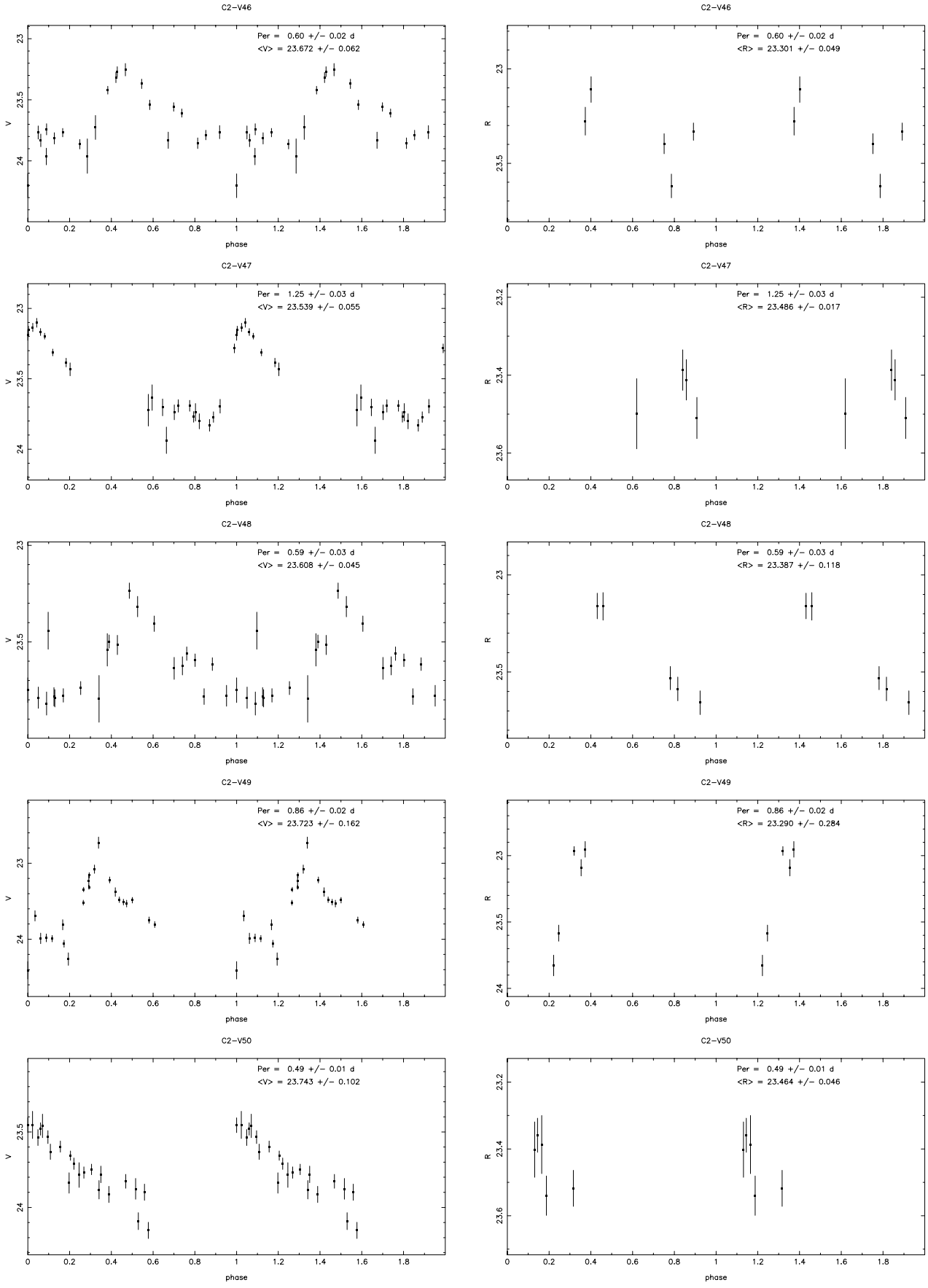

FIG. 4.—*Continued*

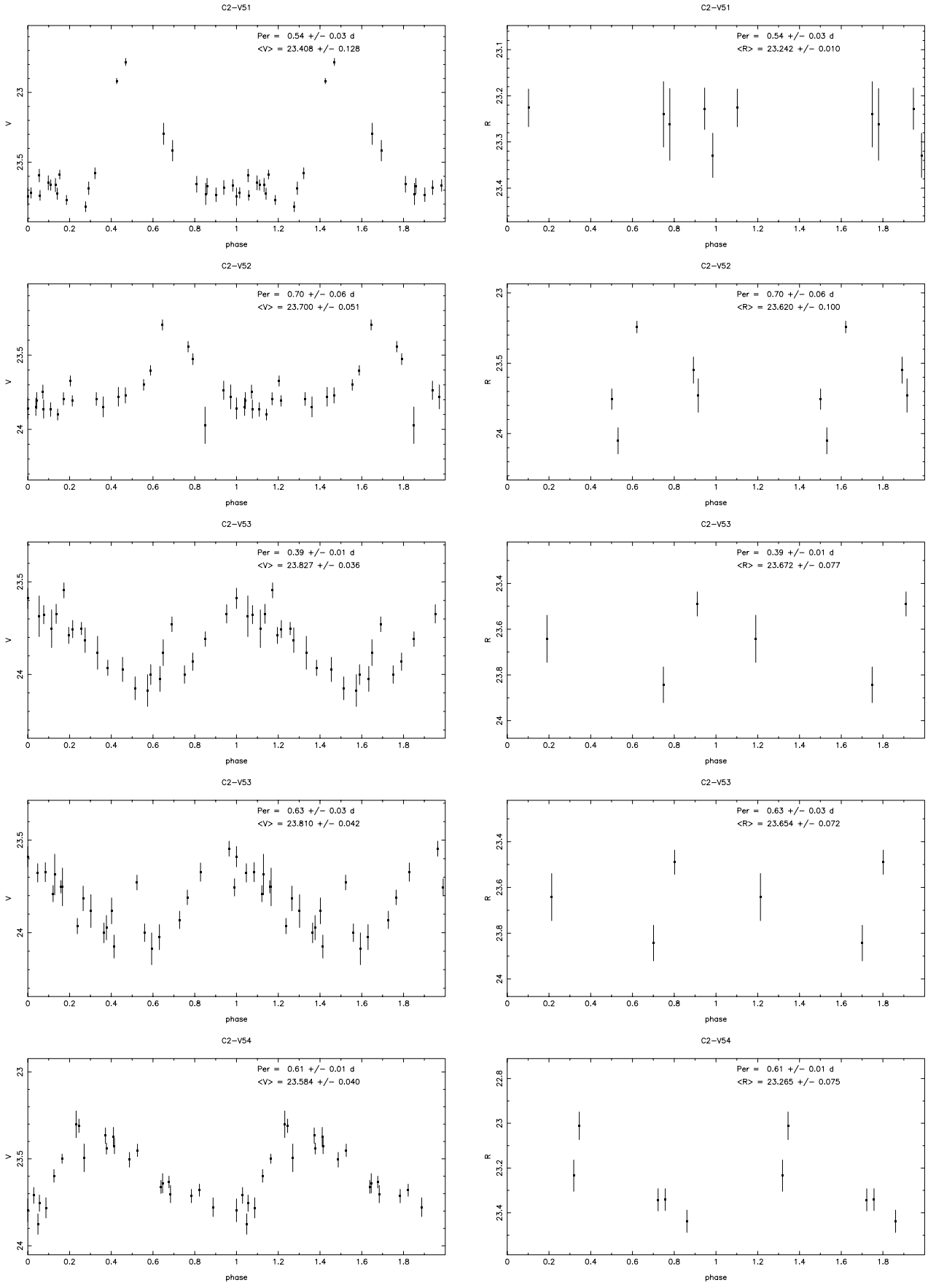

FIG. 4.—*Continued*

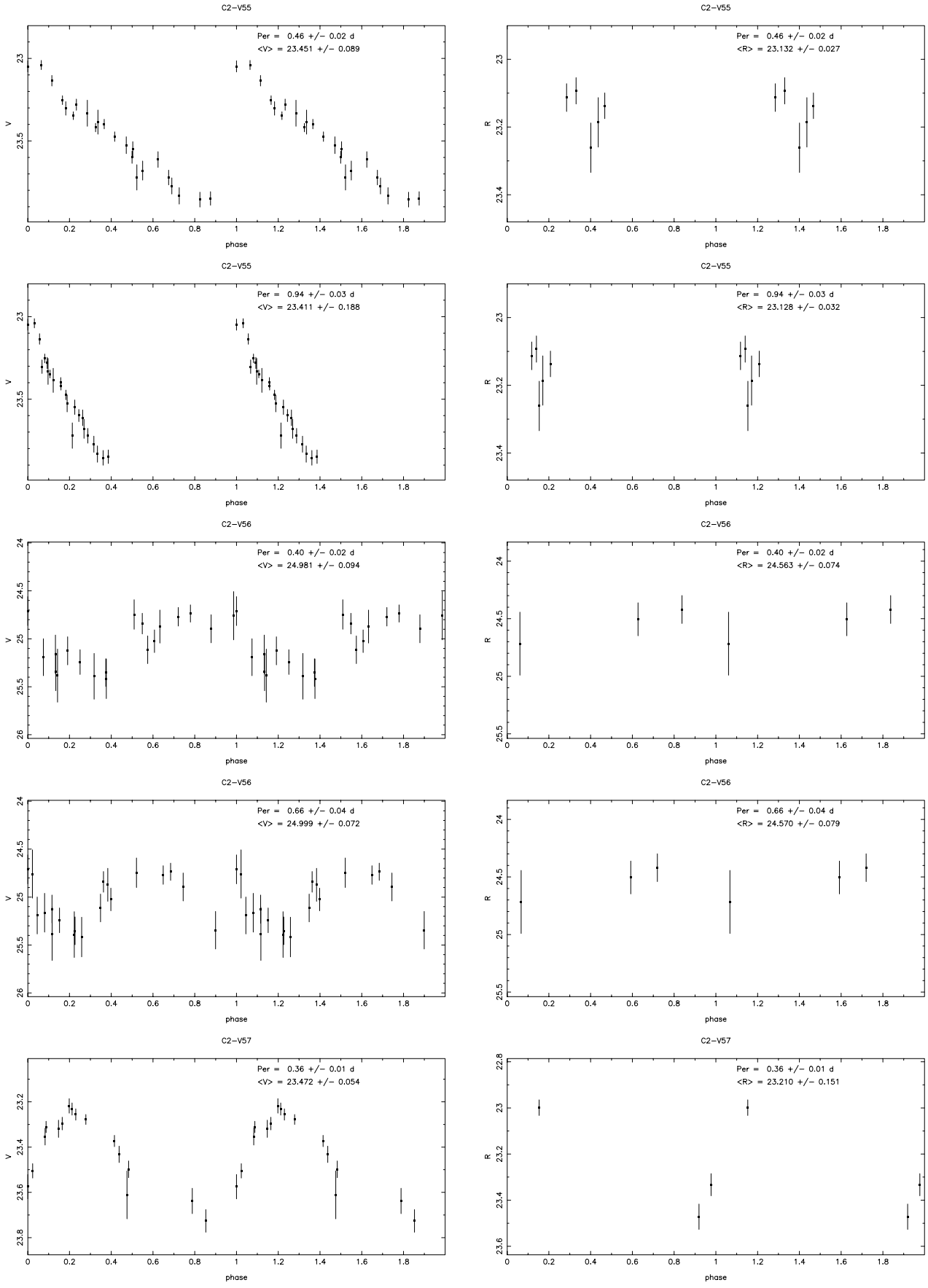

FIG. 4.—*Continued*

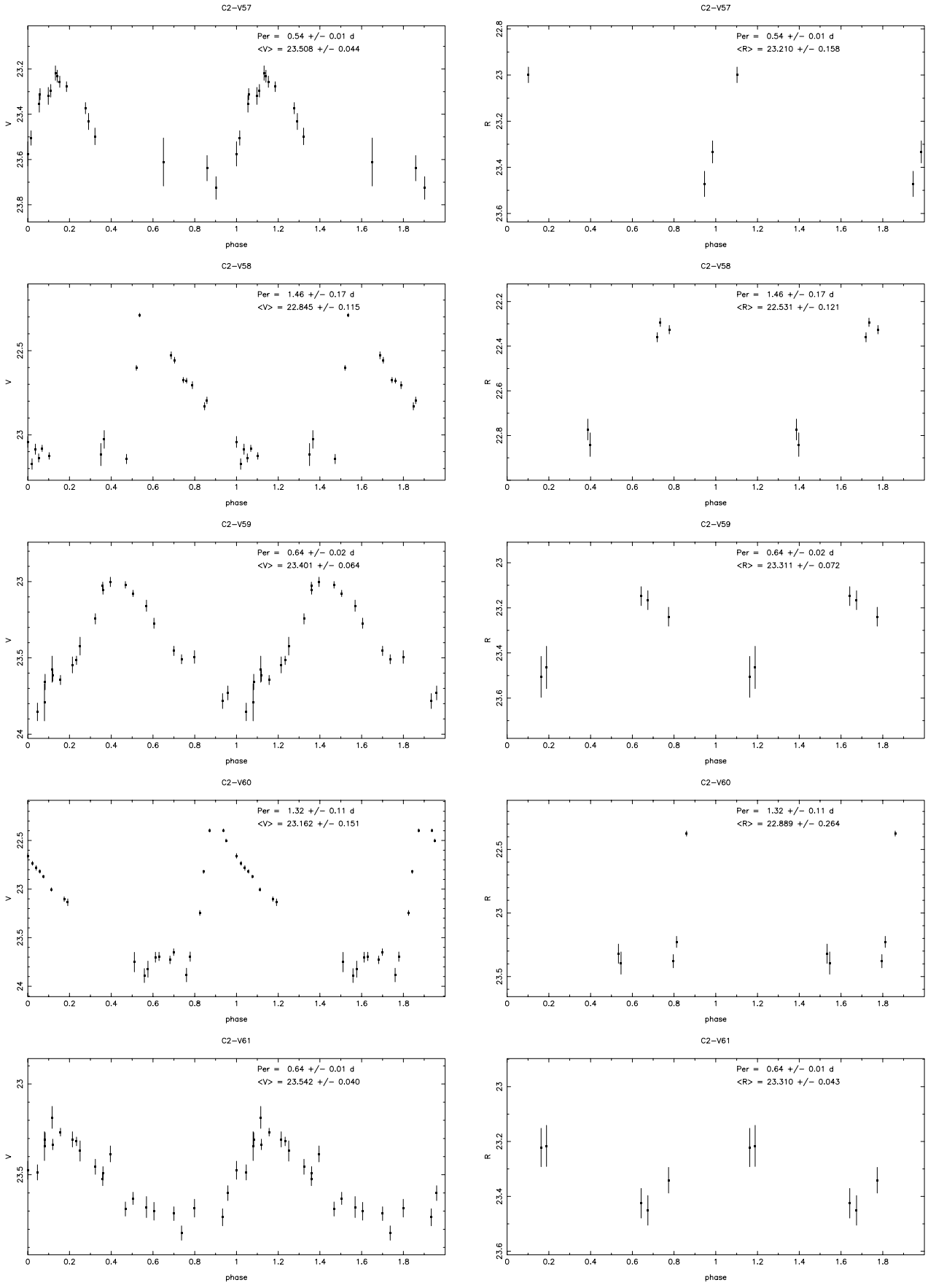

FIG. 4.—*Continued*

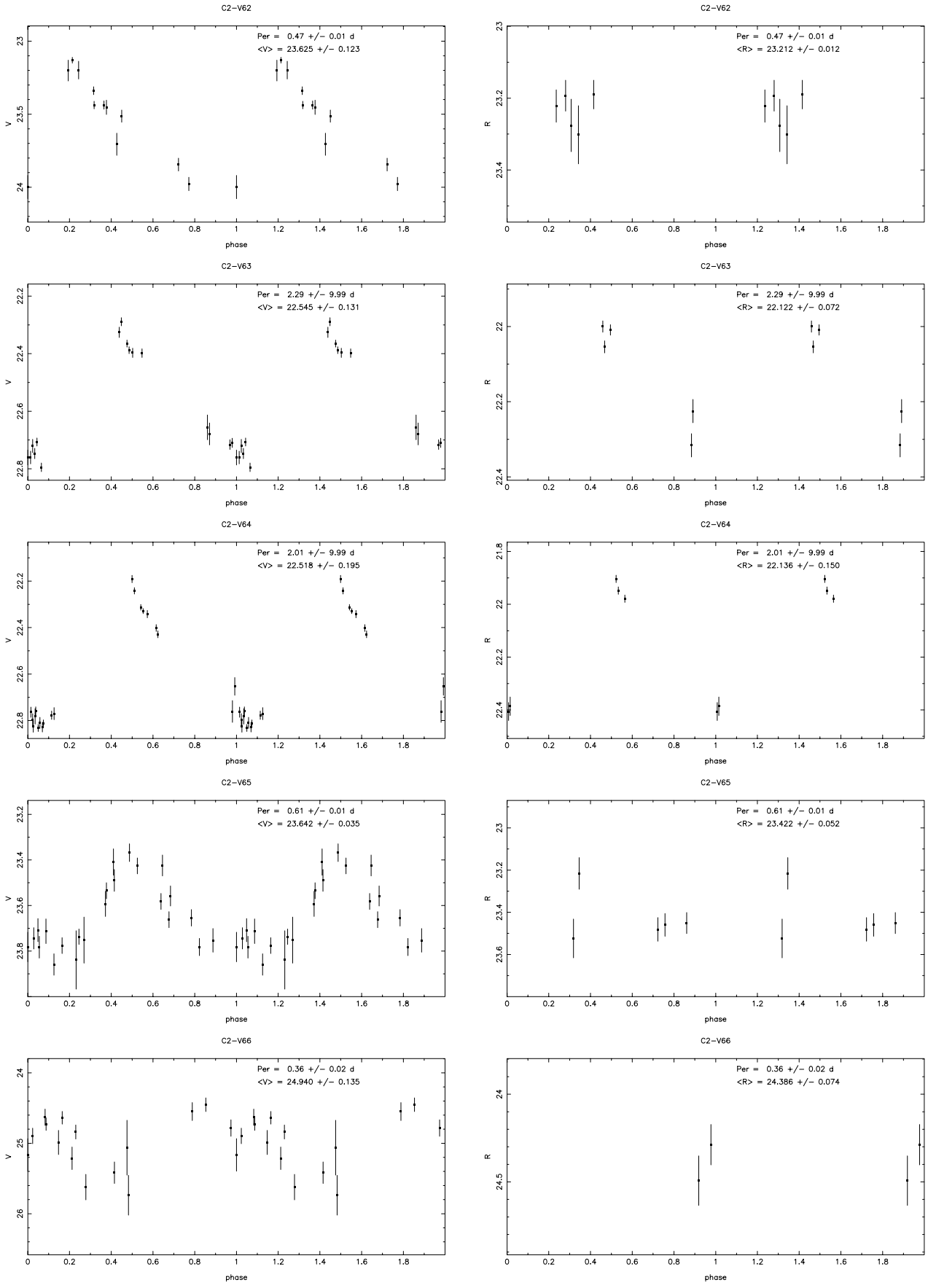

FIG. 4.—*Continued*

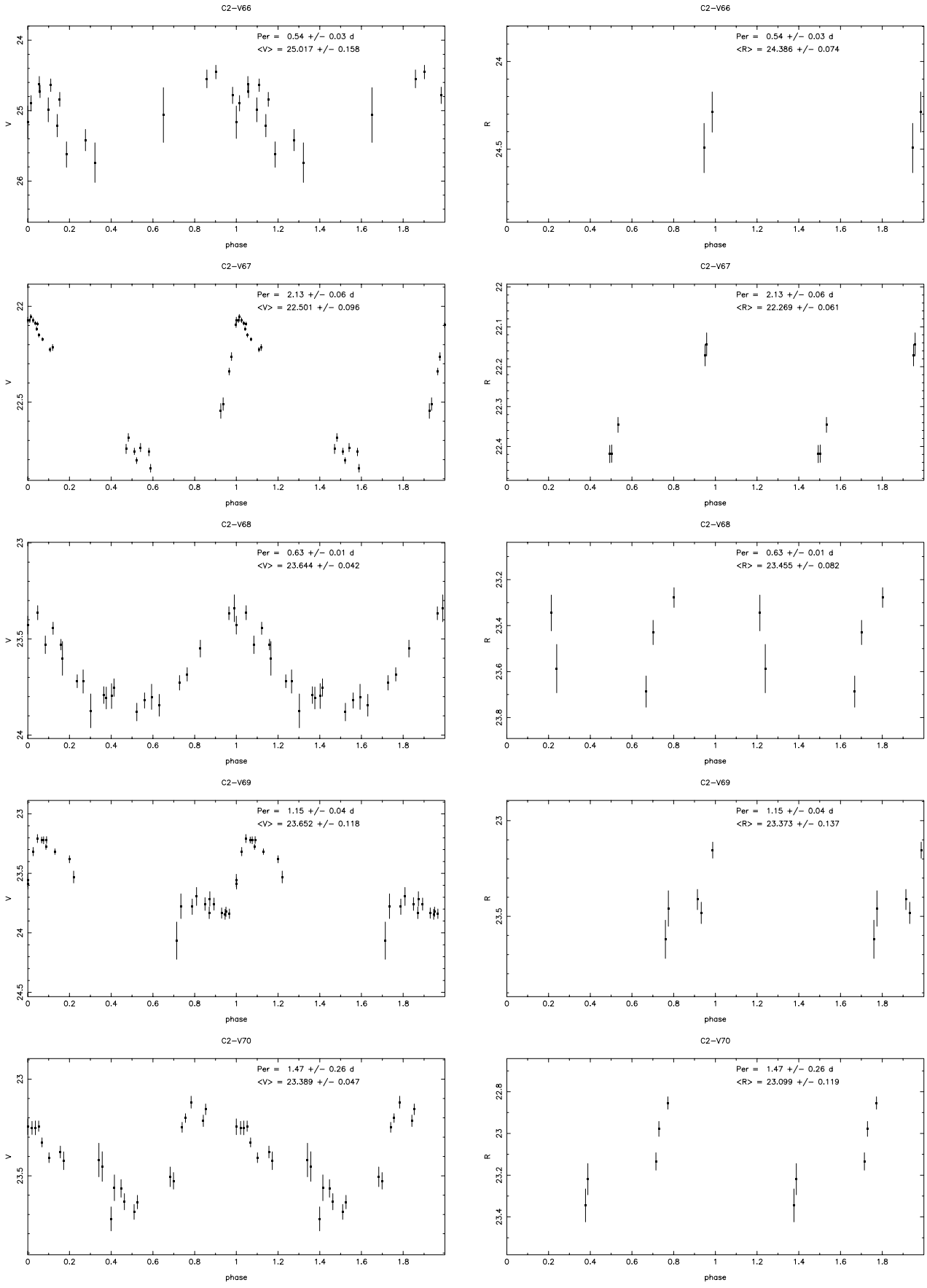

FIG. 4.—*Continued*

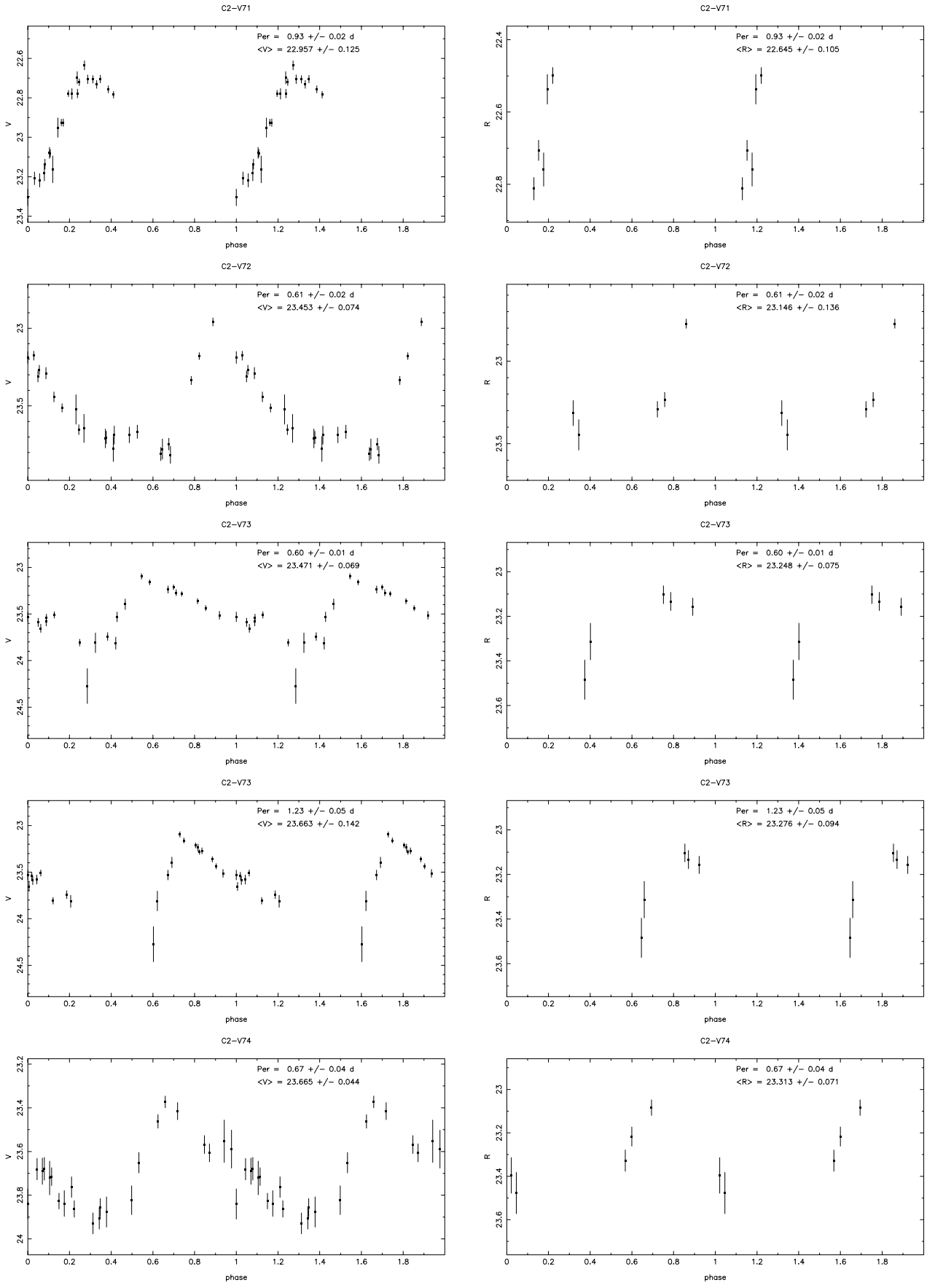

FIG. 4.—*Continued*

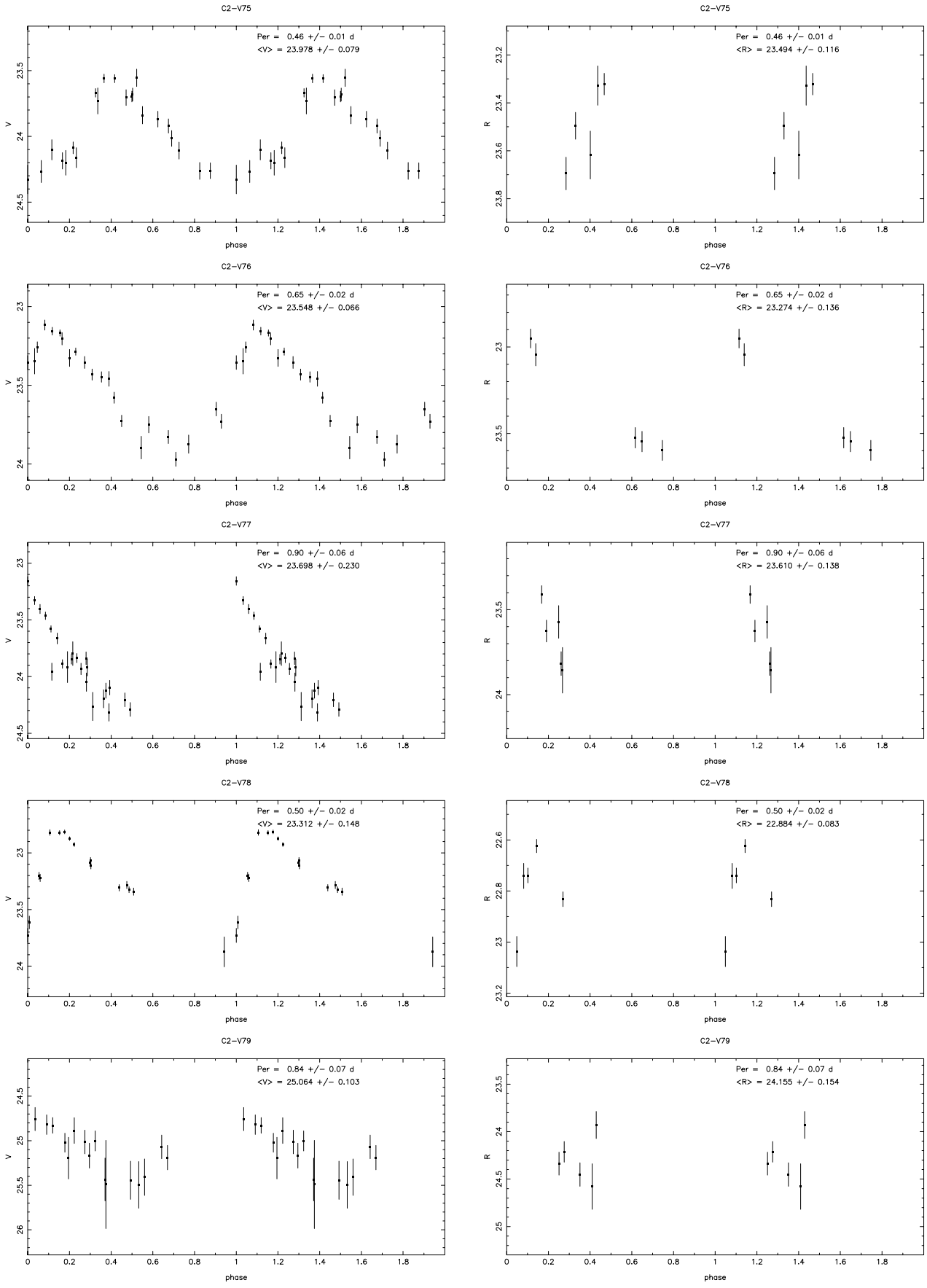

FIG. 4.—*Continued*

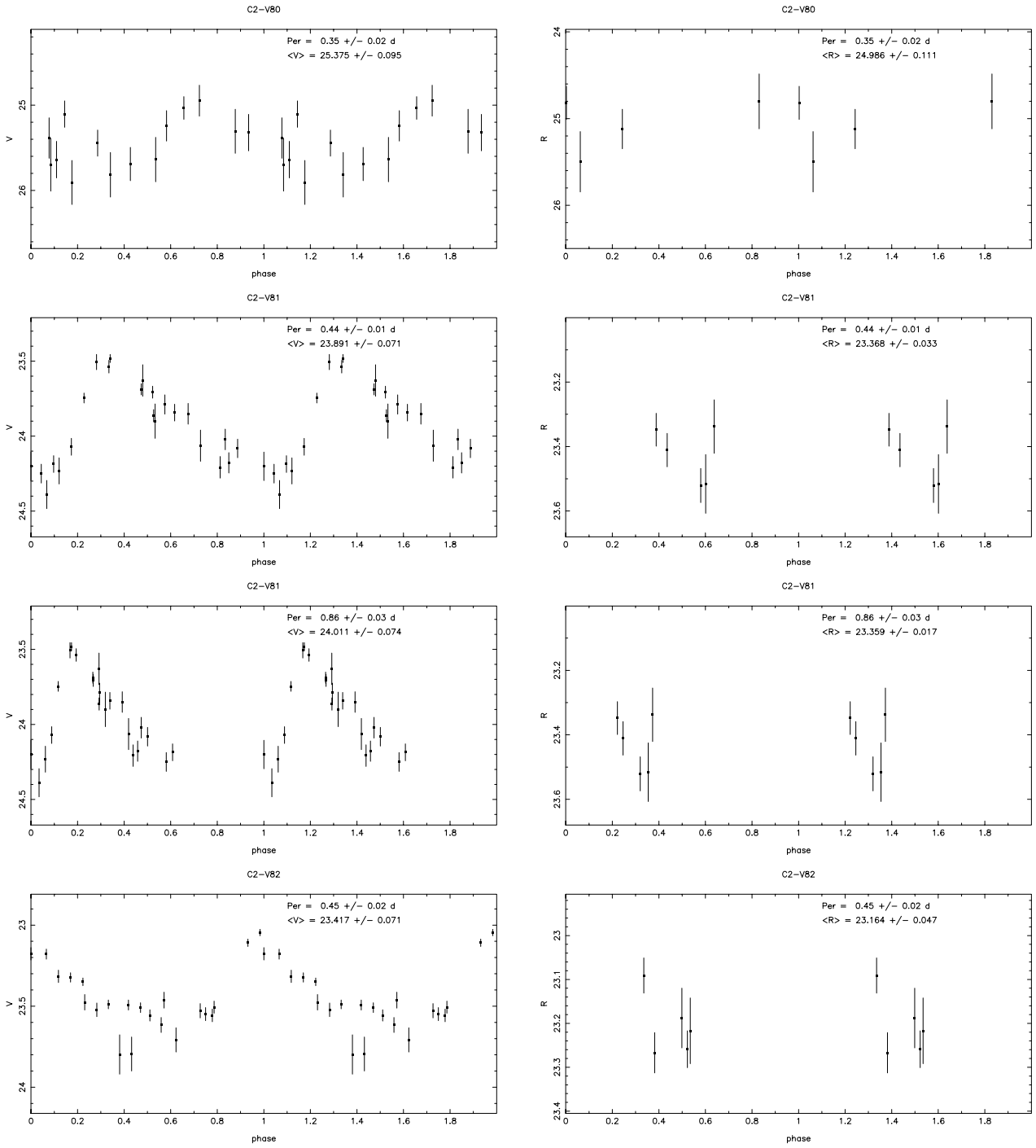

FIG. 4.—*Continued*

Of particular interest are three fundamental mode Cepheids with periods of less than 1 day: C1-V08, C2-V49, and C2-V77. With periods of ~0.8 days, these objects fall in the period regime generally populated by RR Lyrae stars and overtone-pulsating Cepheids. That these objects are not RR Lyrae stars is clear from the fact that they are ~1.4 mag brighter than the RR Lyrae stars. The likelihood of their being overtone-pulsating Cepheids is also small, given that they fall 0.6 mag below the overtone P-L relation in Figure 8 but only 0.06 mag away from an extrapolation of the fundamental mode relation. Thus we conclude that these objects are fundamental mode Cepheids, despite having periods similar to those of RR Lyrae stars.

There is some ambiguity as to whether these objects should be classified as classical or anomalous Cepheids, as the anomalous Cepheid P-L relations of Nemec, Nemec, & Lutz (1994) are very similar to those given above. By adjusting their M15 distance to $(m-M)_0 = 15.23$ (Reid 1999),

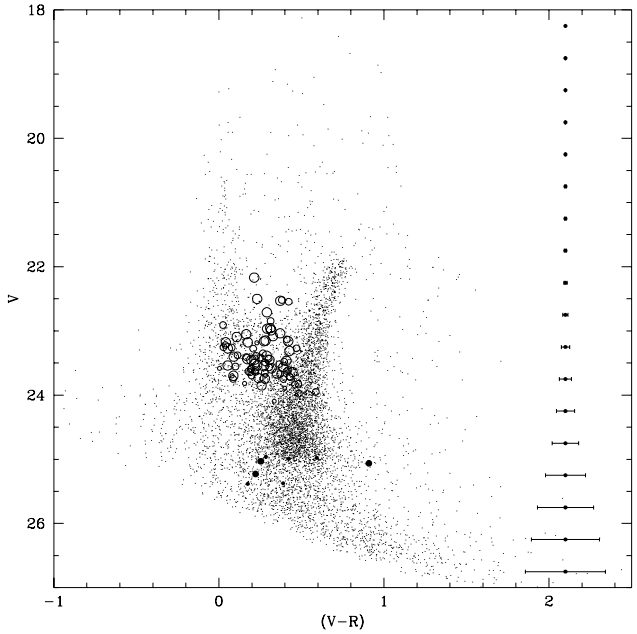

FIG. 5.—Color-magnitude diagram of Leo A, showing variable stars: our brighter population of variables (Cepheids; *open circles*), and our fainter population (RR Lyrae stars; *filled circles*). Circle size indicates the quality of the star's light curve (larger circles indicate higher quality). Error bars are taken from our photometry of the deep V and R frames. Uncertainties in R-band magnitudes dominate the color error bars.

their relations become

$$M_V(\text{fundamental}) = -3.13 \log (P) - 0.99 , \quad (5)$$

$$M_V(\text{overtone}) = -3.13 \log (P) - 1.54 . \quad (6)$$

The fundamental mode relations are clearly the same; the overtone relations are also consistent in the period range of Nemec et al. (1994) once the slope differences are accounted for. To further confuse matters, there is an overlap in period

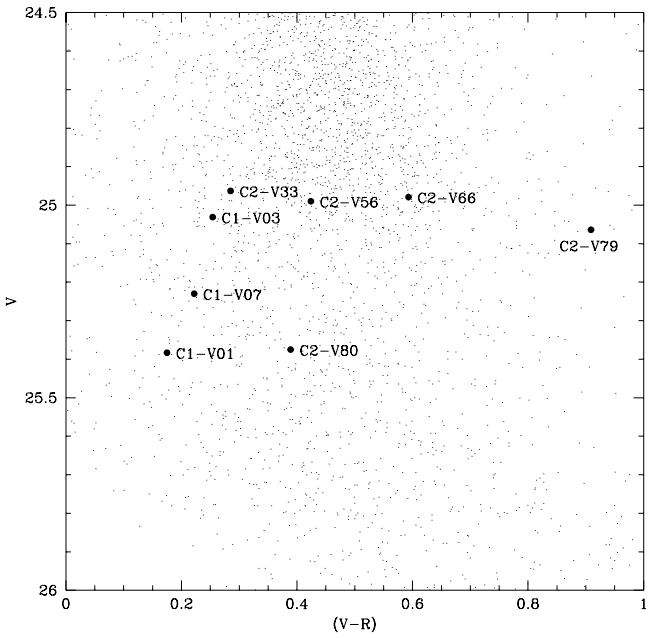

FIG. 6.—Leo A CMD, expanded to show the RR Lyrae stars in detail

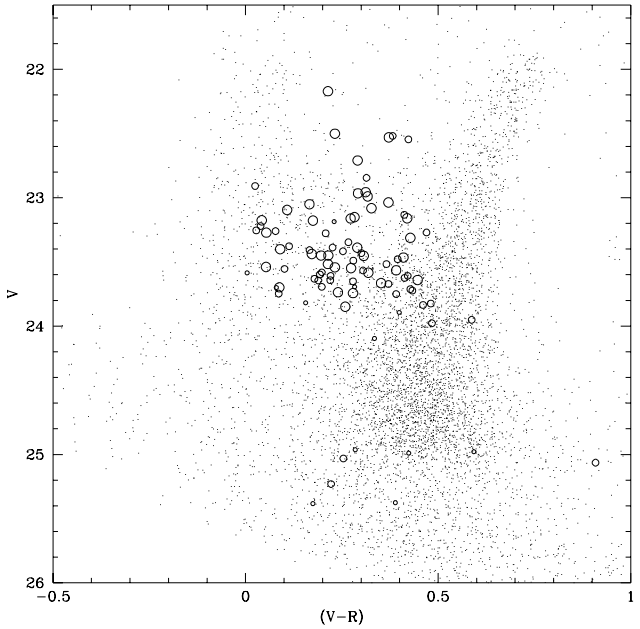

FIG. 7.—Leo A CMD, expanded to show the Cepheids in detail. Our mean R magnitudes of the variables have more scatter than our V magnitudes because of the limited phase coverage (five epochs).

between the SMC classical Cepheids of Udalski et al. (1999a) and the anomalous Cepheids of Nemec et al. (1994). Thus no clear distinction between these two classes of objects appears to exist in terms of position in a P-L rela-

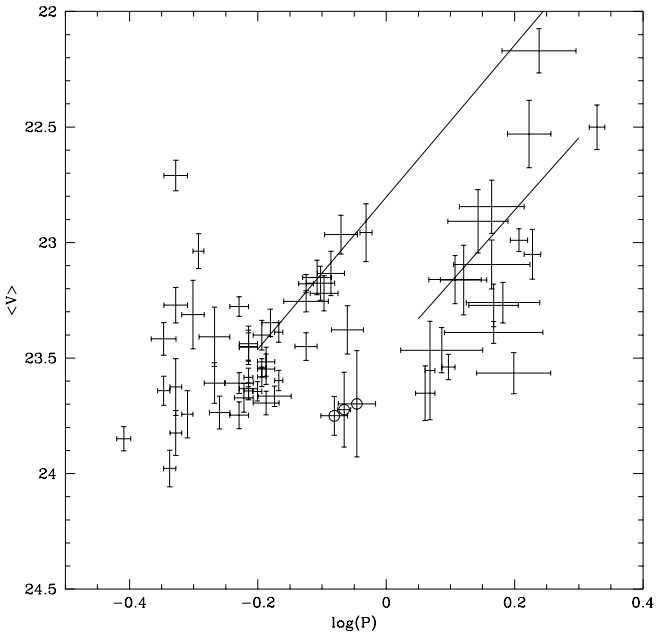

FIG. 8.—Period-luminosity diagram of bright variables in Leo A, showing only Cepheids with unambiguous periods and quality ratings of 3 or 4 and the three short-period fundamental mode Cepheids (*circles*). The lines represent the P-L relations for short-period SMC Cepheids in the OGLE database (Udalski et al. 1999b), assuming an SMC distance modulus of $(m-M)_0 = 18.88$ (Dolphin et al. 2001c). The lines are truncated near $\langle V \rangle = 23.4$ because the SMC does not contain a sufficient number of fainter Cepheids to constrain the P-L relations. Note that the lack of variables with periods of a day is caused by our inability to measure unambiguous periods for such objects.

tion. For the sake of clarity, we will define "classical" Cepheids as Population I (young) stars, and "anomalous" Cepheids as Population II (old) stars.

5.1. *Period-Luminosity Relations*

A brief review of the origin of the P-L relations may help explain this apparent contradiction of finding Cepheids with periods normally associated with RR Lyrae stars. What follows is only a back-of-the-envelope calculation, but it is sufficiently accurate to demonstrate the nature of these objects. The pulsation period (P) is related to the mean density (ρ) as follows:

$$P \propto \rho^{-1/2} . \tag{7}$$

We can use the definition of density ($\rho \propto M/R^3$) and effective temperature ($T^4 \propto L/R^2$) to rewrite equation (7) as

$$P \propto \frac{L^{3/4}}{M^{1/2} T_{\rm eff}^3} . \tag{8}$$

Since effective temperature as a function of luminosity is constrained to a small range within the instability strip, the pulsation period is essentially a function of luminosity and mass.

For evolving Population I stars, evolutionary motion is approximately horizontal in the H-R diagram. Therefore the main-sequence mass-luminosity relation, $L/(1\ L_\odot) \approx [M/(1\ M_\odot)]^{3.5}$, is roughly true also for pulsating variables, reducing equation (8) to

$$P = C \frac{[L/(1\ L_\odot)]^{0.61}}{T_{\rm eff}^3} , \tag{9}$$

where C is a constant. Incorporating the dependence of $T_{\rm eff}$ on L within the instability strip, one obtains the well-known Cepheid P-L relation.

This relation does not hold true for Population II stars, however, which become significantly brighter after leaving the main sequence and arriving at the horizontal branch ($M_V \approx +0.6$ or $L \approx 50\ L_\odot$) with a mass of only $\approx 0.6\ M_\odot$. With the mass thus fixed, the period should be given by

$$P = 1.29 C \frac{[L/(1\ L_\odot)]^{0.75}}{T_{\rm eff}^3} , \tag{10}$$

where C is the same constant as in equation (9).

We note that this Population II P-L relation has a very similar slope to the Population I P-L relation given in equation (9), a feature observed by Baade & Swope (1963) in their observations of M31. Using equations (9) and (10), we predict that a Population II variable with $L = 10^4\ L_\odot$ (a typical luminosity of Baade's Population II variables) will have a period $\sim$5 times that of a Population I variable of the same luminosity. This corresponds to a difference of $\Delta \log P \sim 0.7$, consistent with the value of 0.8 measured by Baade & Swope (1963).

More pertinent to our discussion of Leo A, one can use these equations to determine the expected luminosity of a classical Cepheid with the same period as that of an RR Lyrae star. For a Population I and a Population II variable with the same period and effective temperature, we find

$$(L_{\rm Ceph}/1\ L_\odot)^{0.61} = 1.29 (L_{\rm RR}/1\ L_\odot)^{0.75} = 24 . \tag{11}$$

Using the mass and luminosity given above for the RR Lyrae stars and the main-sequence mass-luminosity relation for the Cepheid, we find $L_{\rm Ceph} \approx 190\ L_\odot$, meaning that an RR Lyrae star will be $\sim$1.45 mag fainter than a Cepheid of equal period and luminosity. Even though the above calculations are rough approximations, it is interesting to note that this is almost exactly the magnitude difference observed in our data between the three variables in question [$\langle V_{\rm Ceph} \rangle = 23.74$], which we have inferred are fundamental mode pulsators, and our RR Lyrae stars [$\langle V_{\rm RR} \rangle = 25.11$].

5.2. *Metallicity Effects on the Cepheid Population*

While we have demonstrated that fundamental mode Cepheids *can* be found with the period and absolute magnitude claimed, it is somewhat disturbing that a population of such objects has not been previously observed. The Cepheid P-L relations of Udalski et al. (1999b) show LMC Cepheids reaching $M_{\rm V} \approx -2.6$ in large numbers and SMC Cepheids reaching $M_V \approx -1.4$. Likewise, IC 1613 (a dwarf slightly more metal-poor than the SMC) shows Cepheids reaching $M_V = -1.3$ (Dolphin et al. 2001a). First-overtone pulsators fall off at about the same absolute magnitude in each of those data sets; however, we observe significant numbers of both classes of Leo A Cepheids down to $M_V = -0.8$. In fact, the median V magnitude of the Cepheids in our sample is $M_V = -1.1$, which is fainter than 95.5% of the OGLE SMC Cepheids and 98.9% of their LMC Cepheids. Note that this is not a completeness problem with the OGLE observations. Their survey of the SMC shows a completeness (estimated from artificial star counts) of roughly 96% at $I = 19.5$ ($M_I \approx +0.6$) for their lower density fields and above 80% for their densest field (Udalski et al. 1998). Comparison of stars in overlapping regions of their survey shows an overall 94% completeness in their Cepheid catalog (Udalski et al. 1999a). Because of its smaller distance, the OGLE LMC catalog should be even less prone to completeness problems. This is conceivably a selection effect in our Leo A data; however, if a significant number of longer period Cepheids were present, they would have been found by Hoessel et al. (1994).

In addition to the low luminosities, another surprise was the large number of Cepheids recovered in Leo A. With a luminosity 1.5% that of the SMC, one would expect the 2083 OGLE Cepheids to scale to $\sim$30. Instead, we find 3 times that number.

The solutions to both of these dilemmas rest in the metallicity dependency of the blue loop position on the CMD. Synthetic CMDs for a variety of metallicities, calculated using the Girardi et al. (2000) isochrones using constant star formation rates from 0 to 15 Gyr ago, are shown in Figure 9. At solar metallicity, blue helium-burning stars (BHeB's) remain to the blue of the instability strip at magnitudes of $M_V < -4$. This can be seen in Figure 9 (*top left*), where no stars fall in the instability strip. At lower metallicity, however, BHeB's become increasingly blue.

The effect of this metallicity dependence is twofold. First, at lower metallicities, the intersection of the blue loop with the instability strip falls at fainter magnitudes. This is apparent in Figure 9; the absolute magnitude is $M_V = -1.8$ at $Z = 0.004$, $M_V = -0.9$ at $Z = 0.001$, and $M_V = -0.4$ at $Z = 0.0004$. Second, because the blue loops are more strongly populated at fainter absolute magnitudes (a result of evolutionary timescales and the stellar IMF), more stars

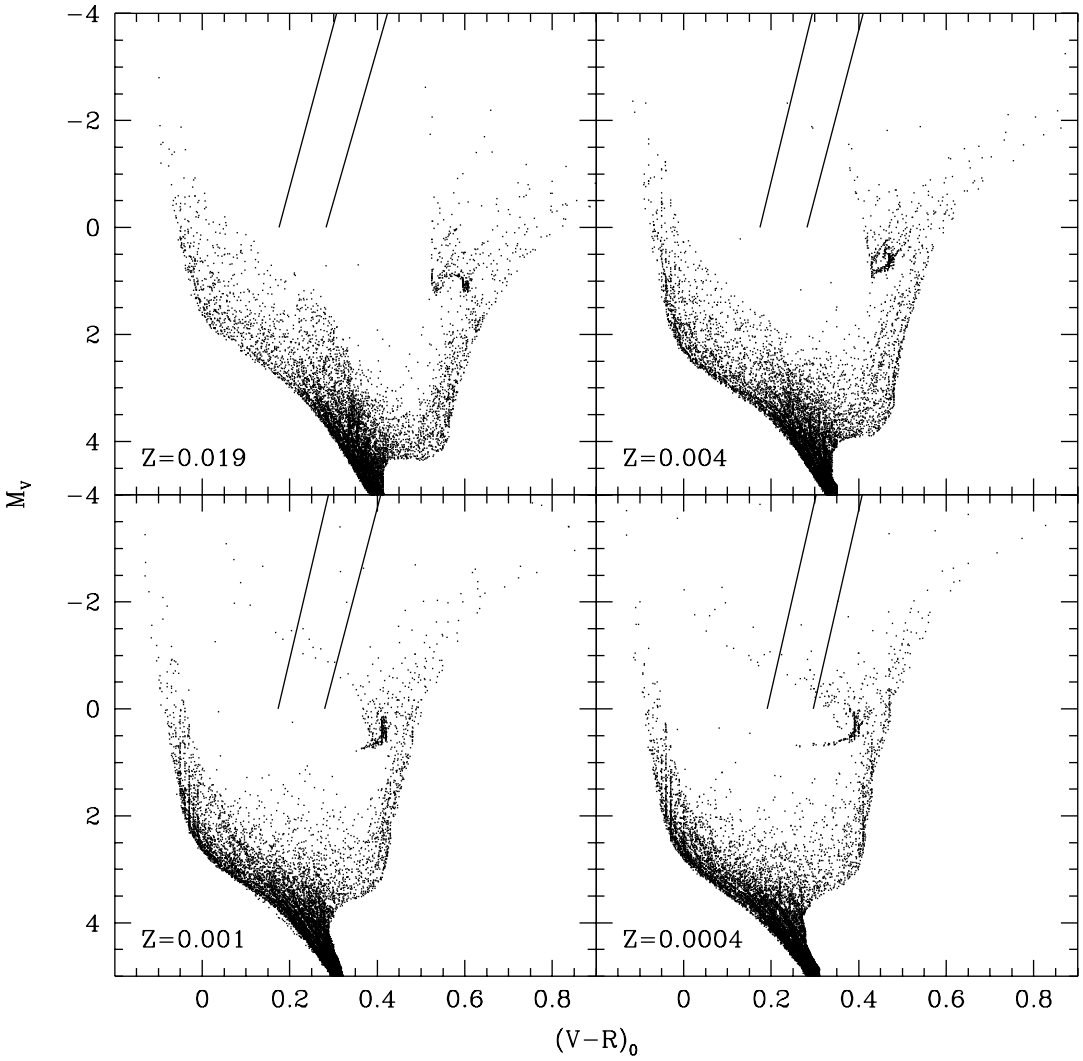

FIG. 9.—Synthetic CMDs based on the Girardi et al. (2000) isochrones, calculated for the stated metallicities and assuming a constant star formation rate. The lines indicate the rough location of the instability strip.

will fall within the instability strip for a low-metallicity system than for a high-metallicity system with equal star formation rates.

The presence of short-period Cepheids in young low-metallicity populations is not a new discovery. For example, the theoretical models of Bono et al. (1997) show this effect. However, we note that such objects are ordinary post–main-sequence Population I stars and thus are properly classified as classical Cepheids and not as anomalous Cepheids.

5.3. *Star Formation History from the Cepheid Population*

A nagging question in our new variable-star search is to explain the unsuccessful search of Hoessel et al. (1994). Despite an 11 year baseline and observations spaced as close as 1 day apart, they failed to conclusively identify any Cepheids. In contrast, we report the discovery of 84 Cepheid candidates based on three nights of data.

It is clear that Hoessel et al. (1994) would not have been sensitive to the many ~1 day Cepheids that we find in abundance because of the BHeB's. However, the population of the instability strip is nonzero at magnitudes brighter than $M_V = -2.3$. Figure 10 shows a more strongly populated synthetic CMD, with a constant star formation rate from 0 to 1 Gyr ago and a metallicity of $Z = 0.0004$; stars are present in the instability strip up to the top of the CMD.

While it is possible that the lack of bright Cepheids may result from a recent decrease in the star formation rate, we do not find this to be essential. Of the 5405 stars inside the instability strip of Figure 10, only 75 have absolute magnitudes brighter than $M_V = -2.5$ (corresponding to $P > 3$ days). Scaling to the number of observed Cepheids in Leo A (84), we would expect only ~1.2 bright (long period) Cepheids in Leo A because of both the stellar IMF and evolutionary timescales. This is also seen in our CMD, which shows no clear evidence of stars brighter than $V = 22$ in the instability strip, although foreground contamination prohibits a definitive measurement. Thus we find no evidence of an unusual star formation rate. The recent (less than 100 Myr) star formation rate cannot have been significantly higher than that at older ages (~650 Myr), in which case we would

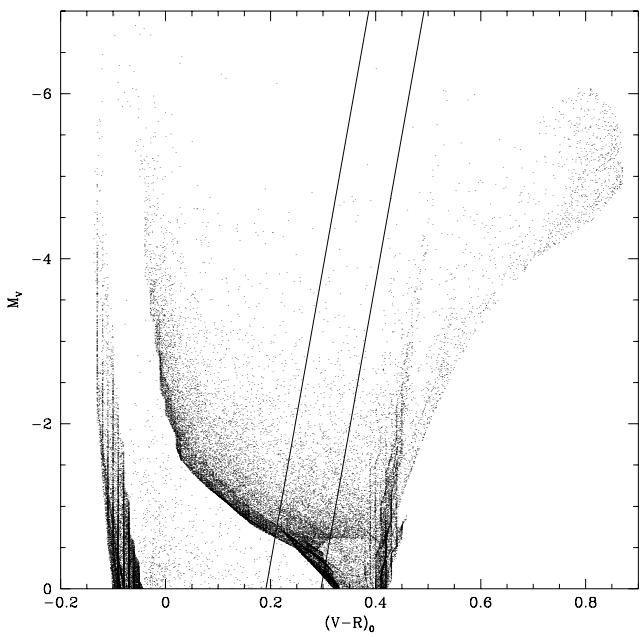

FIG. 10.—Synthetic CMD based on the Girardi et al. (2000) isochrones, calculated for $Z = 0.0004$ ([M/H] = −1.7), with a constant star formation rate from 0 to 1 Gyr. The lines indicate the rough location of the instability strip.

expect to see significant numbers of bright Cepheids, but Cepheid statistics provide no lower limit on the recent star formation rate.

This is not the first time that the absence of long-period Cepheids in a dwarf irregular galaxy has been pondered. In their study of WLM, Sandage & Carlson (1985) found numerous Cepheids with periods between 3 and 10 days, but none with periods longer than 10 days. They speculated that the absence of the longer period Cepheids could be due to either stochastic variations in the rate of star formation or (their favored explanation) a metallicity dependency of the lengths of the blue loop excursions of the post–main-sequence evolutionary tracks. Later, Skillman, Terlevich, & Melnick (1989) measured H II region abundances in WLM, showing it to be more metal-rich than Sextans A, which was known to have several longer period Cepheids. Today we know that Sextans A has experienced a relatively high rate of star formation in the last 50 Myr (Dohm-Palmer et al. 1997), corresponding to main-sequence turnoff masses in excess of 7 $M_\odot$ and thus Cepheids with periods in excess of 10 days, while the star formation rate in WLM has been relatively low during this period (Dolphin 2000b). Thus, given the relatively small numbers of total stars in the low-mass, low-metallicity dwarf irregular galaxies, small numbers of long-period Cepheid variables are expected. Only enhanced recent star formation rates will produce statistically meaningful samples of long-period Cepheid variable stars in a single dwarf galaxy.

6. STELLAR POPULATIONS

Although the primary topic of this paper is the variable-star content of Leo A, we have found an interesting difference in the distributions of young and old stars in Leo A, with red stars ($22.0 < V < 23.5$ and $0.45 < V-R < 0.8$) distributed over a larger scale than blue stars ($21.5 < V < 23.5$ and $-0.3 < V-R < 0.2$). The distributions of these populations are shown in Figure 11. The population difference is also supported by the observation that one of out two bona fide RR Lyrae stars (C1-V03) falls beyond the outermost contour of the blue stars and the other between the outermost and second contours.

To better quantify the population differences, we have divided the galaxy into three regions based on the blue star density. The three resulting CMDs are shown in Figure 12. The inner region shows a blue-to-red ratio of 0.87, the middle region a ratio of 0.25, and the outer region a ratio of 0.03. We interpret this gradient as the sign of an old stellar halo surrounding the body of the galaxy, similar to those found in many other galaxies, such as WLM (Minniti & Zijl-

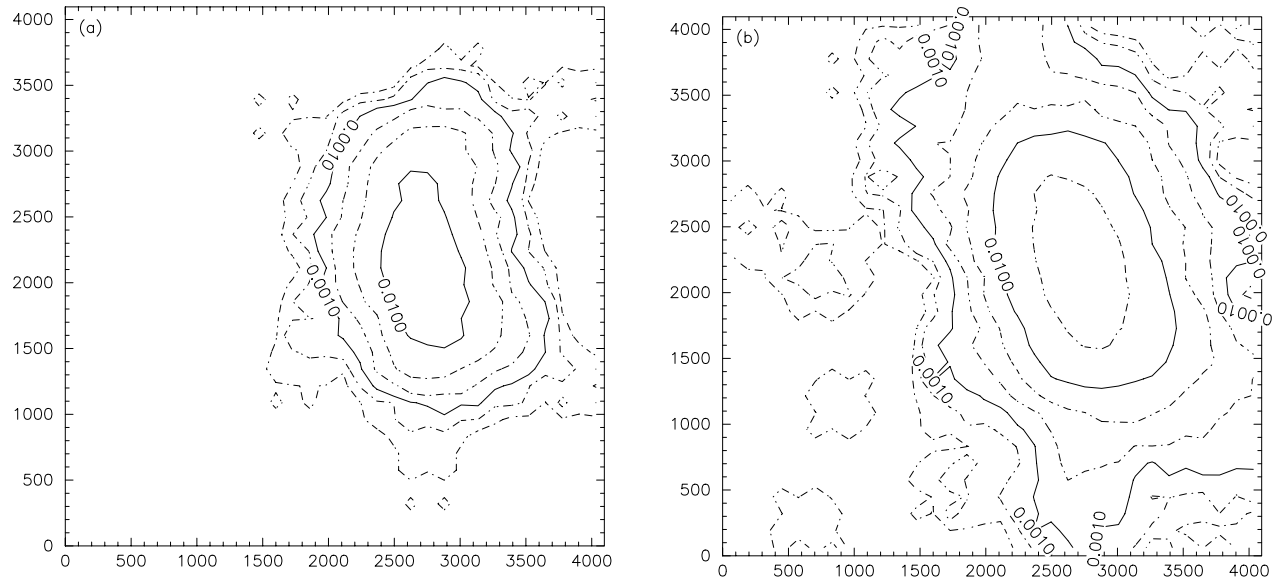

FIG. 11.—Density maps of blue plume stars ($21.5 < V < 23.5$ and $-0.3 < V-R < 0.2$; *left*) and red giants ($22.0 < V < 23.5$ and $0.45 < V-R < 0.8$) (*right*) in arcsec^{-2}. Contour levels are plotted every 0.33 dex. Note that the red star distribution is larger than the blue star distribution (as evidenced by the spacing between contours), indicating an old halo.

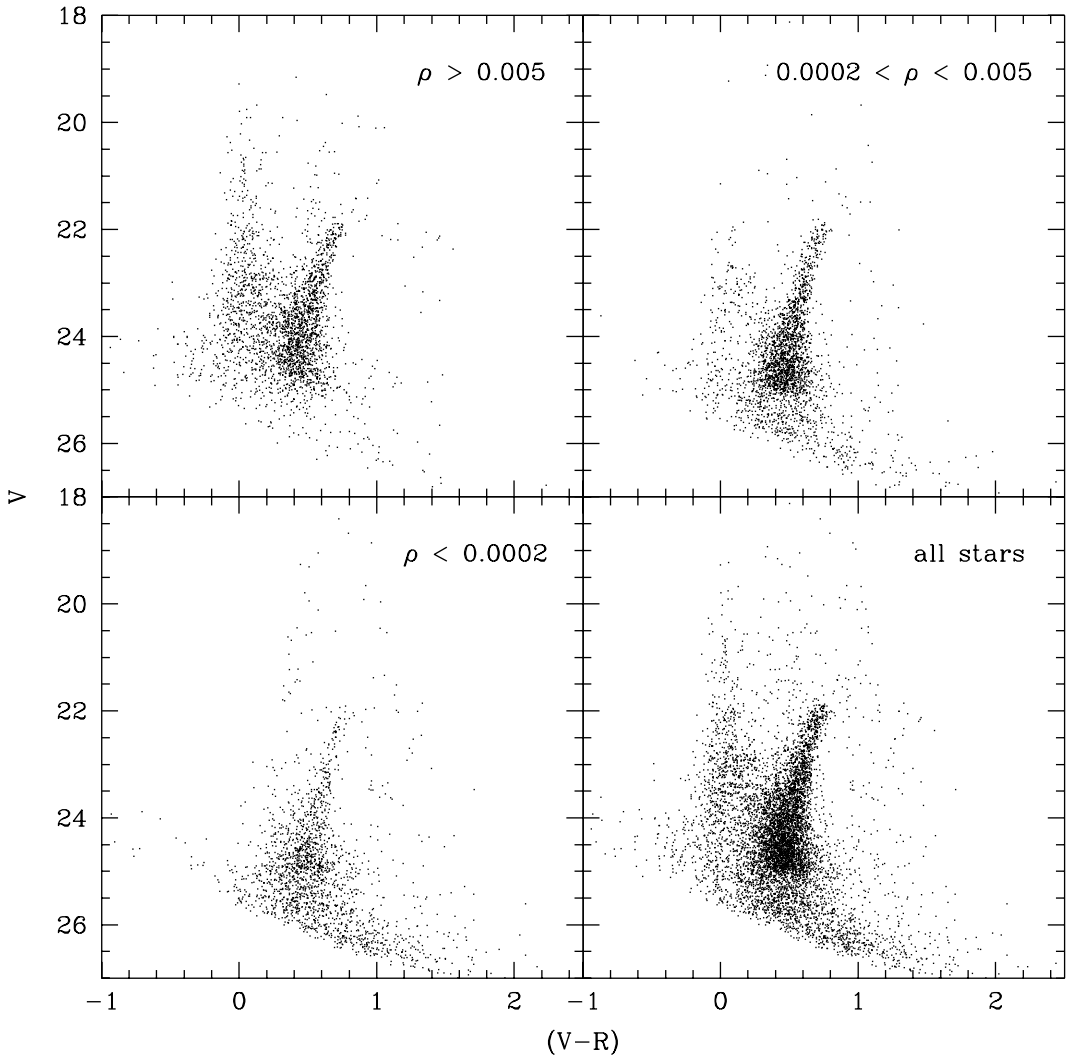

FIG. 12.—Color-magnitude diagram of Leo A, divided by density of blue plume stars ($21.5 < V < 23.5$ and $-0.3 < V-R < 0.2$) as described in the text.

stra 1997), UGC 4483 (Dolphin et al. 2001a), and LGS 3 (Miller et al. 2001). By comparing contour spacing, this stellar halo appears more compact than the H I halo found by Young & Low (1996). As our data were optimized for a variable-star search rather than CMD analysis (thus giving us extremely deep photometry in V and very shallow photometry in R), we cannot make a more detailed analysis of the populations. We note that the population gradient we observe would require that such a study sample the entire galaxy to obtain a complete picture of the stellar populations and their spatial distributions.

We note that our CMD shows a lack of bright supergiants in Leo A. The brightest blue star falls at $V = 19.23$, or $M_V = -5.33$, corresponding to an age of 40 Myr according to the theoretical models of Fagotto et al. (1994) at $Z = 0.0004$. While the presence of H II regions demonstrates that Leo A contains a nonzero number of very young ($\lesssim 6$ Myr) main-sequence stars, a large and steady amount of star formation should have produced blue supergiants roughly 2.5 mag brighter than those observed. The brightest three blue stars have an average magnitude of $\langle V \rangle = 19.39$, or $M_V = -5.17$. This is undoubtedly the cause of the incorrect distances measured by Demers et al. (1984) and Sandage (1986), as the brightest supergiant studies assumed absolute magnitudes of $M_V \sim -7$ for the brightest blue stars in Leo A.

7. SUMMARY

We have presented the results of a search for short-period variables in Leo A, based on three consecutive nights of WIYN MIMO observations. We have located 92 variable-star candidates. When placed on a CMD, the variable stars are clearly divided into two populations. The majority of our variables are short-period classical Cepheids; eight are candidate RR Lyrae stars. From the RR Lyrae stars, we measure a distance modulus of $(m - M)_0 = 24.51 \pm 0.12$. The discovery of RR Lyrae stars in Leo A disproves the hypothesis that the onset of star formation in Leo A was delayed until a few gigayears ago.

We have examined the Cepheid population of Leo A, which appears to be significantly different from previously studied Cepheid populations. We found 84 Cepheid candidates, of which 66 have excellent light curves in V and R and unambiguous periods. Rather than a typical Cepheid population, with periods of 2–60 days and absolute magnitudes of $-2 > M_V > -6.5$, we found very faint ($-0.7 > M_V > -2.3$) Cepheids with short periods, includ-

ing three fundamental pulsators with periods of under 1 day. We have examined this unusual population in terms of pulsation theory and have demonstrated that these objects fall at the expected positions on fundamental and overtone P-L relations. The unusual Cepheid magnitudes are caused by the metallicity dependence of the blue loops. We find that this also explains the relatively large number of Cepheids observed in Leo A (3 times the number expected from scaling the SMC Cepheid population to Leo A's luminosity). We believe that most of these unusual aspects of this Cepheid population should, in fact, be a common feature of low-metallicity star-forming galaxies.

We have also examined the distributions of blue stars (primarily blue helium-burning stars) and red stars (primarily red giants) in our image, and discovered an old stellar halo in Leo A that extends well beyond the extent of the young population. A CMD of the halo looks typical for an old (more than $\sim$2 Gyr) population, with the only obvious feature being the red giant branch; a definitive age-dating of this population will be possible only with deeper photometry.

We would like to thank the National Optical Astronomy Observatory TAC for the allocation of telescope time and the Kitt Peak National Observatory KPNO staff for their assistance. E. D. S. gratefully acknowledges partial support from NASA LTSARP grant NAG 5-9221 and the University of Minnesota.

REFERENCES

Baade, W., & Swope, H. H. 1963, AJ, 68, 435
Bauer, F., et al. 1999, A&A, 348, 175
Bono, G., Caputo, F., Santolamazza, P., Cassisi, S., & Piersimoni, A. 1997, AJ, 113, 2209
Carretta, E., Gratton, R. G., Clementini, G., & Fusi Pecci, F. 2000, ApJ, 533, 215
Demers, S., Kibblewhite, E. J., Irwin, M. J., Bunclark, P. S., & Bridgeland, M. T. 1984, AJ, 89, 1160
Dohm-Palmer, R. C., et al. 1997, AJ, 114, 2527
Dolphin, A. E. 2000a, PASP, 112, 1383
———. 2000b, ApJ, 531, 804
Dolphin, A. E., et al. 2001a, MNRAS, 324, 249
———. 2001b, ApJ, 550, 554
Dolphin, A. E., Walker, A. R., Hodge, P. W., Mateo, M., Olszewski, E. W., Schommer, R. A., & Suntzeff, N. B. 2001c, ApJ, 562, 303
Fagotto, F., Bressan, A., Bertelli, G., & Chiosi, C. 1994, A&AS, 104, 365
Girardi, L., Bressan, A., Bertelli, G., & Chiosi, C. 2000, A&AS, 141, 371
Hoessel, J. G., Saha, A., Krist, J., & Danielson, G. E. 1994, AJ, 108, 645
Kaluzny, J., Olech, A., Thompson, I., Pych, W., Krzeminski, W., & Schwarzenberg-Czerny, A. 2000, A&AS, 143, 215
Lafler, J., & Kinman, T. D. 1965, ApJS, 11, 216
Landolt, A. U. 1992, AJ, 104, 340
Madore, B. F., & Freedman, W. L. 1991, PASP, 103, 933
Miller, B. W., Dolphin, A. E., Lee, M.-G., Kim, S.-C., & Hodge, P. W. 2001, ApJ, 562, 713
Minniti, D., & Zijlstra, A. A. 1997, AJ, 114, 147
Nemec, J. M., Nemec, A. F. L., & Lutz, T. E. 1994, AJ, 108, 222
Reid, I. N. 1996, MNRAS, 278, 367
———. 1999, ARA&A, 37, 191
Rozanski, R., & Rowan-Robinson, M. 1994, MNRAS, 271, 530
Saha, A., Armandroff, T., Sawyer, D. G., & Corson, C. 2000, Proc. SPIE, 4008, 447
Saha, A., & Hoessel, J. G. 1990, AJ, 99, 97
Saha, A., Hoessel, J. G., Krist, J., & Danielson, G. E. 1996, AJ, 111, 197
Sandage, A. 1986, AJ, 91, 496
———. 1993, AJ, 106, 703
Sandage, A., & Carlson, G. 1985, AJ, 90, 1464
Schechter, P. L., Mateo, M., & Saha, A. 1993, PASP, 105, 1342
Schlegel, D. J., Finkbeiner, D. P., & Davis, M. 1998, ApJ, 500, 525
Shetrone, M. D., Côté, P., & Sargent, W. L. W. 2001, ApJ, 548, 592
Skillman, E. D., Terlevich, R., & Melnick, J. 1989, MNRAS, 240, 563
Stetson, P. B. 2000, PASP, 112, 925
Tolstoy, E. 1996, ApJ, 462, 684
Tolstoy, E., et al. 1998, AJ, 116, 1244
Udalski, A., Soszynski, I., Szymanski, M., Kubiak, M., Pietrzynski, G., Wozniak, P., & Zebrun, K. 1999a, Acta Astron., 49, 437
Udalski, A., Szymanski, M., Kubiak, M., Pietrzynski, G., Soszynski, I., Wozniak, P., & Zebrun, K. 1999b, Acta Astron., 49, 201
Udalski, A., Szymanski, M., Kubiak, M., Pietrzynski, G., Wozniak, P., & Zebrun, K. 1998, Acta Astron., 48, 147
van den Bergh, S. 2000, The Galaxies of the Local Group (Cambridge: Cambridge Univ. Press)
van Zee, L., Skillman, E. D., & Haynes, M. P. 1999, BAAS, 194.0504
Venn, K. A. 1999, ApJ, 518, 405
Venn, K. A., et al. 2001, ApJ, 547, 765
Walker, A. R. 1989, PASP, 101, 570
Young, L. M., & Lo, K. Y. 1996, ApJ, 462, 203
Zwicky, F. 1942, Phys. Rev. II, 61, 489